Supplementary Materials: A Quantitative Comparison of Total Suspended Sediment Algorithms: A Case Study of the Last Decade for MODIS and Landsat-Based Sensors

Passang Dorji * and Peter Fearns

S1. Scatter Plot of MODIS TSS Models for CLASS-I Water

Figure S1.1. Scatter plot of MODIS TSS models in CLASS-I water for brown earth sediment, b_b/b ratio of 0.018, solar zenith angle of 30°.

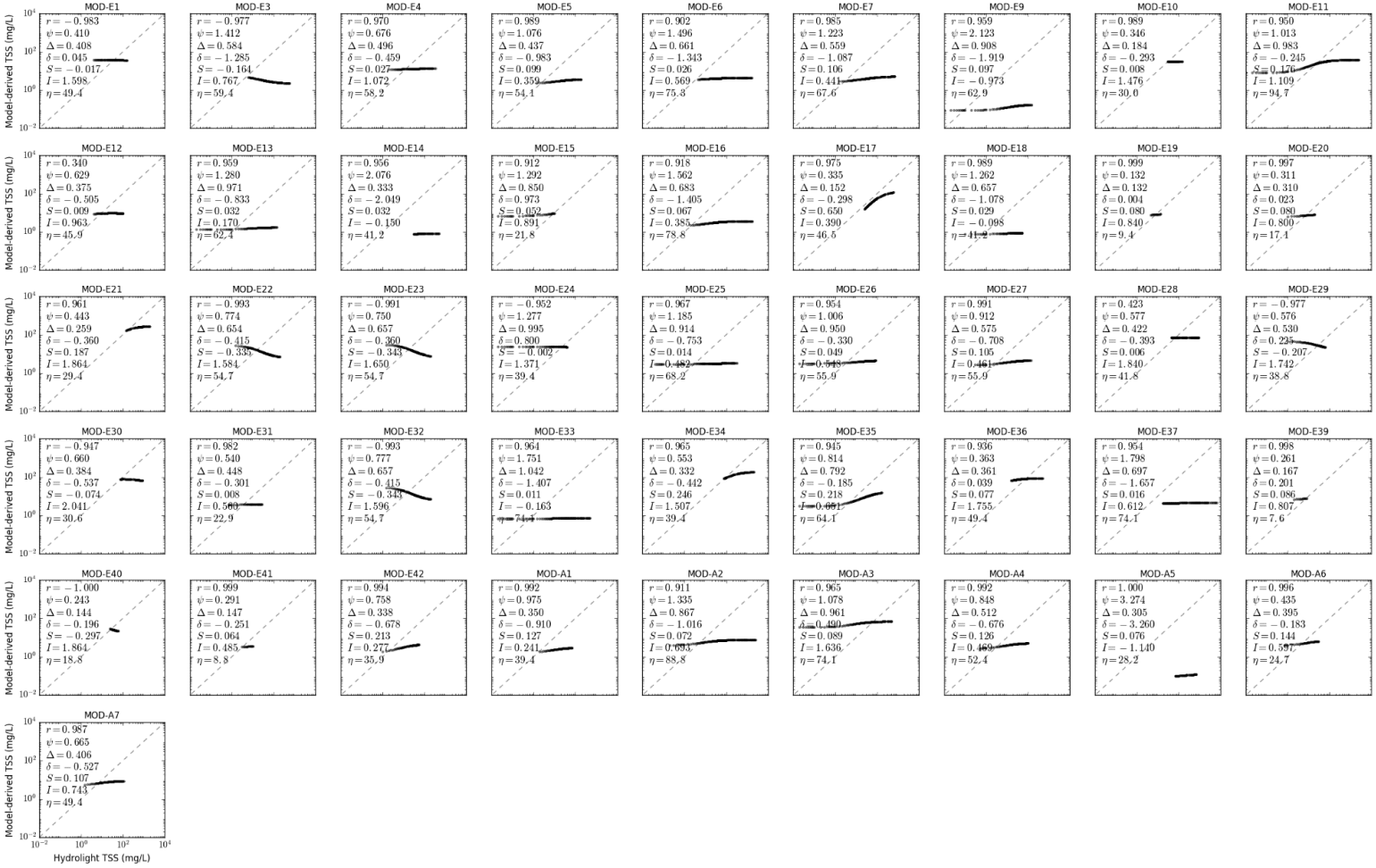

Figure S1.2. Scatter plot of MODIS TSS models in CLASS-I water for bukata sediment, b_b/b ratio of 0.018, solar zenith angle of 30°.

Figure S1.3. Scatter plot of MODIS TSS models in CLASS-I water for calcareous sand sediment, b_b/b ratio of 0.018, solar zenith angle of 30°.

Figure S1.4. Scatter plot of MODIS TSS models in CLASS-I water for red clay sediment, b_b/b ratio of 0.018, solar zenith angle of 30°.

Figure S1.5. Scatter plot of MODIS TSS models in CLASS-I water for yellow clay sediment, b_b/b ratio of 0.018, solar zenith angle of 30°.

Figure S1.6. Scatter plot of MODIS TSS models in CLASS-I water for calcareous sand sediment, b_b/b ratio of 0.001, solar zenith angle of 30°.

Figure S1.7. Scatter plot of MODIS TSS models in CLASS-I water for calcareous sand sediment, b_b/b ratio of 0.01, solar zenith angle of 30°.

Figure S1.8. Scatter plot of MODIS TSS models in CLASS-I water for calcareous sand sediment, b_b/b ratio of 0.05, solar zenith angle of 30°.

Figure S1.9. Scatter plot of MODIS TSS models in CLASS-I water for calcareous sand sediment, b_b/b ratio of 0.1, solar zenith angle of 30°.

Figure S1.10. Scatter plot of MODIS TSS models in CLASS-I water for calcareous sand sediment, b_b/b ratio of 0.018, solar zenith angle of 15°.

Figure S1.11. Scatter plot of MODIS TSS models in CLASS-I water for calcareous sand sediment, b_b/b ratio of 0.018, solar zenith angle of 45°.

Figure S1.12. Scatter plot of MODIS TSS models in CLASS-I water for calcareous sand sediment, b_b/b ratio of 0.018, solar zenith angle of 60°.

Supplementary Materials S2. Scatter Plot of MODIS TSS Models for CLASS-II Water

Figure S2.1. Scatter plot of MODIS TSS models in CLASS-II water for brown earth sediment, b_b/b ratio of 0.018, solar zenith angle of 30°.

Figure S2.2. Scatter plot of MODIS TSS models in CLASS-II water for bukata sediment, b_b/b ratio of 0.018, solar zenith angle of 30°.

Figure S2.3. Scatter plot of MODIS TSS models in CLASS-II water for calcareous sand sediment, b_b/b ratio of 0.018, solar zenith angle of 30°.

Figure S2.4. Scatter plot of MODIS TSS models in CLASS-II water for red clay sediment, b_b/b ratio of 0.018, solar zenith angle of 30°.

Figure S2.5. Scatter plot of MODIS TSS models in CLASS-II water for yellow clay sediment, b_b/b ratio of 0.018, solar zenith angle of 30°.

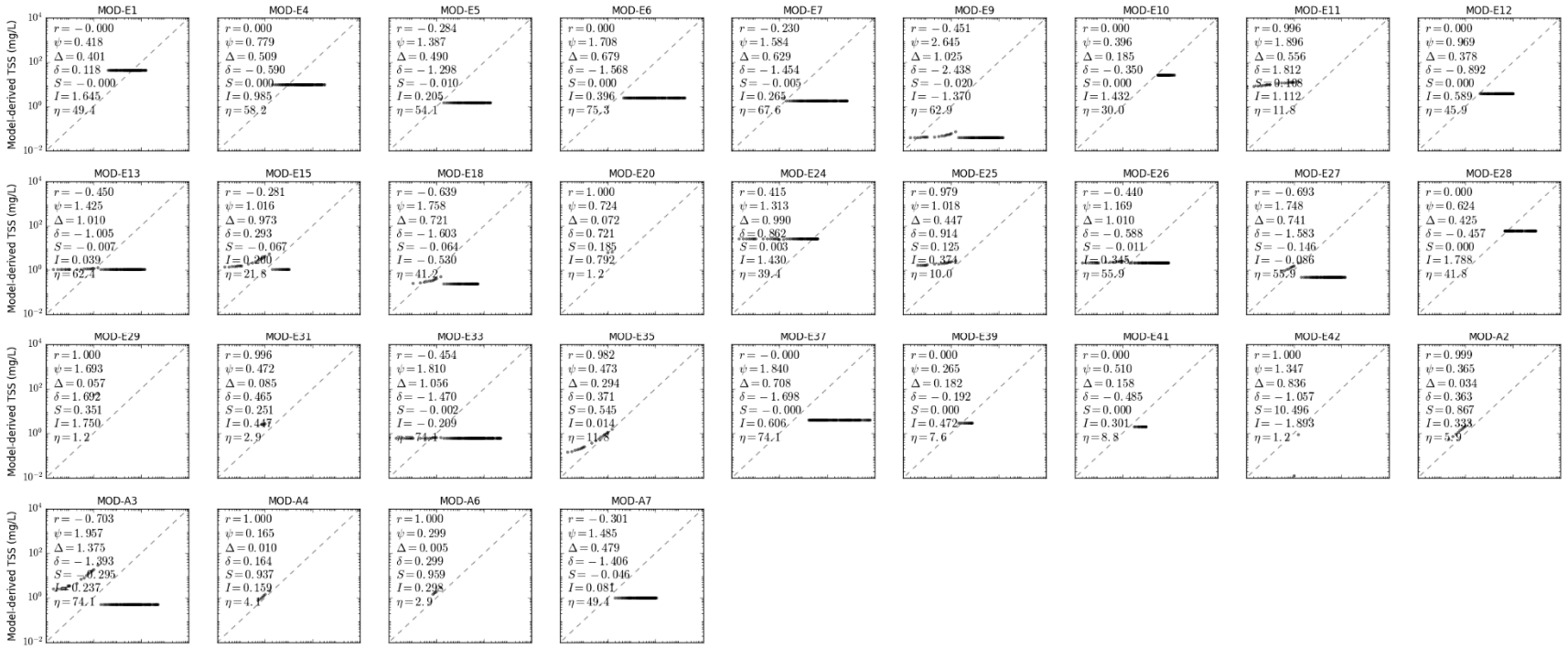

Figure S2.6 Scatter plot of MODIS TSS models in CLASS-II water for calcareous sand sediment, b_b/b ratio of 0.001, solar zenith angle of 30°.

Figure S2.7. Scatter plot of MODIS TSS models in CLASS-II water for calcareous sand sediment, b_b/b ratio of 0.01, solar zenith angle of 30°.

Figure S2.8. Scatter plot of MODIS TSS models in CLASS-II water for calcareous sand sediment, b_b/b ratio of 0.05, solar zenith angle of 30°.

Figure S2.9. Scatter plot of MODIS TSS models in CLASS-II water for calcareous sand sediment, b_b/b ratio of 0.1, solar zenith angle of 30°.

Figure S2.10. Scatter plot of MODIS TSS models in CLASS-II water for calcareous sand sediment, b_b/b ratio of 0.018, solar zenith angle of 15°.

Figure S2.11. Scatter plot of MODIS TSS models in CLASS-II water for calcareous sand sediment, b_b/b ratio of 0.018, solar zenith angle of 45°.

Figure S2.12. Scatter plot of MODIS TSS models in CLASS-II water for calcareous sand sediment, b_b/b ratio of 0.018, solar zenith angle of 60°.

Supplementary Materials S3. Scatter Plot of MODIS TSS Models for CLASS-III Water

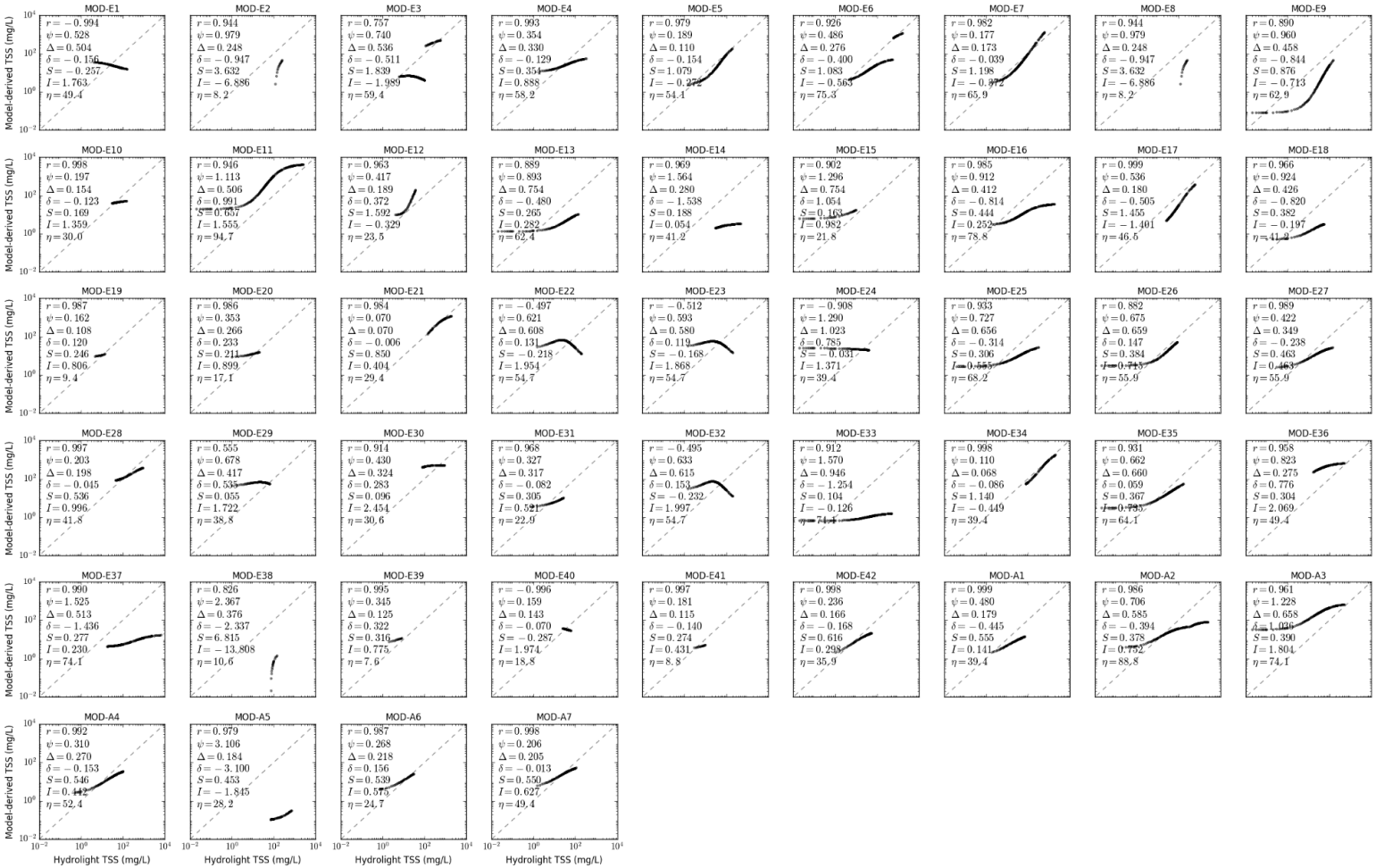

Figure S3.1. Scatter plot of MODIS TSS models in CLASS-III water for brown earth sediment, b_b/b ratio of 0.018, solar zenith angle of 30°.

Figure S3.2. Scatter plot of MODIS TSS models in CLASS-III water for bukata sediment, b_b/b ratio of 0.018, solar zenith angle of 30°.

Figure S3.3. Scatter plot of MODIS TSS models in CLASS-III water for calcareous sand sediment, b_b/b ratio of 0.018, solar zenith angle of 30°.

Figure S3.4. Scatter plot of MODIS TSS models in CLASS-III water for red clay sediment, b_b/b ratio of 0.018, solar zenith angle of 30°.

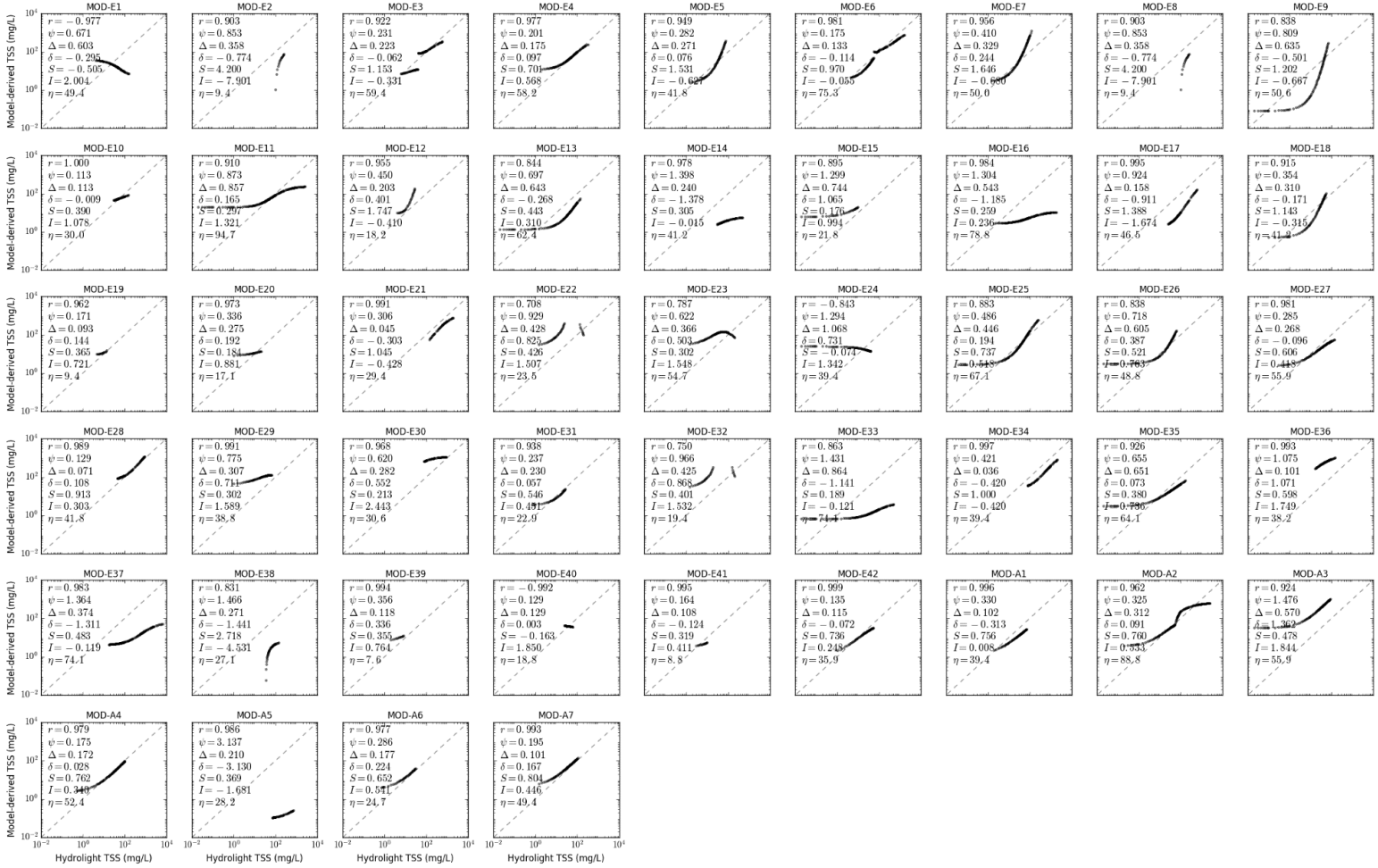

Figure S3.5. Scatter plot of MODIS TSS models in CLASS-III water for yellow clay sediment, b_b/b ratio of 0.018, solar zenith angle of 30°.

Figure S3.6. Scatter plot of MODIS TSS models in CLASS-III water for calcareous sand sediment, b_b/b ratio of 0.001, solar zenith angle of 30°.

Figure S3.7. Scatter plot of MODIS TSS models in CLASS-III water for calcareous sand sediment, b_b/b ratio of 0.01, solar zenith angle of 30°.

Figure S3.8. Scatter plot of MODIS TSS models in CLASS-III water for calcareous sand sediment, b_b/b ratio of 0.05, solar zenith angle of 30°.

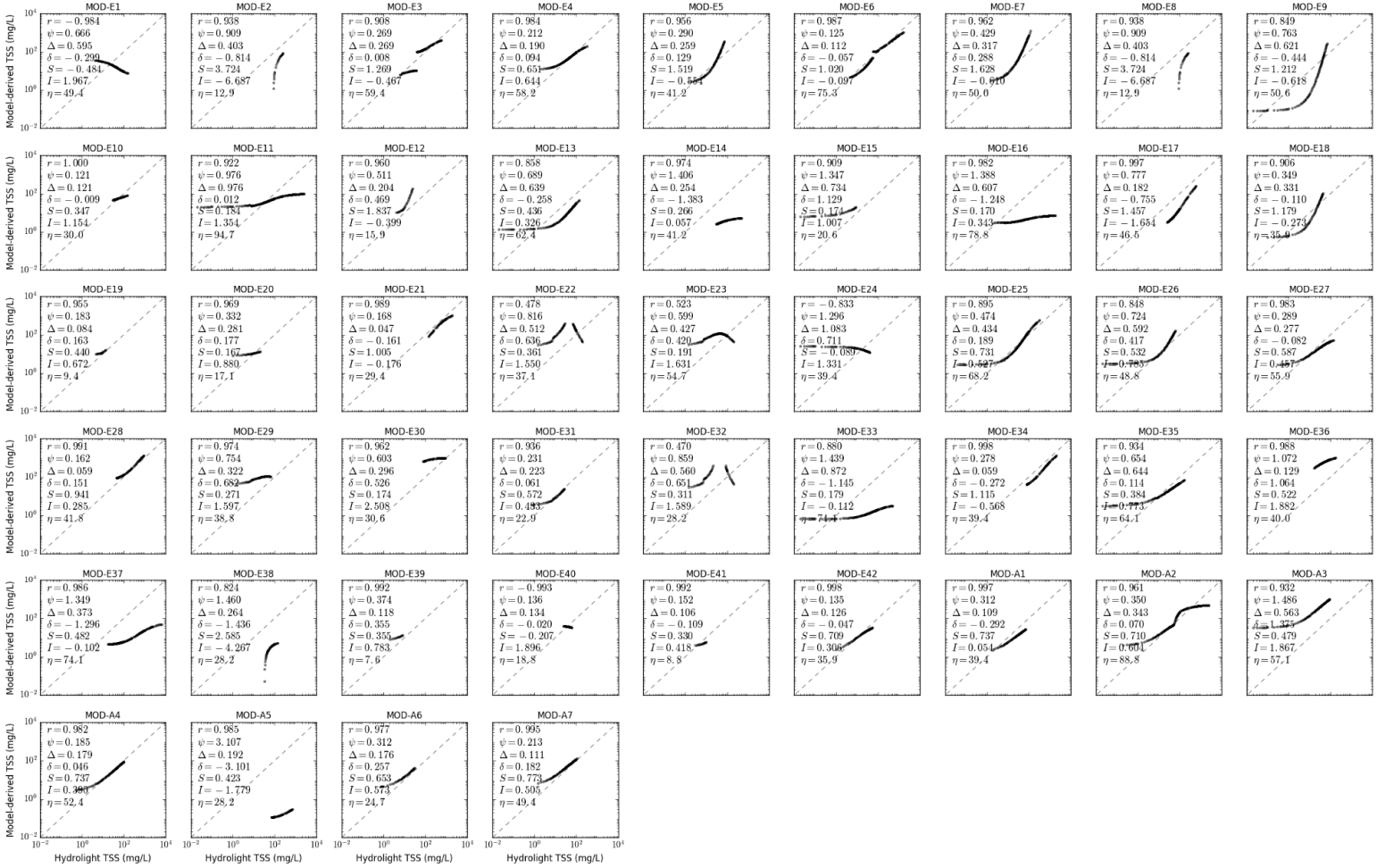

Figure S3.9. Scatter plot of MODIS TSS models in CLASS-III water for calcareous sand sediment, b_b/b ratio of 0.1, solar zenith angle of 30°.

Figure S3.10. Scatter plot of MODIS TSS models in CLASS-III water for calcareous sand sediment, b_b/b ratio of 0.018, solar zenith angle of 15°.

Figure S3.11. Scatter plot of MODIS TSS models in CLASS-III water for calcareous sand sediment, b_b/b ratio of 0.018, solar zenith angle of 45°.

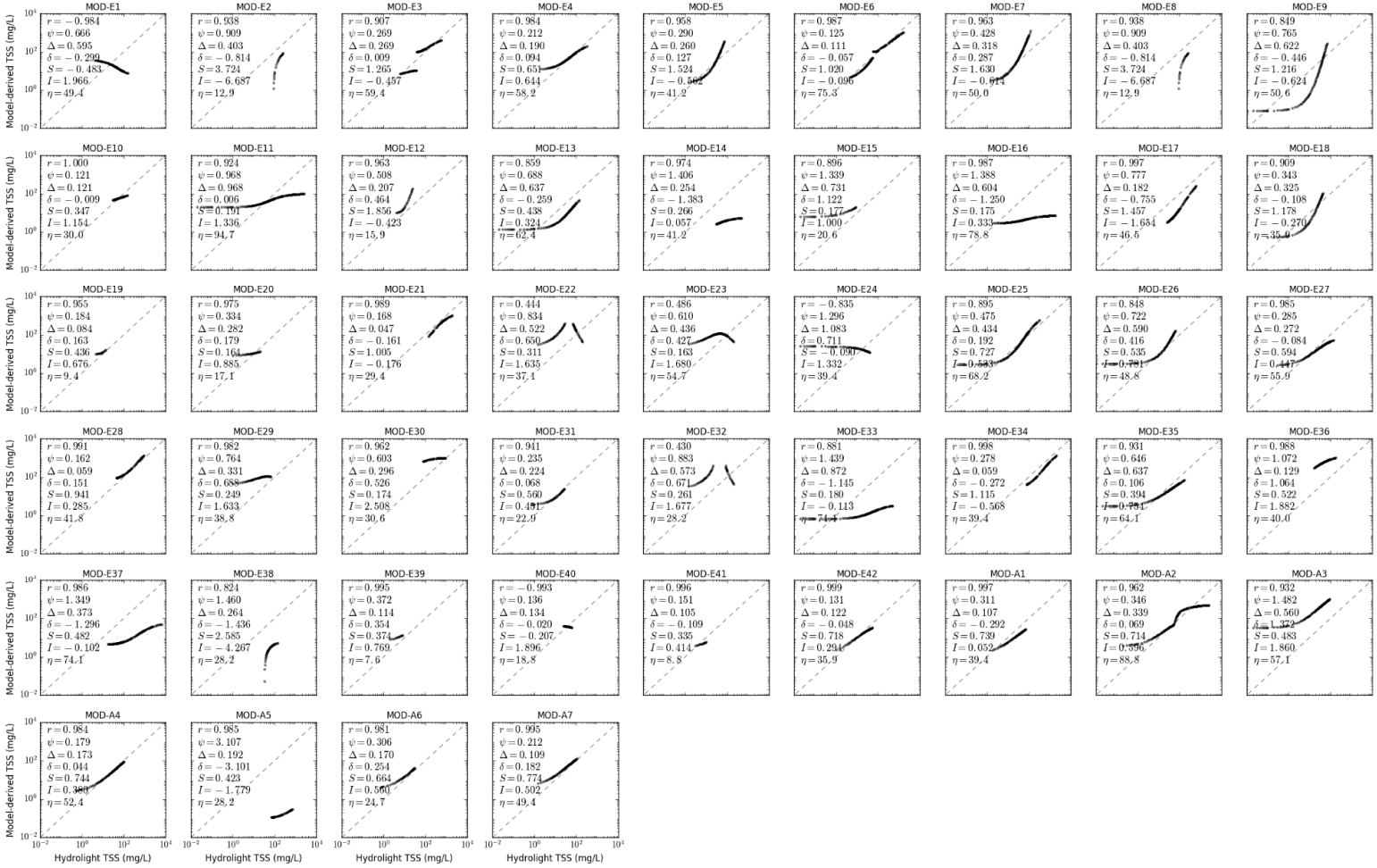

Figure S3.12. Scatter plot of MODIS TSS models in CLASS-III water for calcareous sand sediment, b_b/b ratio of 0.018, solar zenith angle of 60°.

Supplementary Materials S4. Scatter Plot of MODIS TSS Models for CLASS-IV Water

Figure S4.1. Scatter plot of MODIS TSS models in CLASS-IV water for brown earth sediment, b_b/b ratio of 0.018, solar zenith angle of 30°.

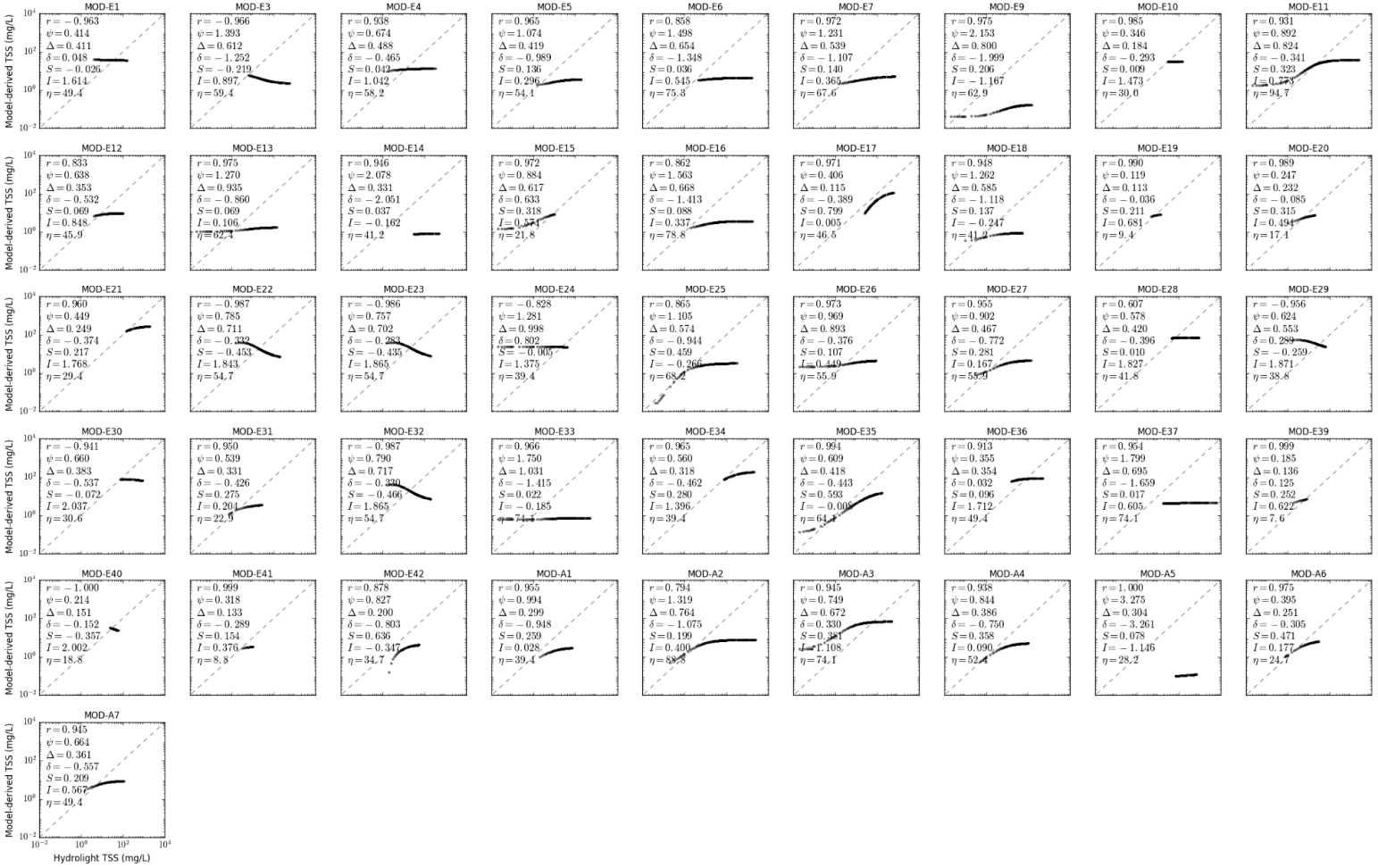

Figure S4.2. Scatter plot of MODIS TSS models in CLASS-IV water for bukata sediment, b_b/b ratio of 0.018, solar zenith angle of 30°.

Figure S4.3. Scatter plot of MODIS TSS models in CLASS-IV water for calcareous sand sediment, b_b/b ratio of 0.018, solar zenith angle of 30°.

Figure S4.4. Scatter plot of MODIS TSS models in CLASS-IV water for red clay sediment, b_b/b ratio of 0.018, solar zenith angle of 30°.

Figure S4.5. Scatter plot of MODIS TSS models in CLASS-IV water for yellow clay sediment, b_b/b ratio of 0.018, solar zenith angle of 30°.

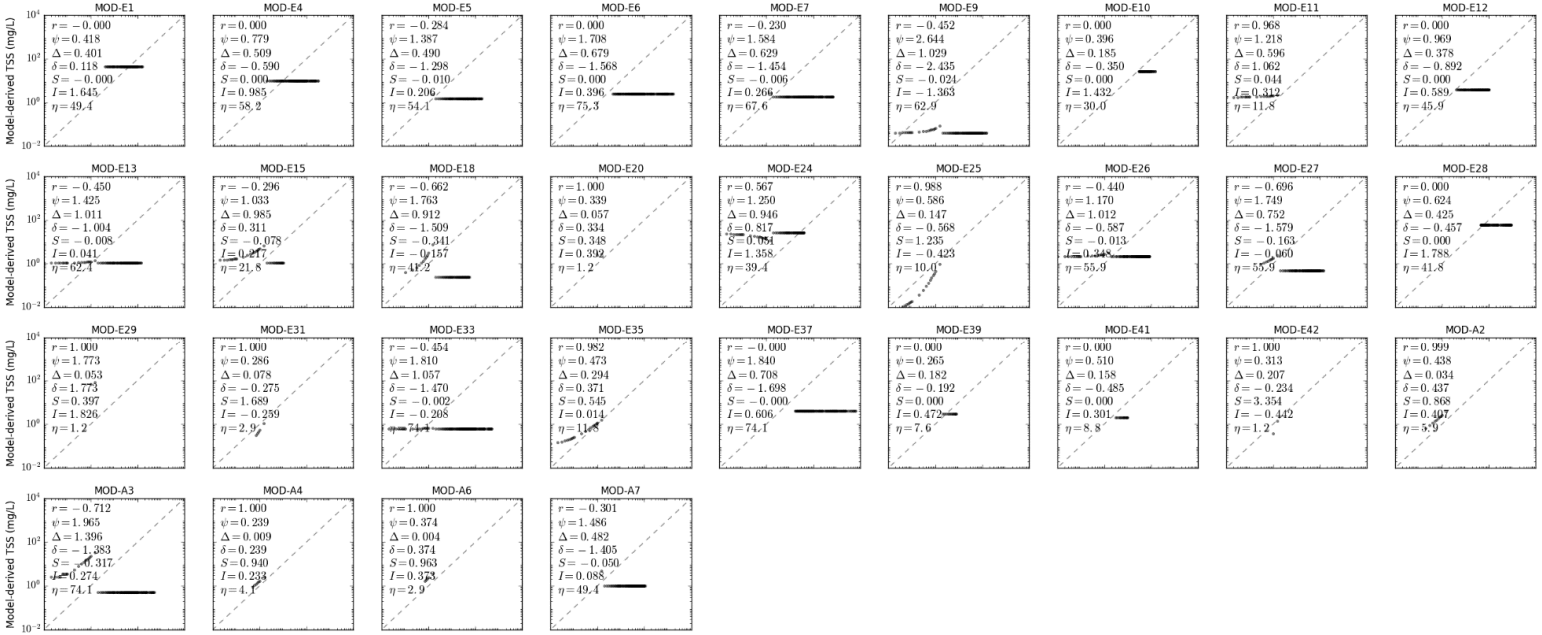

Figure S4.6. Scatter plot of MODIS TSS models in CLASS-IV water for calcareous sand sediment, b_b/b ratio of 0.001, solar zenith angle of 30°.

Figure S4.7. Scatter plot of MODIS TSS models in CLASS-IV water for calcareous sand sediment, b_b/b ratio of 0.01, solar zenith angle of 30°.

Figure S4.8. Scatter plot of MODIS TSS models in CLASS-IV water for calcareous sand sediment, b_b/b ratio of 0.05, solar zenith angle of 30°.

Figure S4.9. Scatter plot of MODIS TSS models in CLASS-IV water for calcareous sand sediment, b_b/b ratio of 0.1, solar zenith angle of 30°.

Figure S4.10. Scatter plot of MODIS TSS models in CLASS-IV water for calcareous sand sediment, b_b/b ratio of 0.018, solar zenith angle of 15°.

Figure S4.11. Scatter plot of MODIS TSS models in CLASS-IV water for calcareous sand sediment, b_b/b ratio of 0.018, solar zenith angle of 45°.

Figure S4.12. Scatter plot of MODIS TSS models in CLASS-IV water for calcareous sand sediment, b_b/b ratio of 0.018, solar zenith angle of 60°.

Supplementary Materials S5. Scatter Plot of MODIS TSS Models for CLASS-V Water

Figure S5.1. Scatter plot of MODIS TSS models in CLASS-V water for brown earth sediment, b_b/b ratio of 0.018, solar zenith angle of 30°.

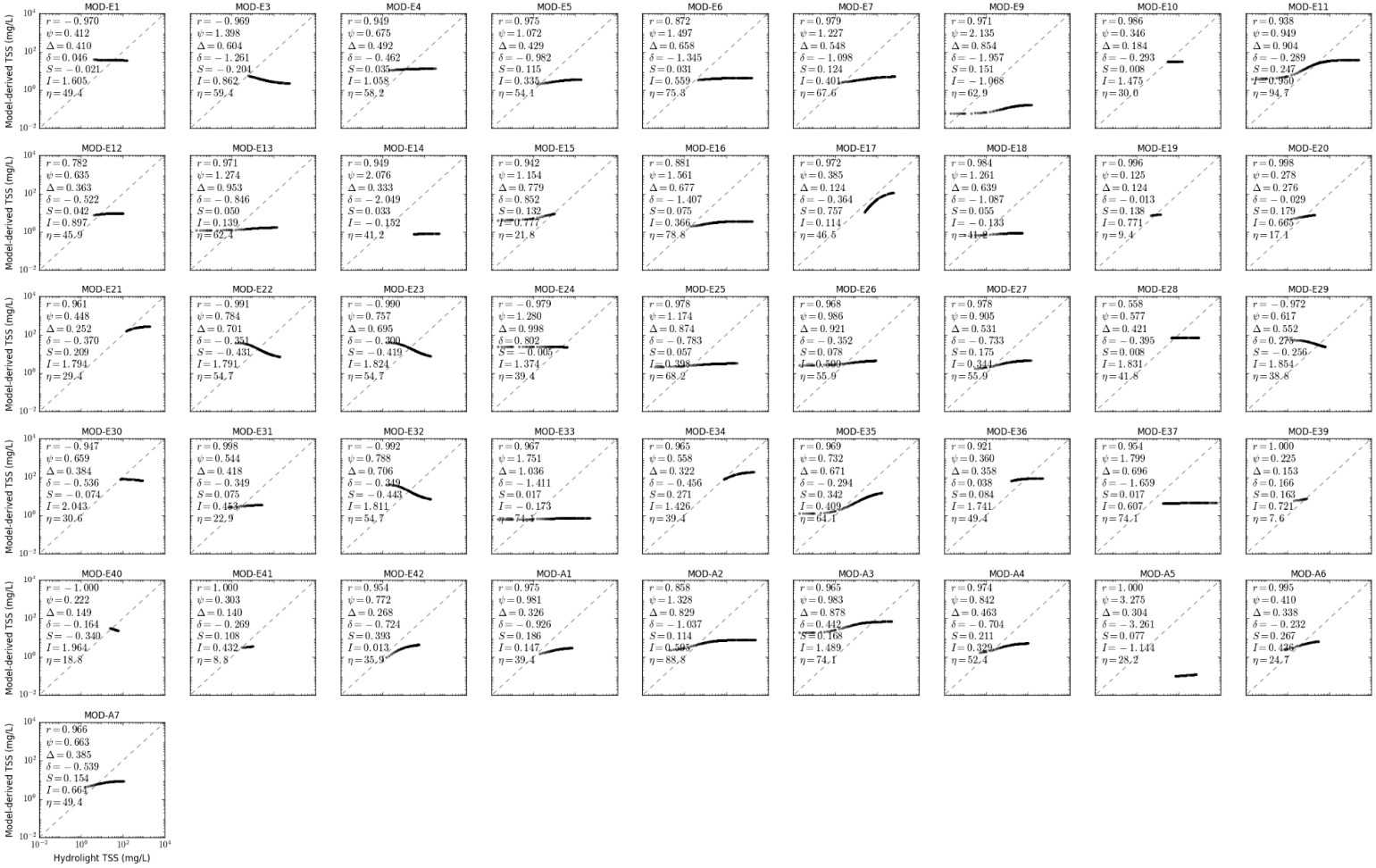

Figure S5.2. Scatter plot of MODIS TSS models in CLASS-V water for bukata sediment, b_b/b ratio of 0.018, solar zenith angle of 30°.

Figure S5.3. Scatter plot of MODIS TSS models in CLASS-V water for calcareous sand sediment, b_b/b ratio of 0.018, solar zenith angle of 30°.

Figure S5.4. Scatter plot of MODIS TSS models in CLASS-V water for red clay sediment, b_b/b ratio of 0.018, solar zenith angle of 30°.

Figure S5.5. Scatter plot of MODIS TSS models in CLASS-V water for yellow clay sediment, b_b/b ratio of 0.018, solar zenith angle of 30°.

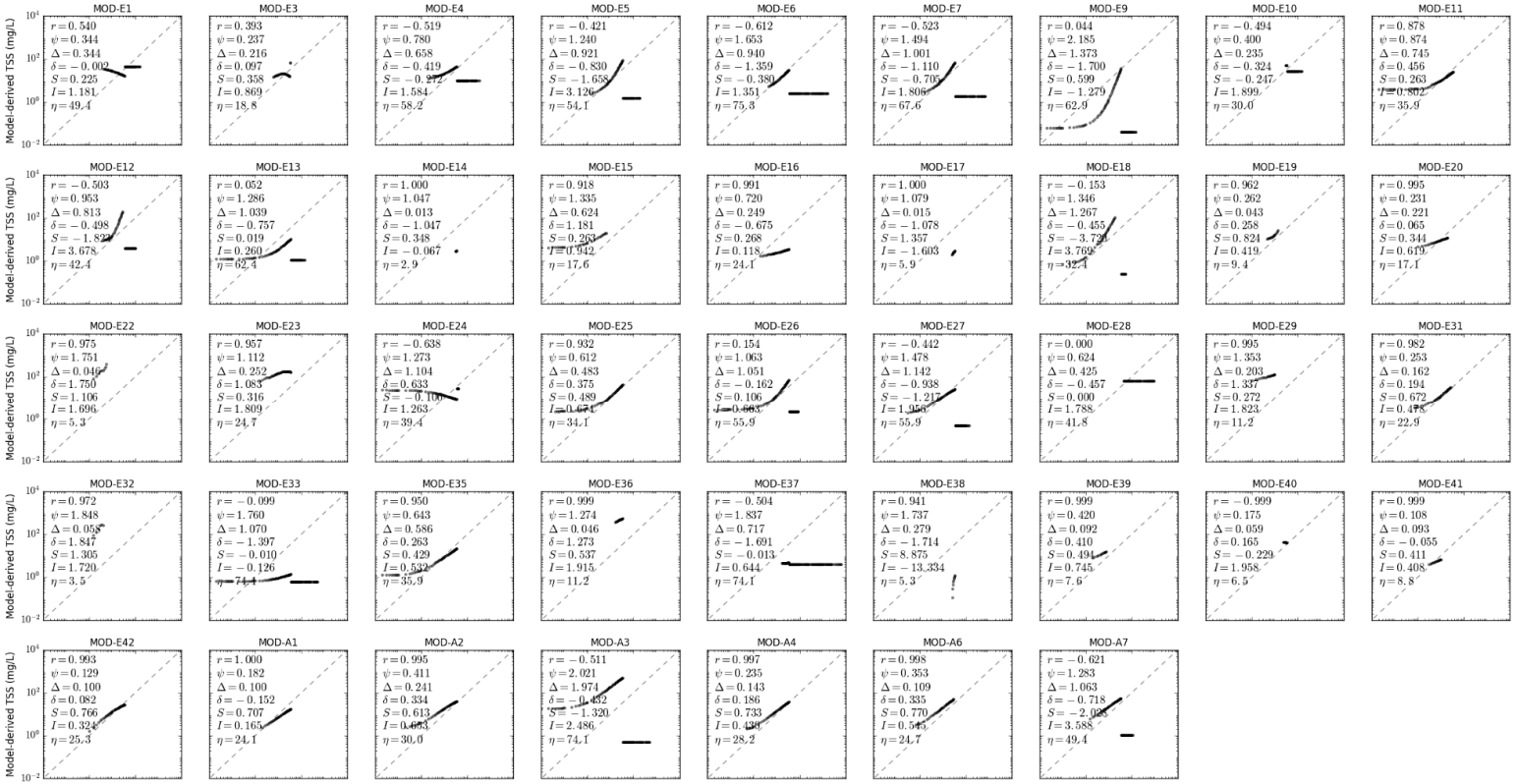

Figure S5.6. Scatter plot of MODIS TSS models in CLASS-V water for calcareous sand sediment, b_b/b ratio of 0.001, solar zenith angle of 30°.

Figure S5.7. Scatter plot of MODIS TSS models in CLASS-V water for calcareous sand sediment, b_b/b ratio of 0.01, solar zenith angle of 30°.

Figure S5.8. Scatter plot of MODIS TSS models in CLASS-V water for calcareous sand sediment, b_b/b ratio of 0.05, solar zenith angle of 30°.

Figure S5.9. Scatter plot of MODIS TSS models in CLASS-V water for calcareous sand sediment, b_b/b ratio of 0.1, solar zenith angle of 30°.

Figure S5.10. Scatter plot of MODIS TSS models in CLASS-V water for calcareous sand sediment, b_b/b ratio of 0.018, solar zenith angle of 15°.

Figure S5.11. Scatter plot of MODIS TSS models in CLASS-V water for calcareous sand sediment, b_b/b ratio of 0.018, solar zenith angle of 45°.

Figure S5.12. Scatter plot of MODIS TSS models in CLASS-5V water for calcareous sand sediment, b_b/b ratio of 0.018, solar zenith angle of 60°.

Supplementary Materials S6. Scatter Plot of LANDSAT TSS Models for CLASS-I Water

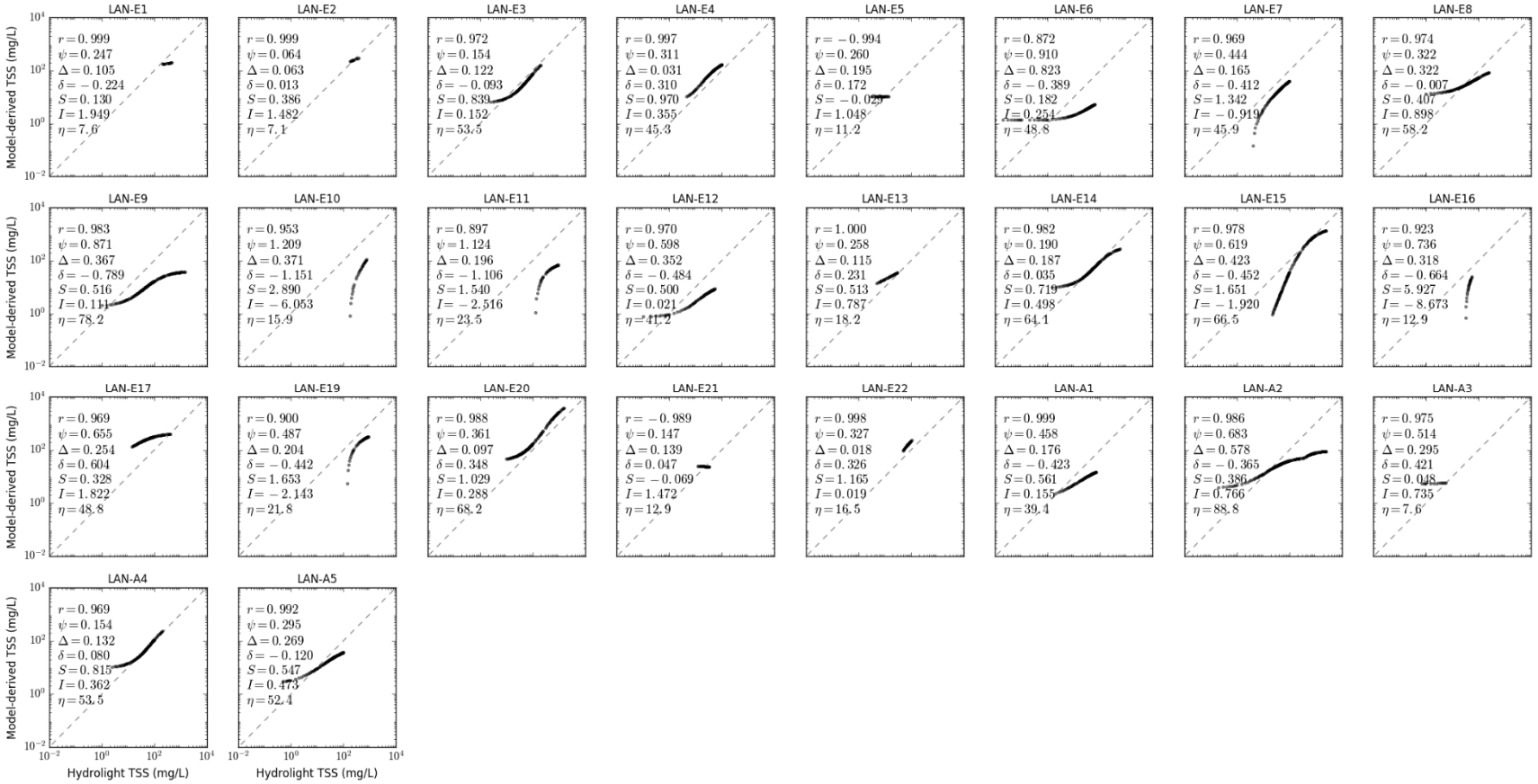

Figure S6.1. Scatter plot of LANDSAT TSS models in CLASS-I water for brown earth sediment, b_b/b ratio of 0.018, solar zenith angle of 30°.

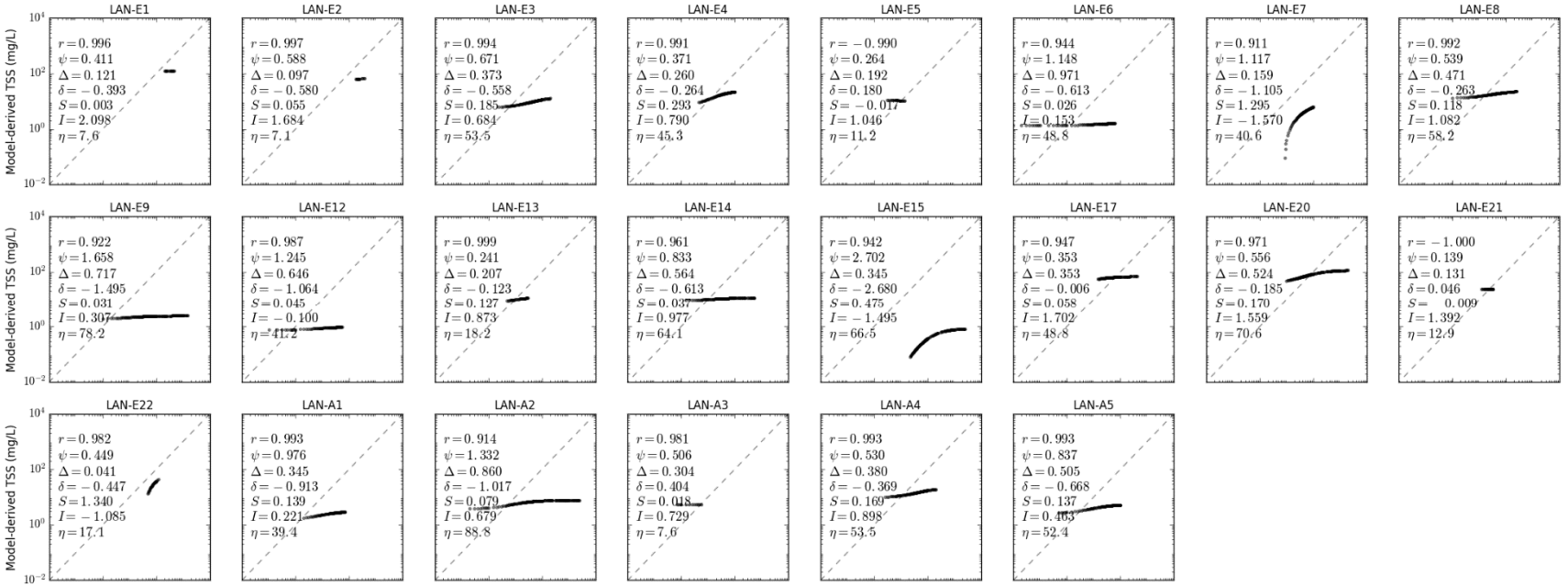

Figure S6.2. Scatter plot of LANDSAT TSS models in CLASS-I water for bukata sediment, b_b/b ratio of 0.018, solar zenith angle of 30°.

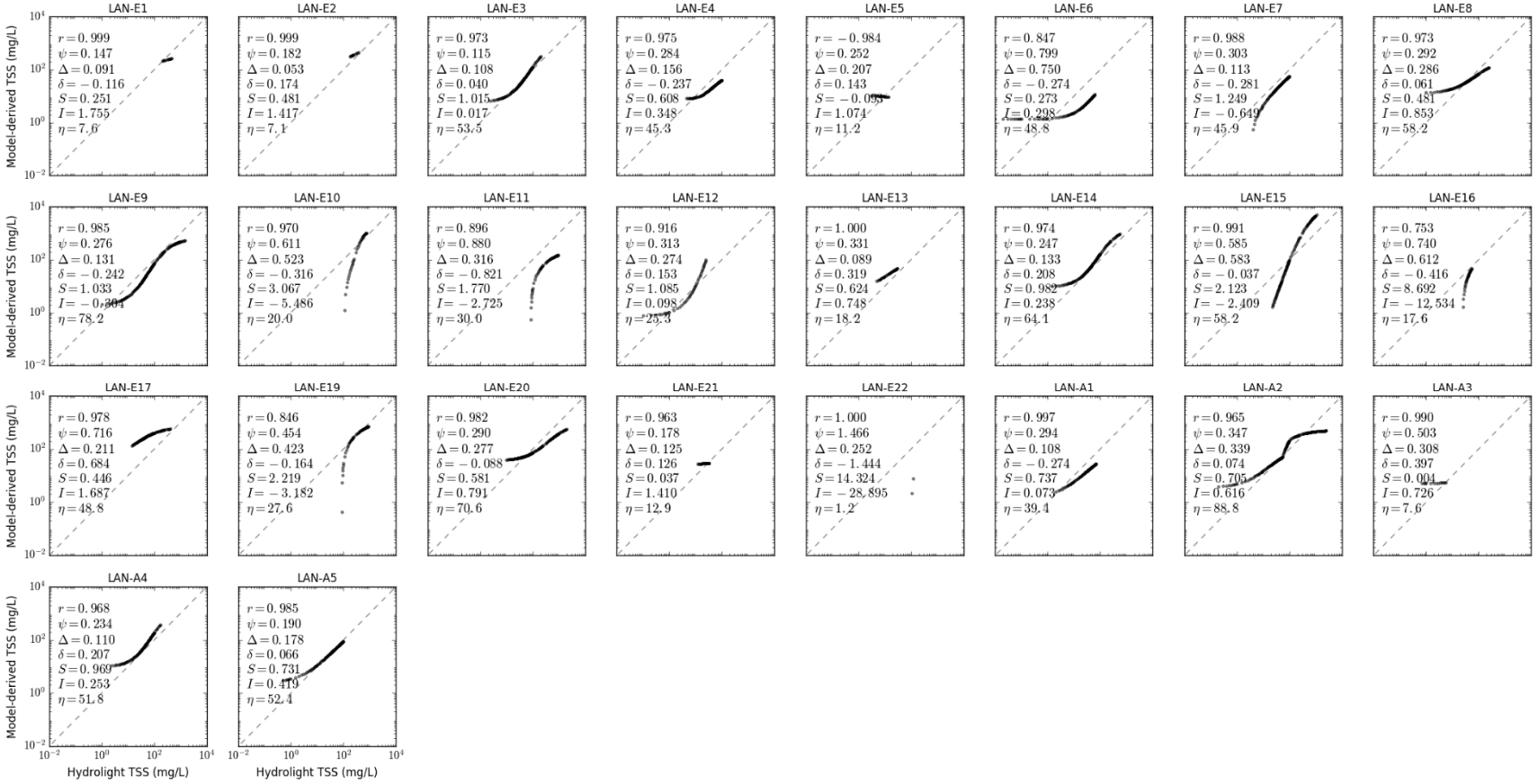

Figure S6.3. Scatter plot of LANDSAT TSS models in CLASS-I water for calcareous sand sediment, b_b/b ratio of 0.018, solar zenith angle of 30°.

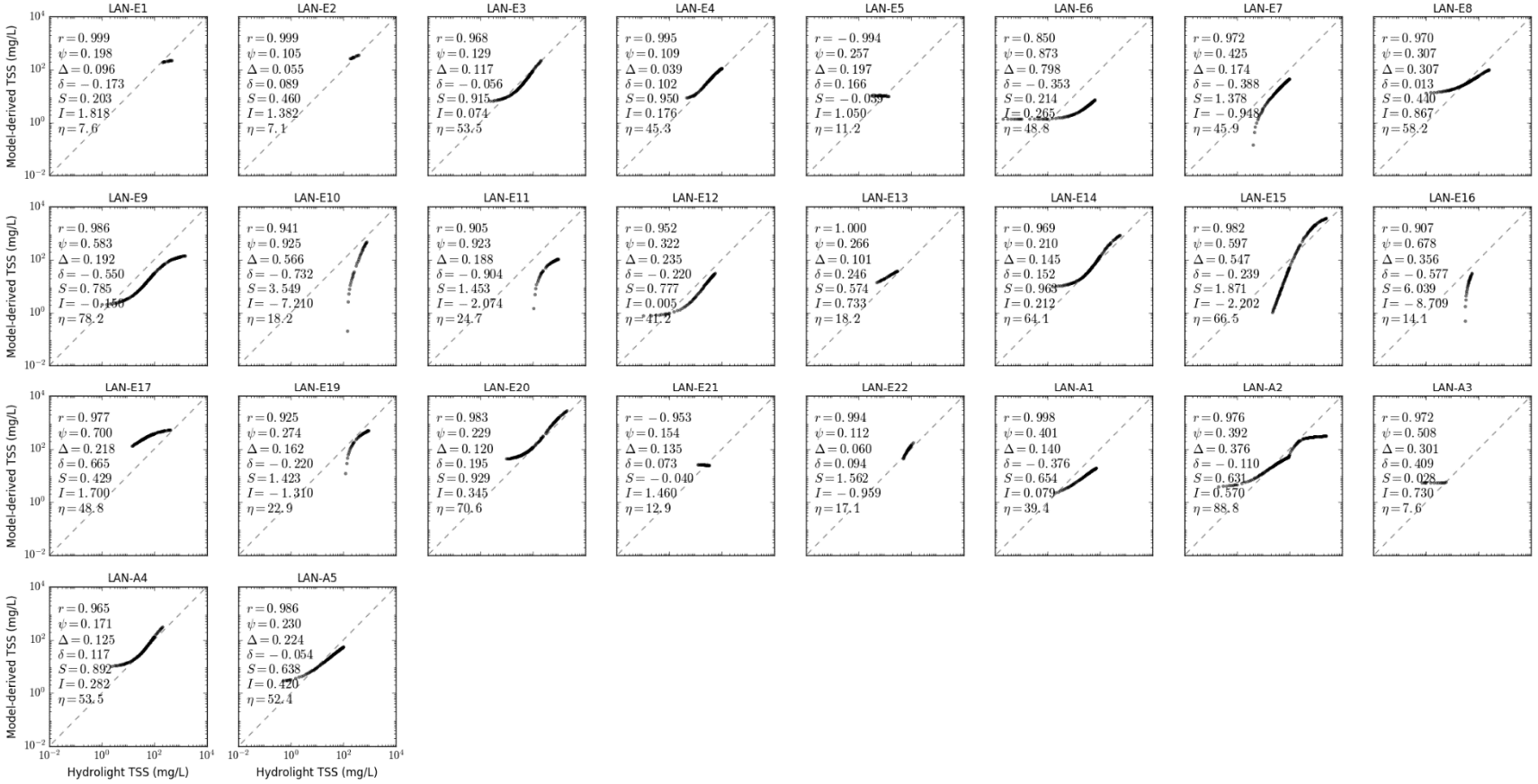

Figure S6.4. Scatter plot of LANDSAT TSS models in CLASS-I water for red clay sediment, b_b/b ratio of 0.018, solar zenith angle of 30°.

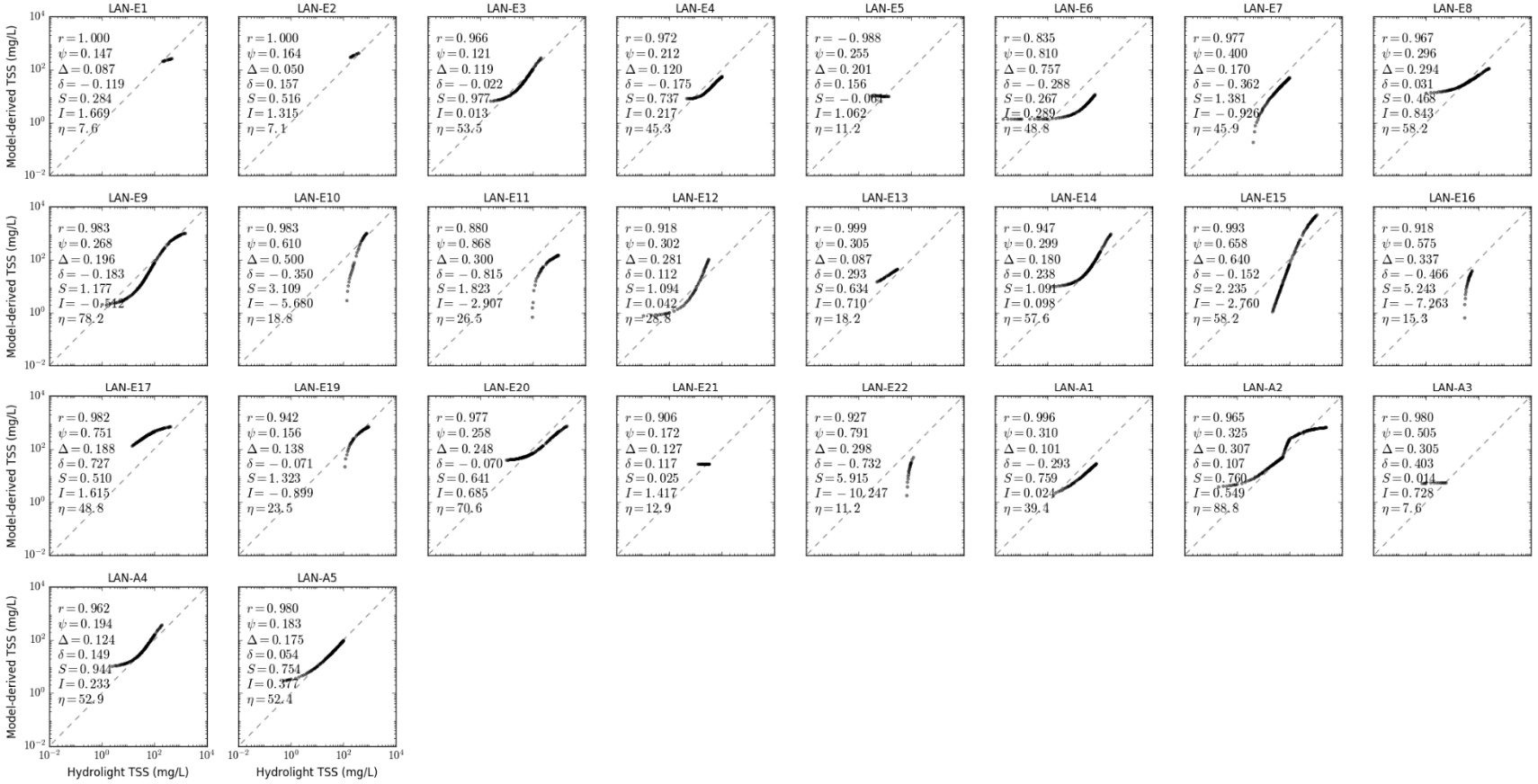

Figure S6.5. Scatter plot of LANDSAT TSS models in CLASS-I water for yellow clay sediment, b_b/b ratio of 0.018, solar zenith angle of 30°.

Figure S6.6. Scatter plot of LANDSAT TSS models in CLASS-I water for calcareous sand sediment, b_b/b ratio of 0.001, solar zenith angle of 30°.

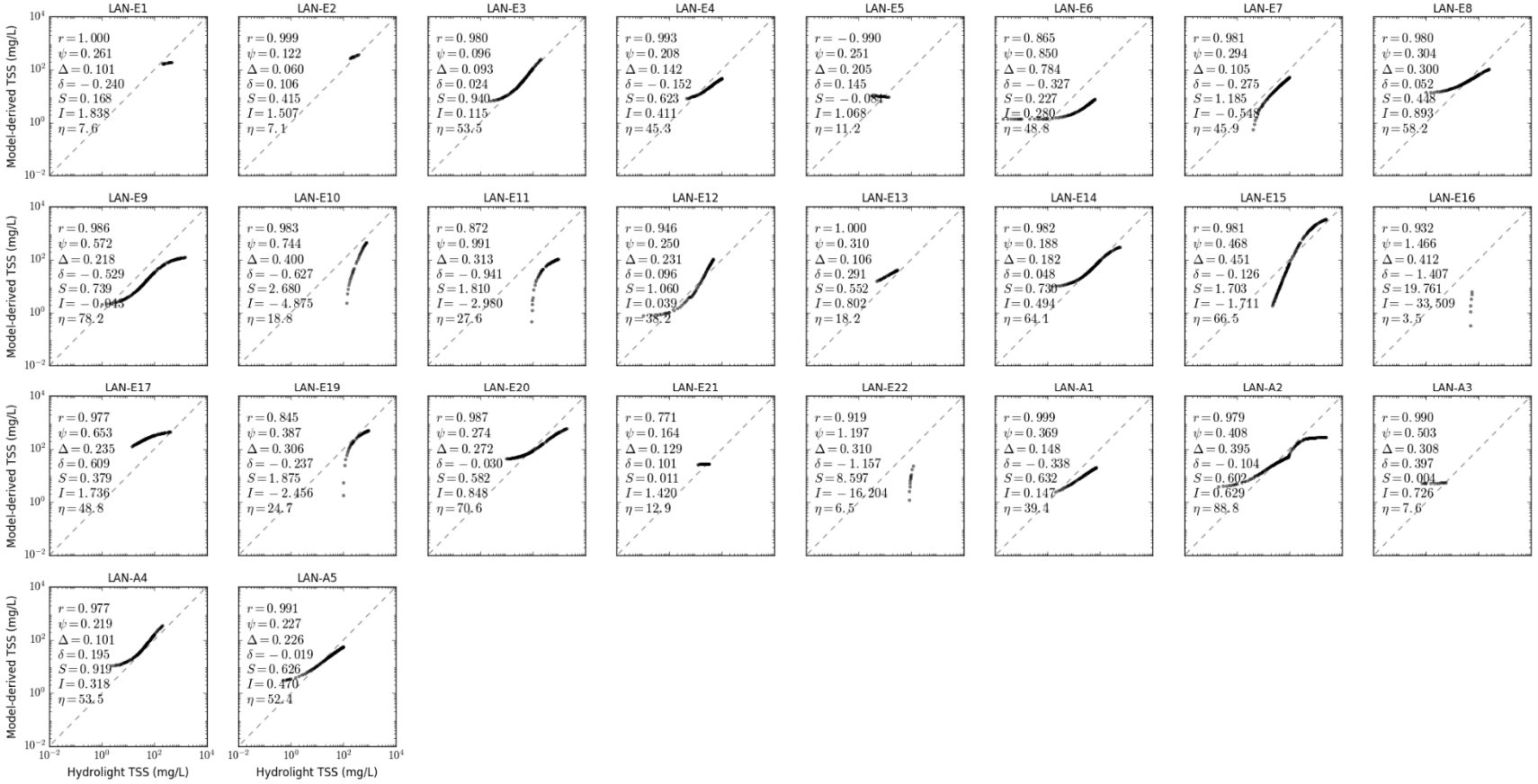

Figure S6.7. Scatter plot of LANDSAT TSS models in CLASS-I water for calcareous sand sediment, b_b/b ratio of 0.01, solar zenith angle of 30°.

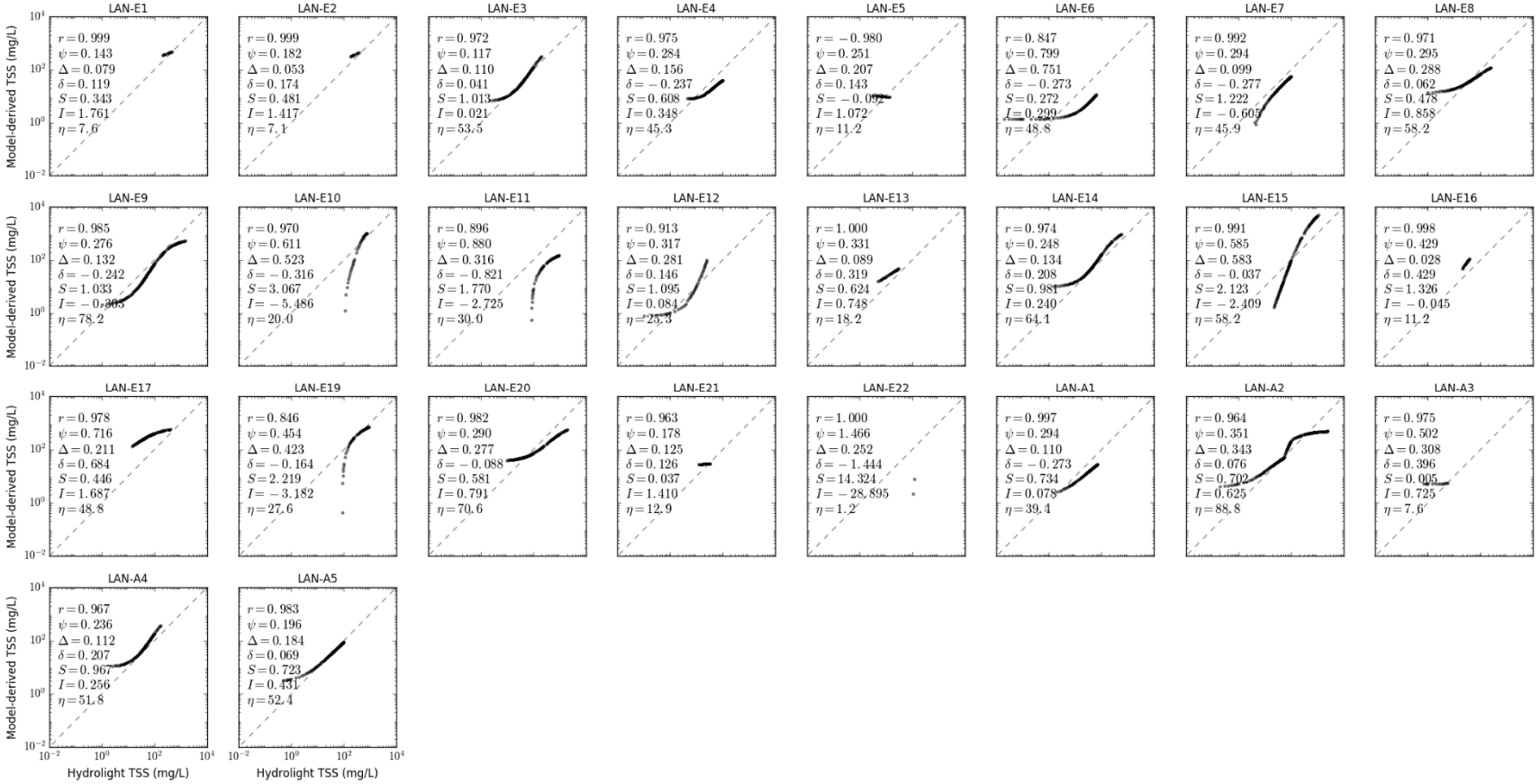

Figure S6.8. Scatter plot of LANDSAT TSS models in CLASS-I water for calcareous sand sediment, b_b/b ratio of 0.05, solar zenith angle of 30°.

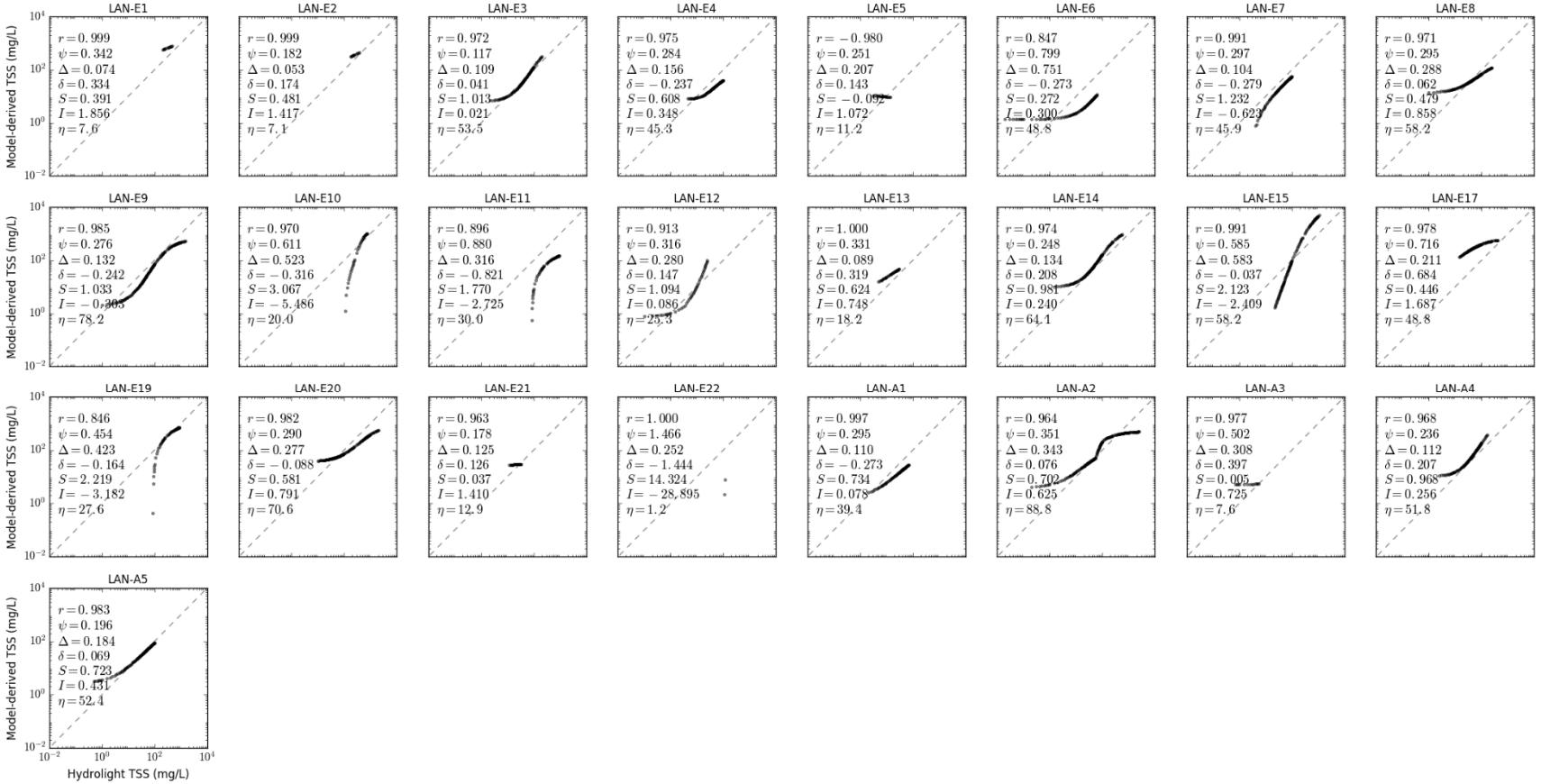

Figure S6.9. Scatter plot of LANDSAT TSS models in CLASS-I water for calcareous sand sediment, b_b/b ratio of 0.1, solar zenith angle of 30°.

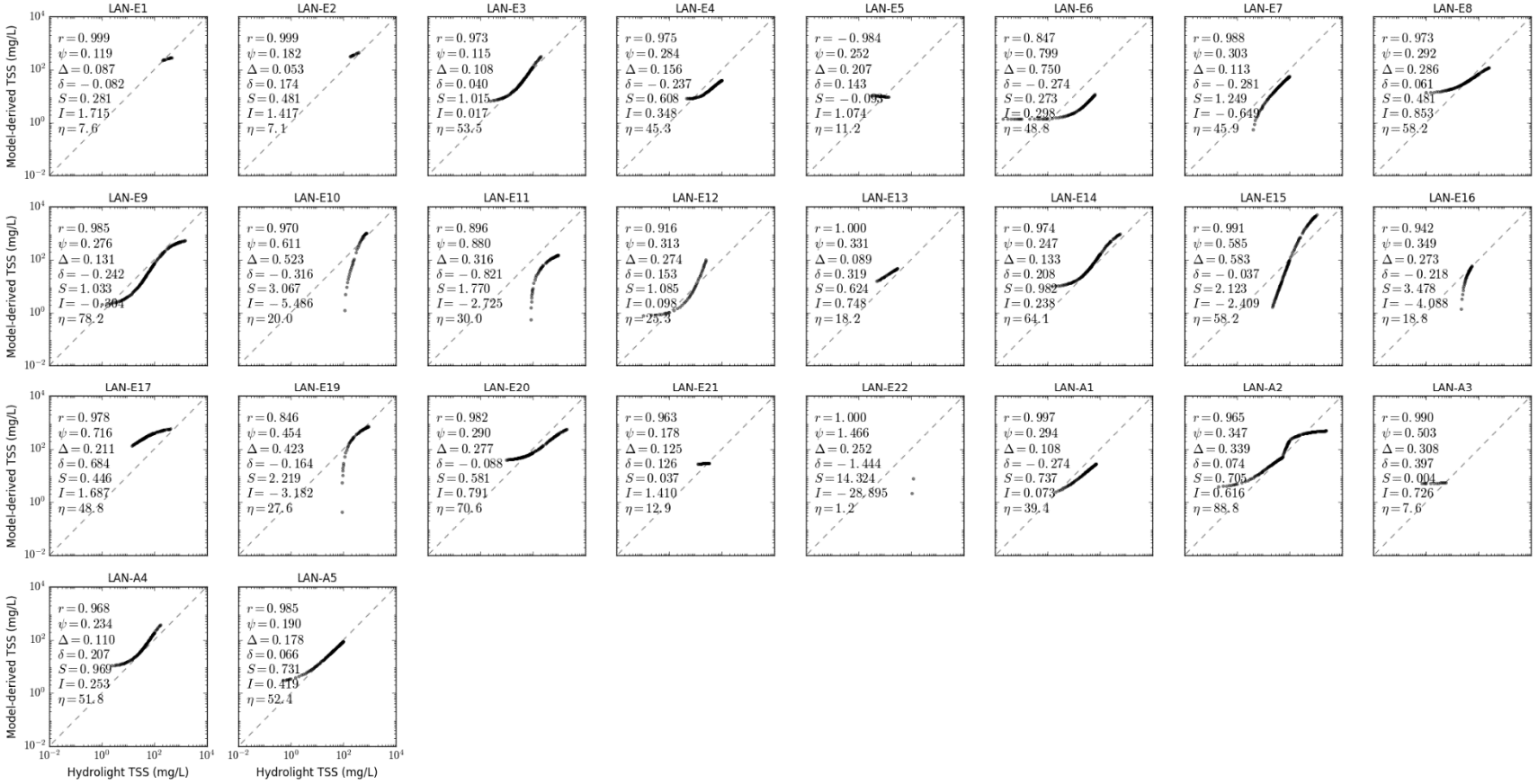

Figure S6.10. Scatter plot of LANDSAT TSS models in CLASS-I water for calcareous sand sediment, b_b/b ratio of 0.018, solar zenith angle of 15°.

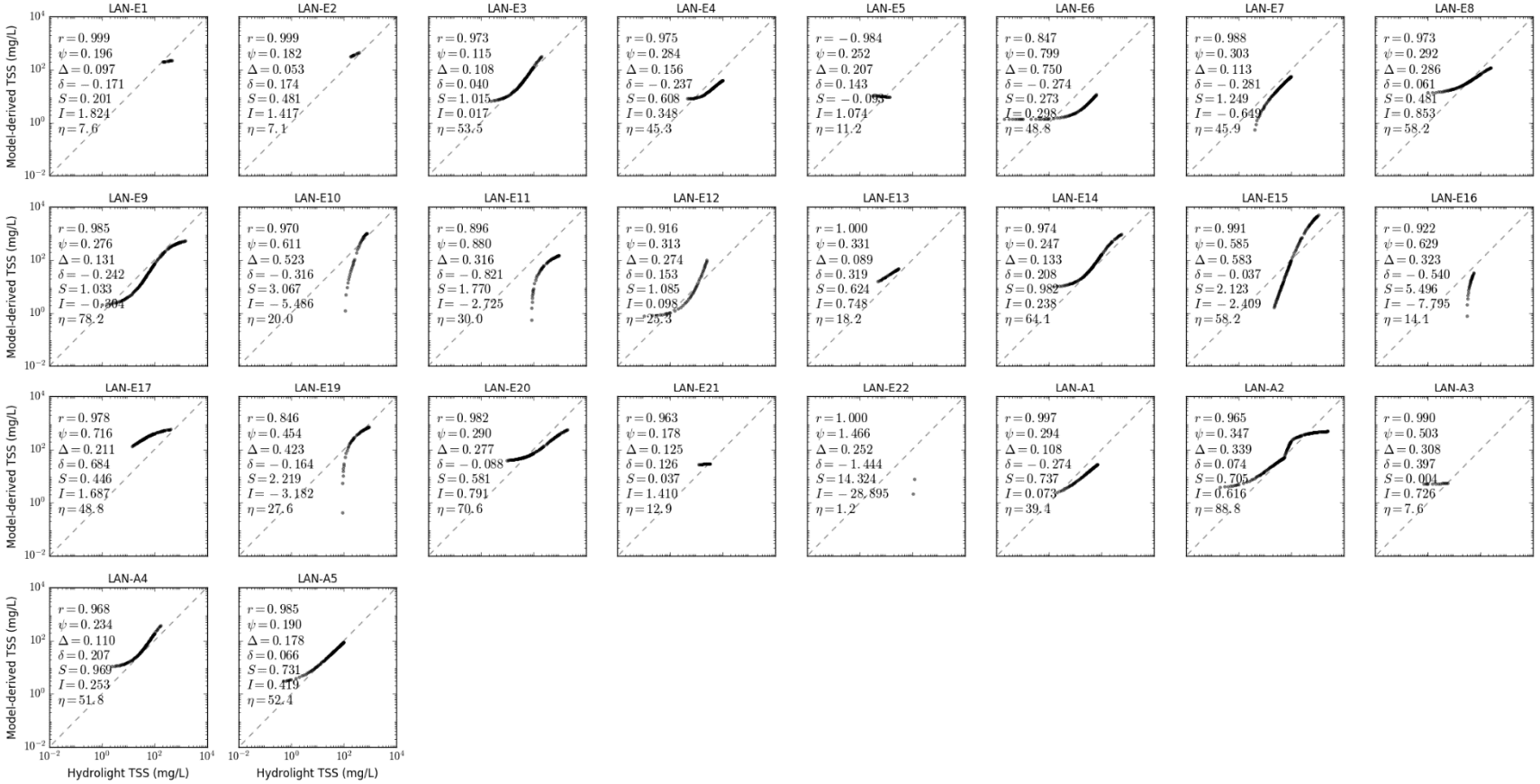

Figure S6.11. Scatter plot of LANDSAT TSS models in CLASS-I water for calcareous sand sediment, b_b/b ratio of 0.018, solar zenith angle of 45°.

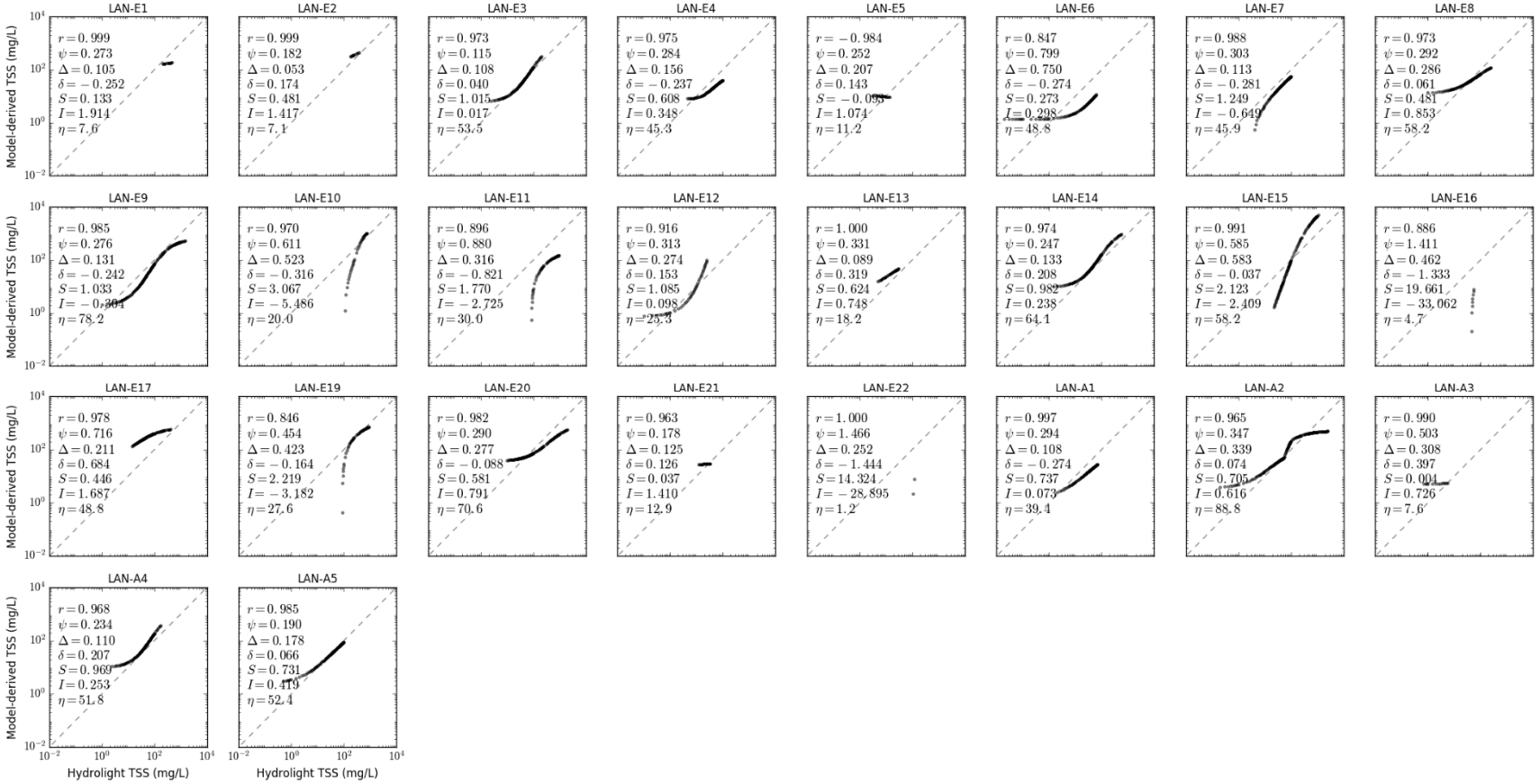

Figure S6.12. Scatter plot of LANDSAT TSS models in CLASS-I water for calcareous sand sediment, b_b/b ratio of 0.018, solar zenith angle of 60°.

Supplementary Materials S7. Scatter Plot of LANDSAT TSS Models for CLASS-II Water

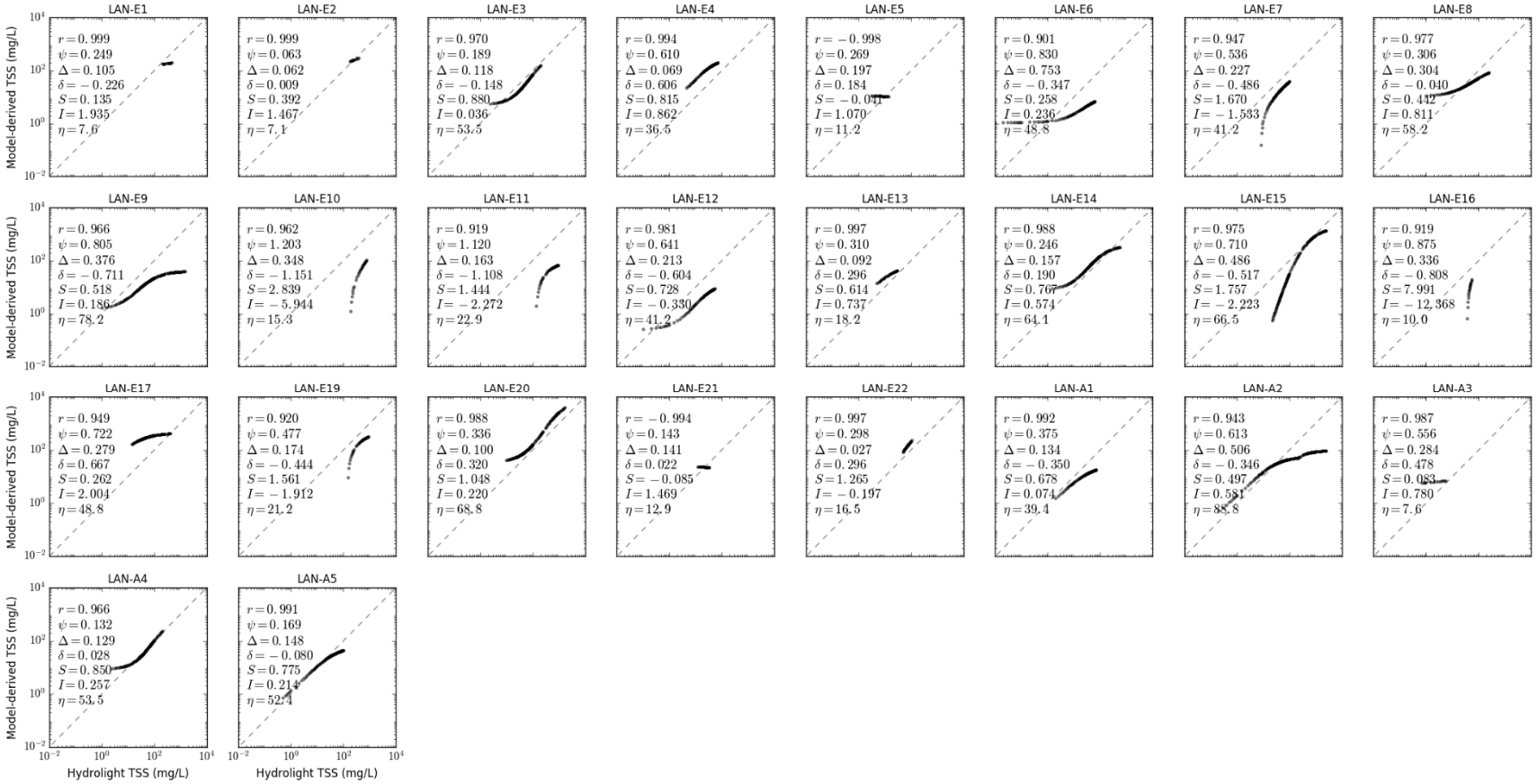

Figure S7.1. Scatter plot of LANDSAT TSS models in CLASS-II water for brown earth sediment, b_b/b ratio of 0.018, solar zenith angle of 30°.

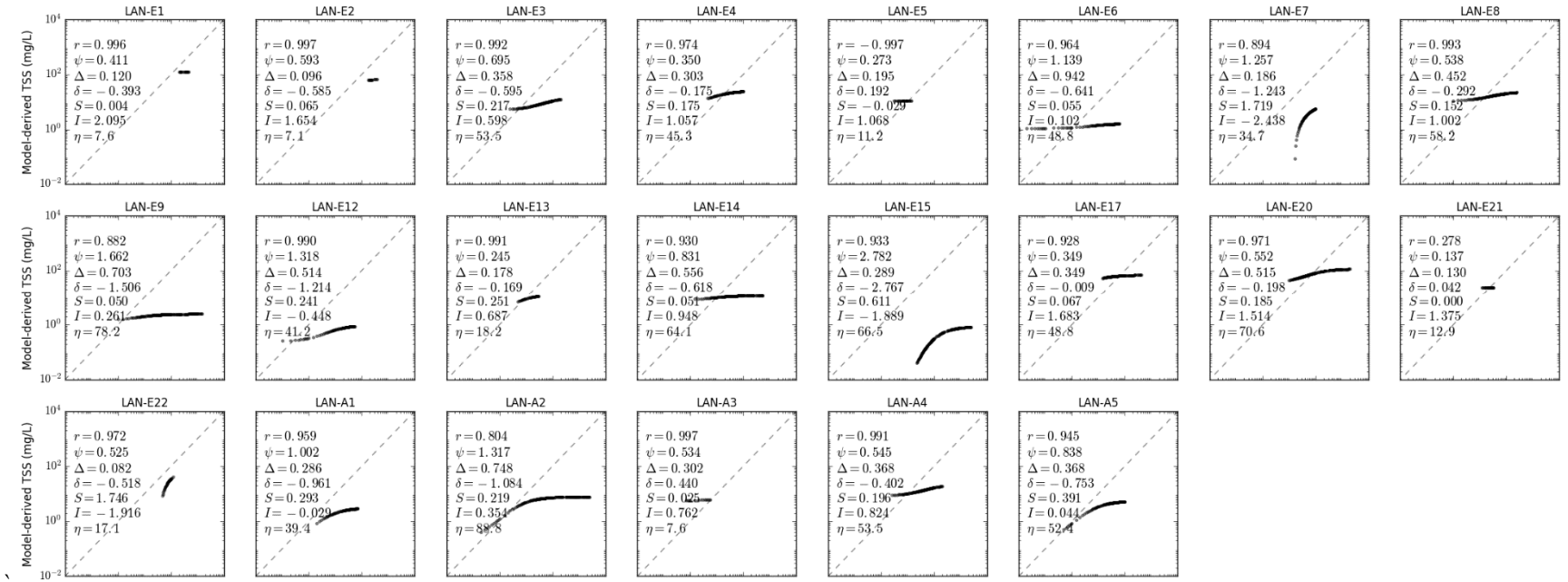

Figure S7.2. Scatter plot of LANDSAT TSS models in CLASS-II water for bukata sediment, b_b/b ratio of 0.018, solar zenith angle of 30°.

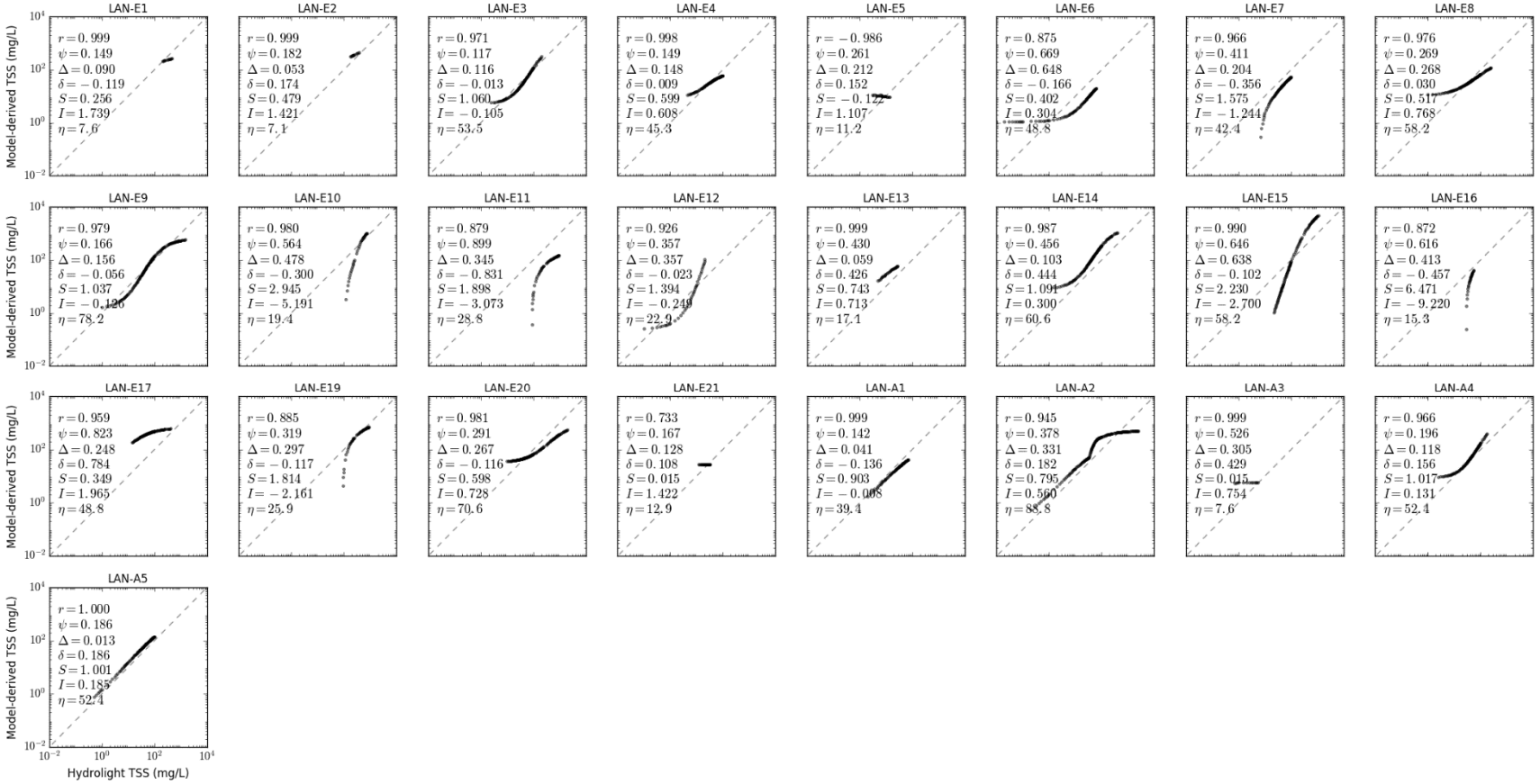

Figure S7.3. Scatter plot of LANDSAT TSS models in CLASS-II water for calcareous sand sediment, b_b/b ratio of 0.018, solar zenith angle of 30°.

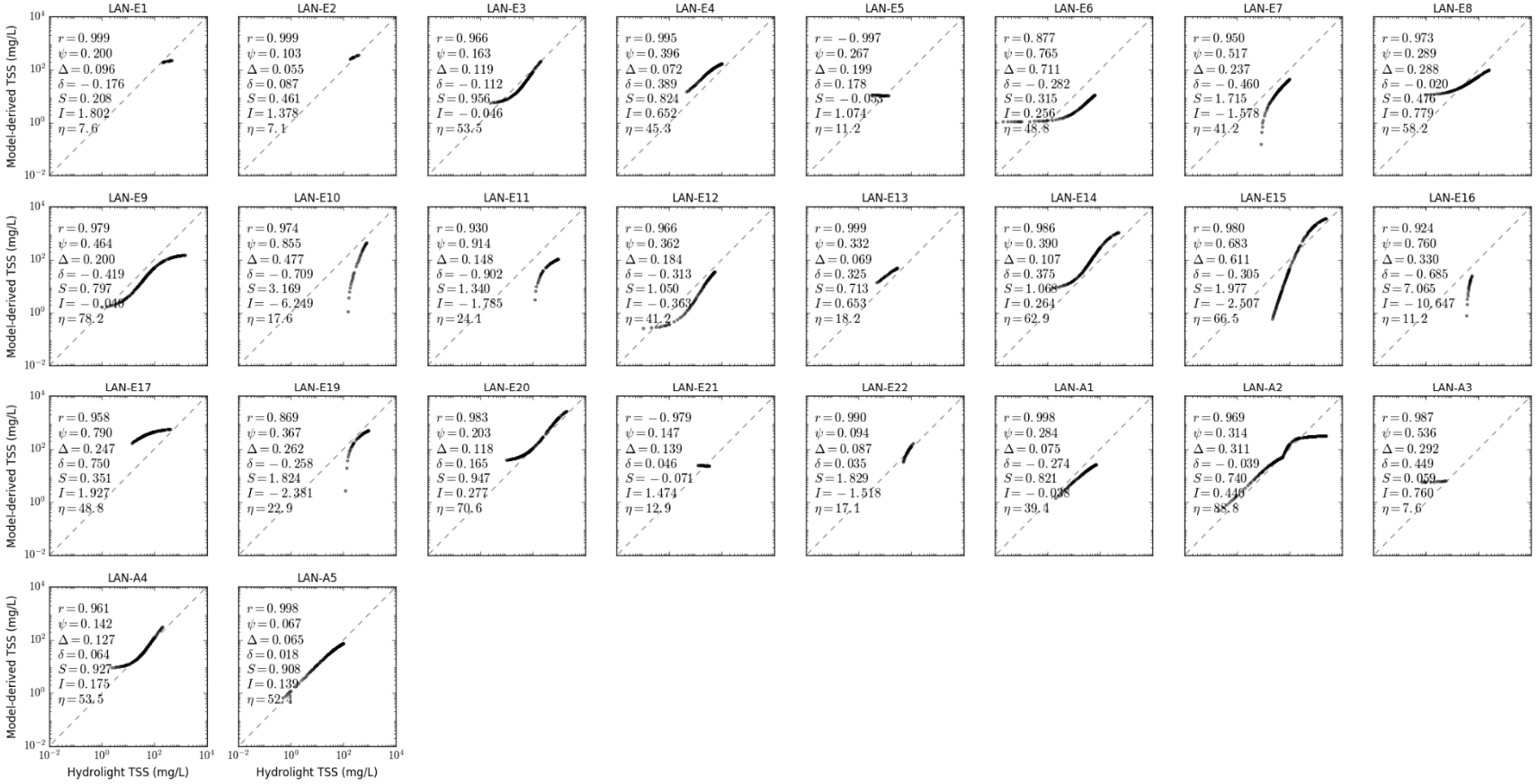

Figure S7.4. Scatter plot of LANDSAT TSS models in CLASS-II water for red clay sediment, b_b/b ratio of 0.018, solar zenith angle of 30°.

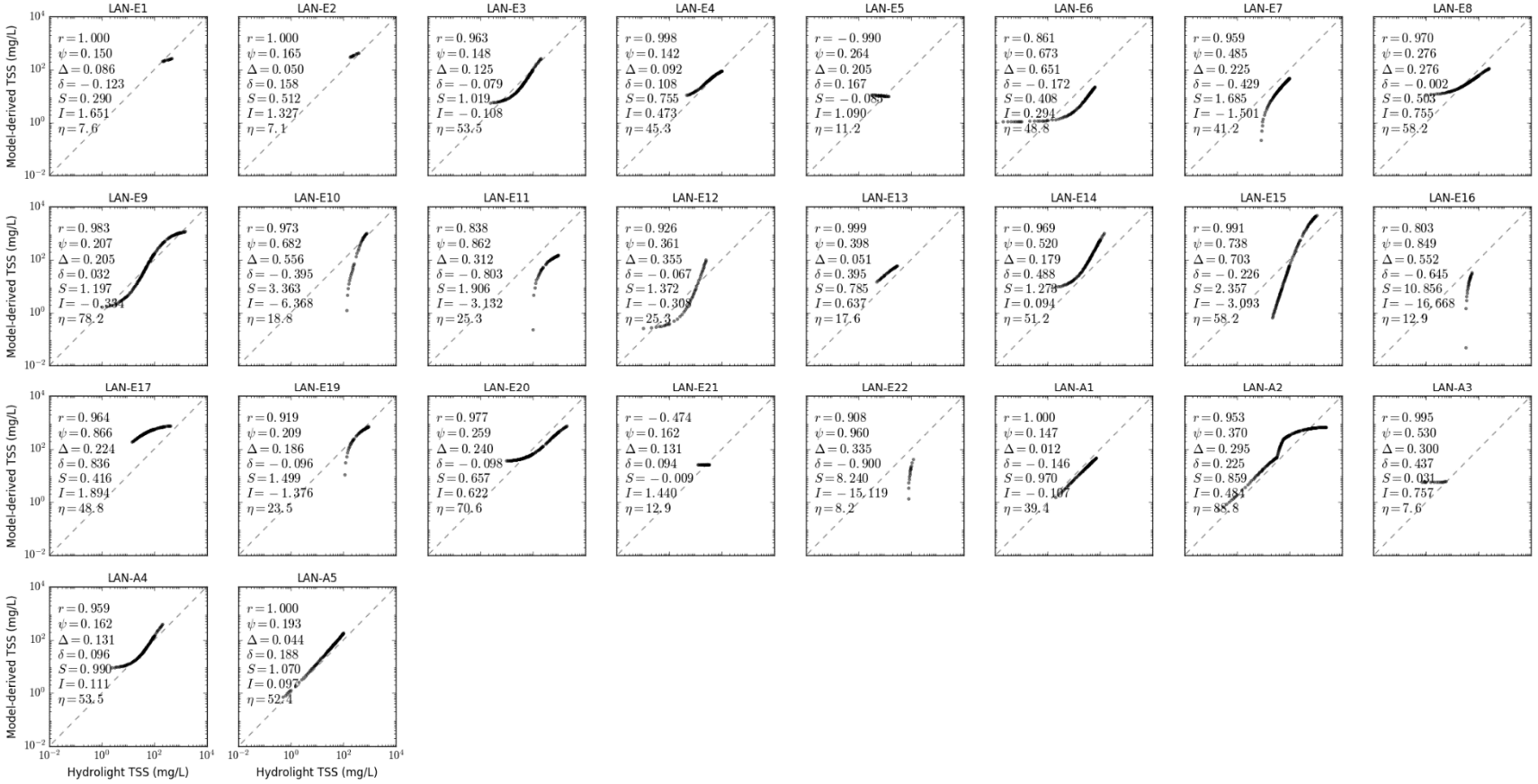

Figure S7.5. Scatter plot of LANDSAT TSS models in CLASS-II water for yellow clay sediment, b_b/b ratio of 0.018, solar zenith angle of 30°.

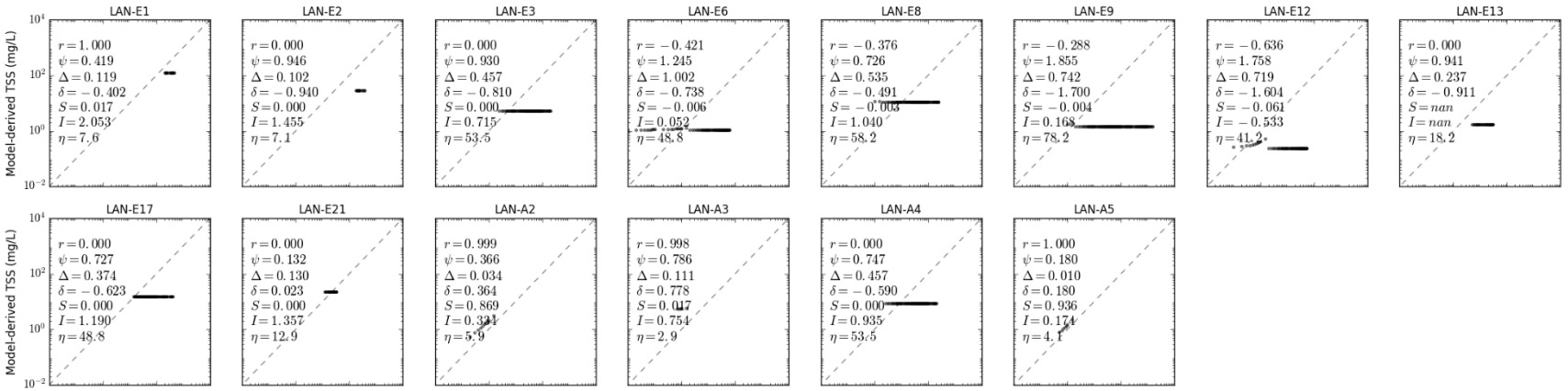

Figure S7.6. Scatter plot of LANDSAT TSS models in CLASS-II water for calcareous sand sediment, b_b/b ratio of 0.001, solar zenith angle of 30°.

Figure S7.7. Scatter plot of LANDSAT TSS models in CLASS-II water for calcareous sand sediment, b_b/b ratio of 0.01, solar zenith angle of 30°.

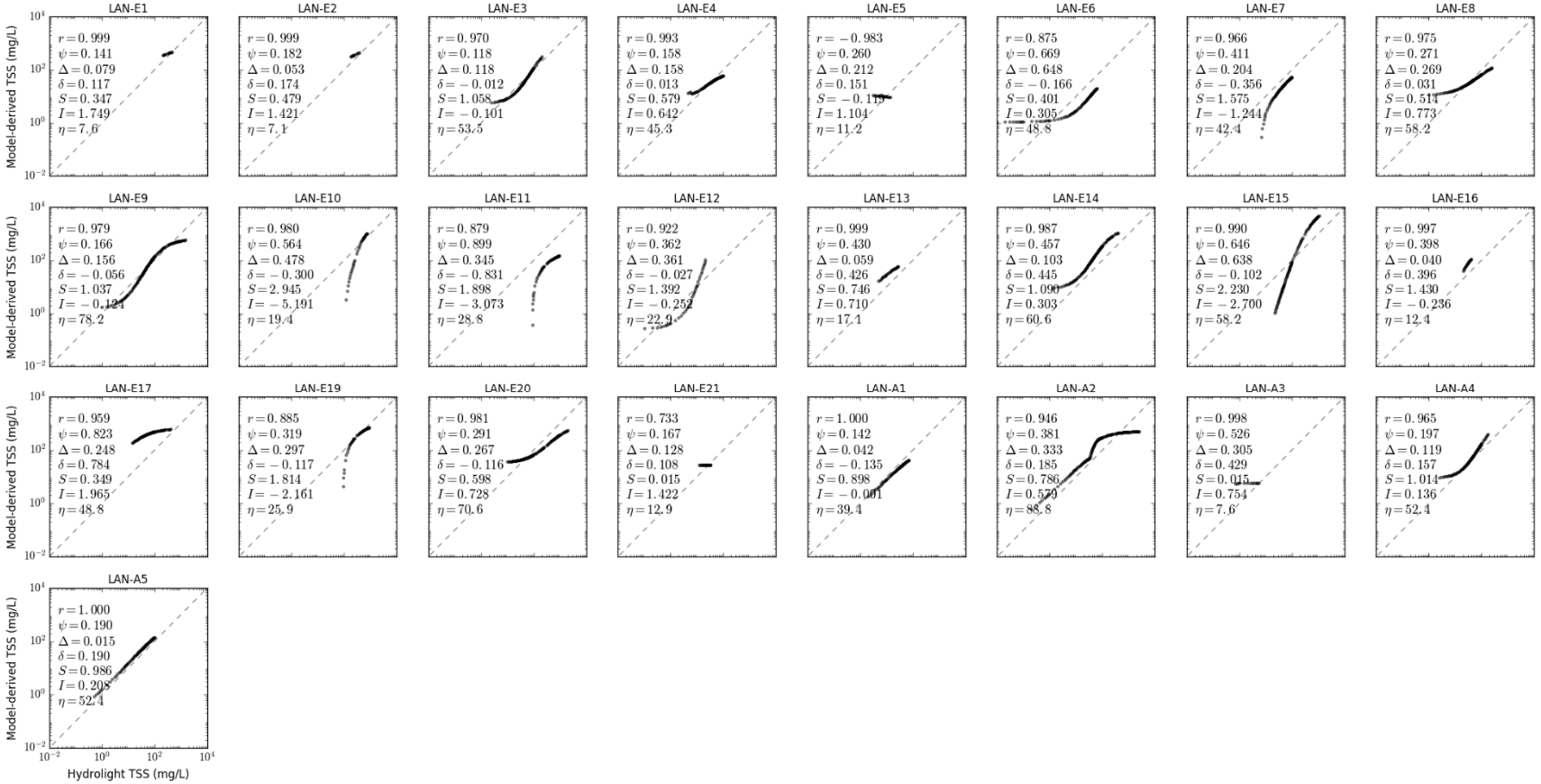

Figure S7.8. Scatter plot of LANDSAT TSS models in CLASS-II water for calcareous sand sediment, b_b/b ratio of 0.05, solar zenith angle of 30°.

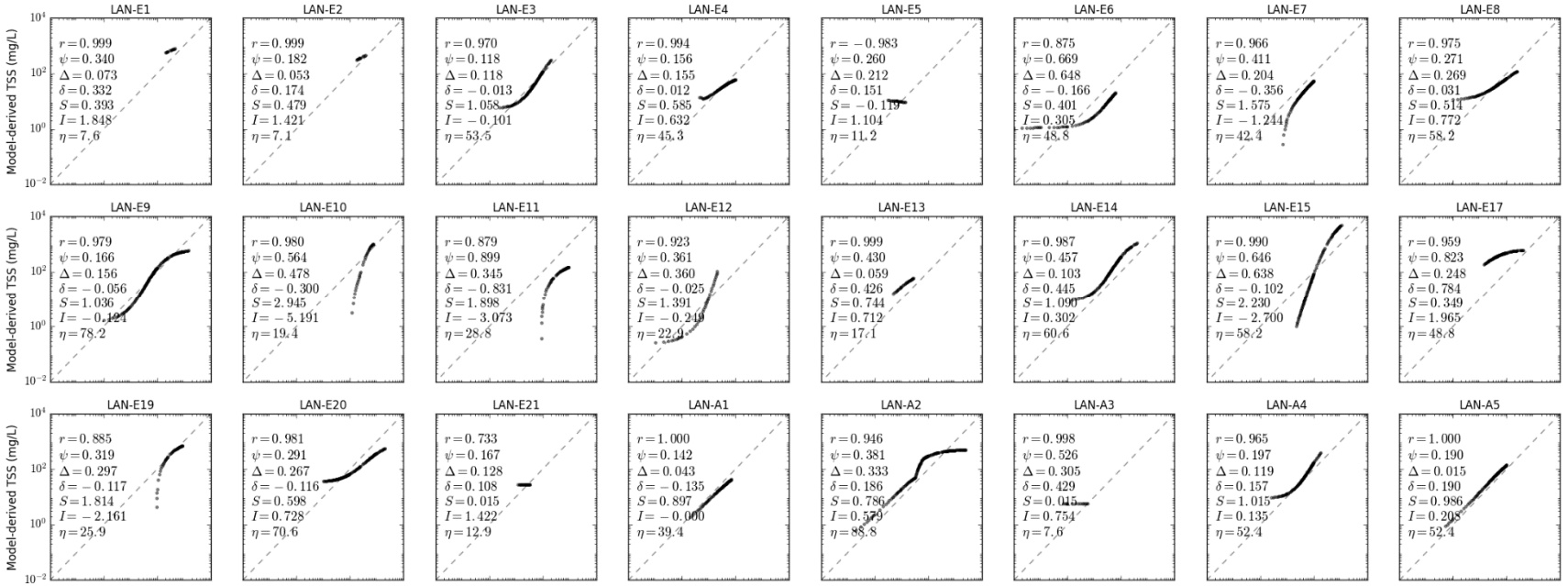

Figure S7.9. Scatter plot of LANDSAT TSS models in CLASS-II water for calcareous sand sediment, b_b/b ratio of 0.1, solar zenith angle of 30°.

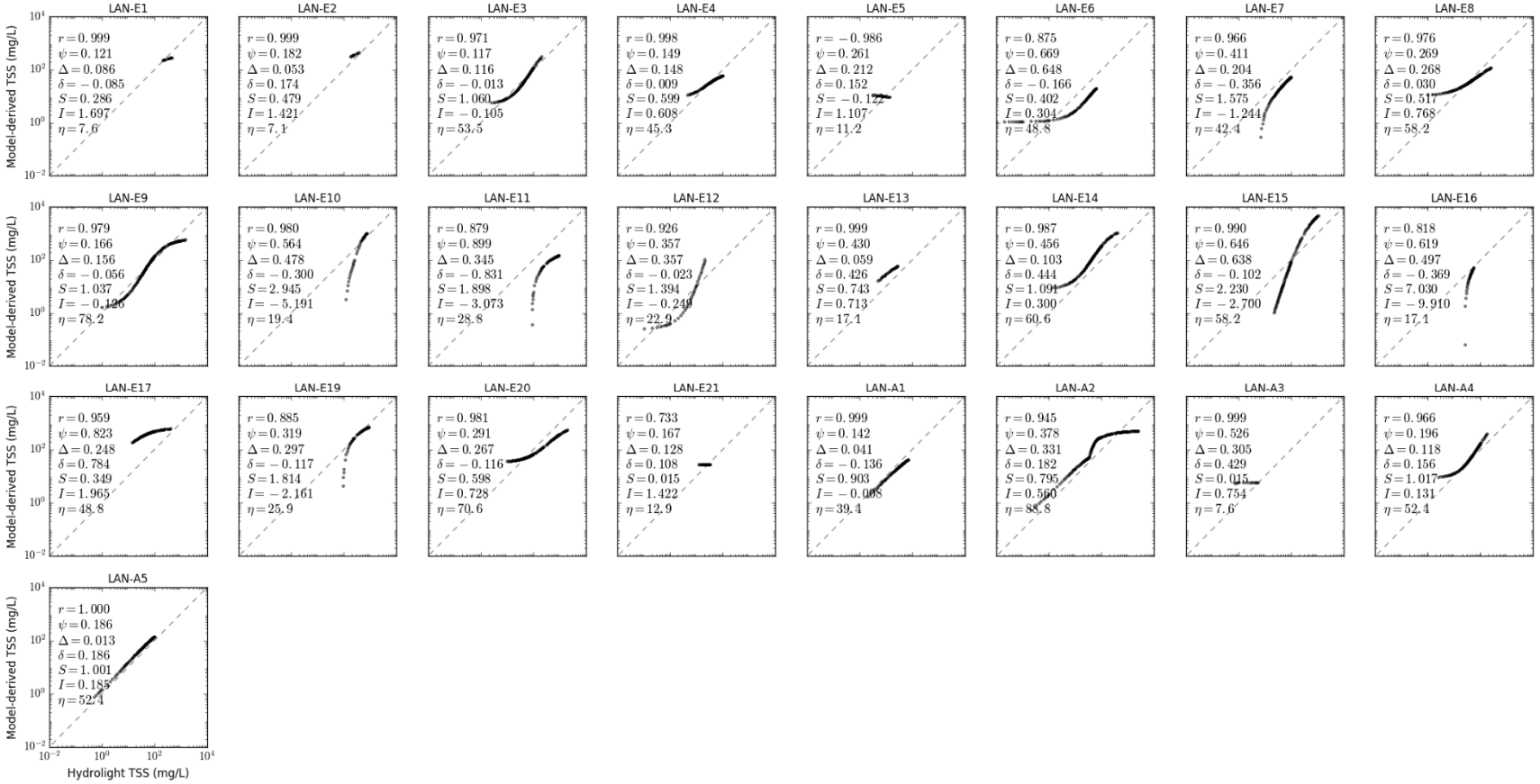

Figure S7.10. Scatter plot of LANDSAT TSS models in CLASS-II water for calcareous sand sediment, b_b/b ratio of 0.018, solar zenith angle of 15°.

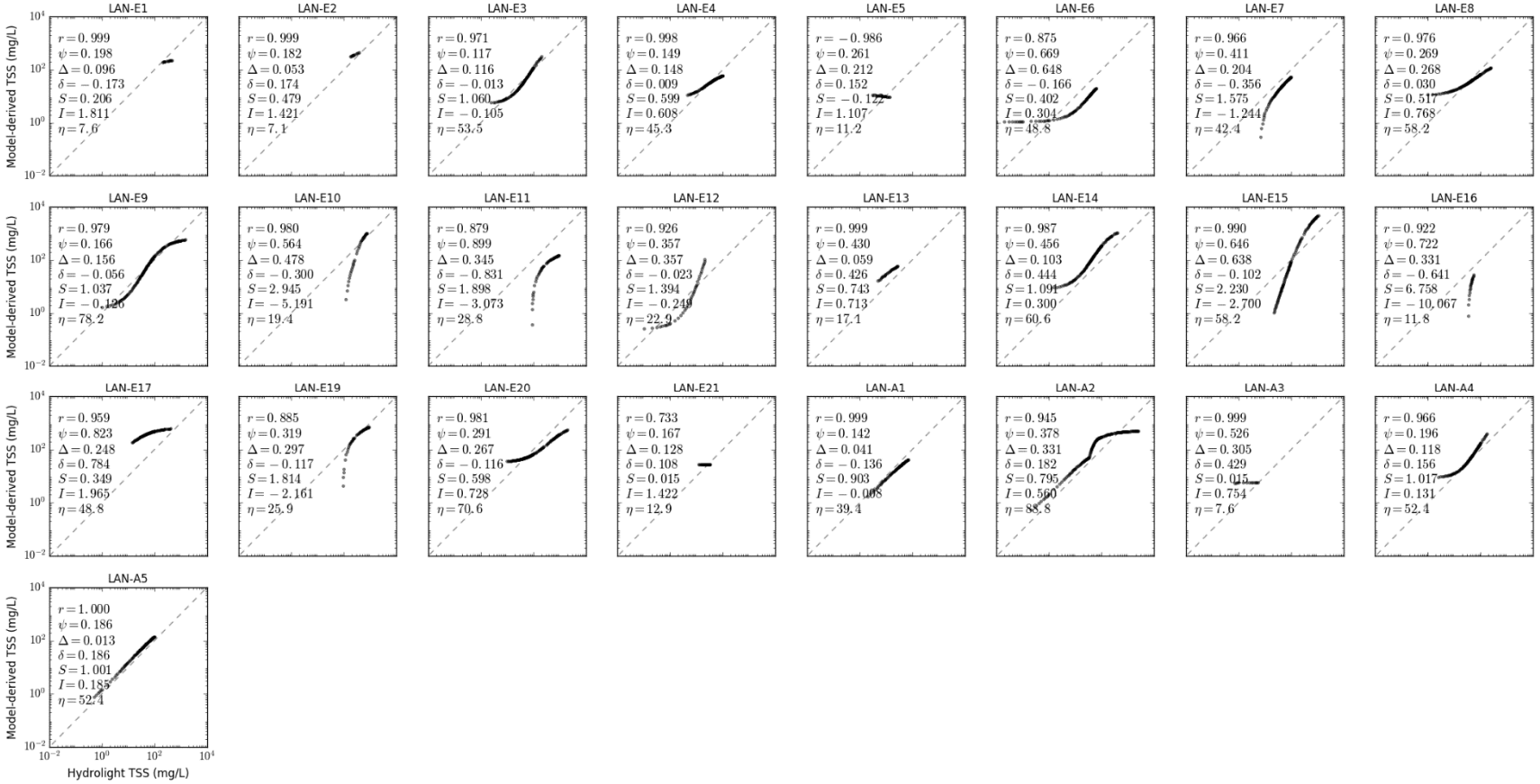

Figure S7.11. Scatter plot of LANDSAT TSS models in CLASS-II water for calcareous sand sediment, b_b/b ratio of 0.018, solar zenith angle of 45°.

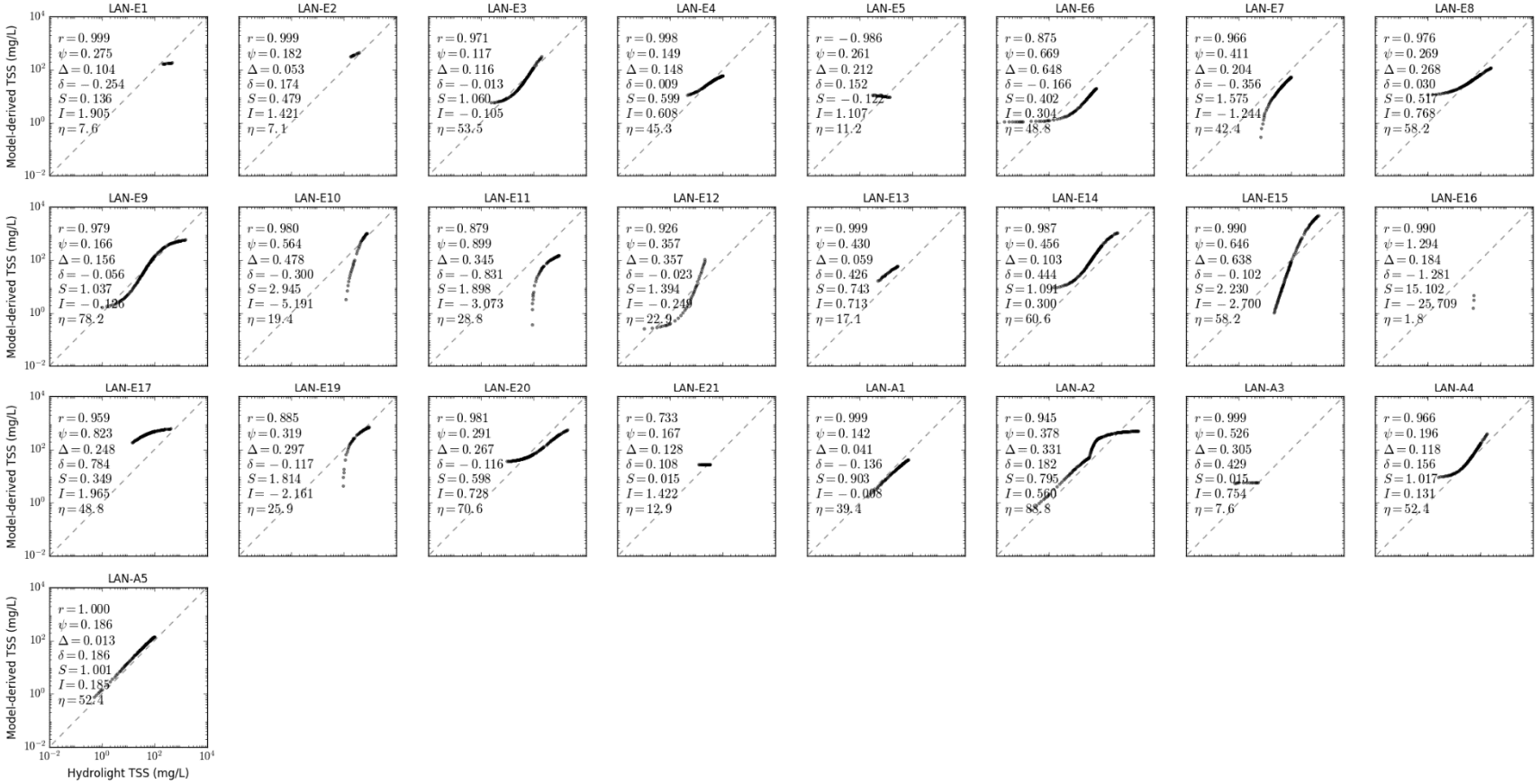

Figure S7.12. Scatter plot of LANDSAT TSS models in CLASS-II water for calcareous sand sediment, b_b/b ratio of 0.018, solar zenith angle of 60°.

Supplementary Materials S8. Scatter Plot of LANDSAT TSS Models for CLASS-III Water

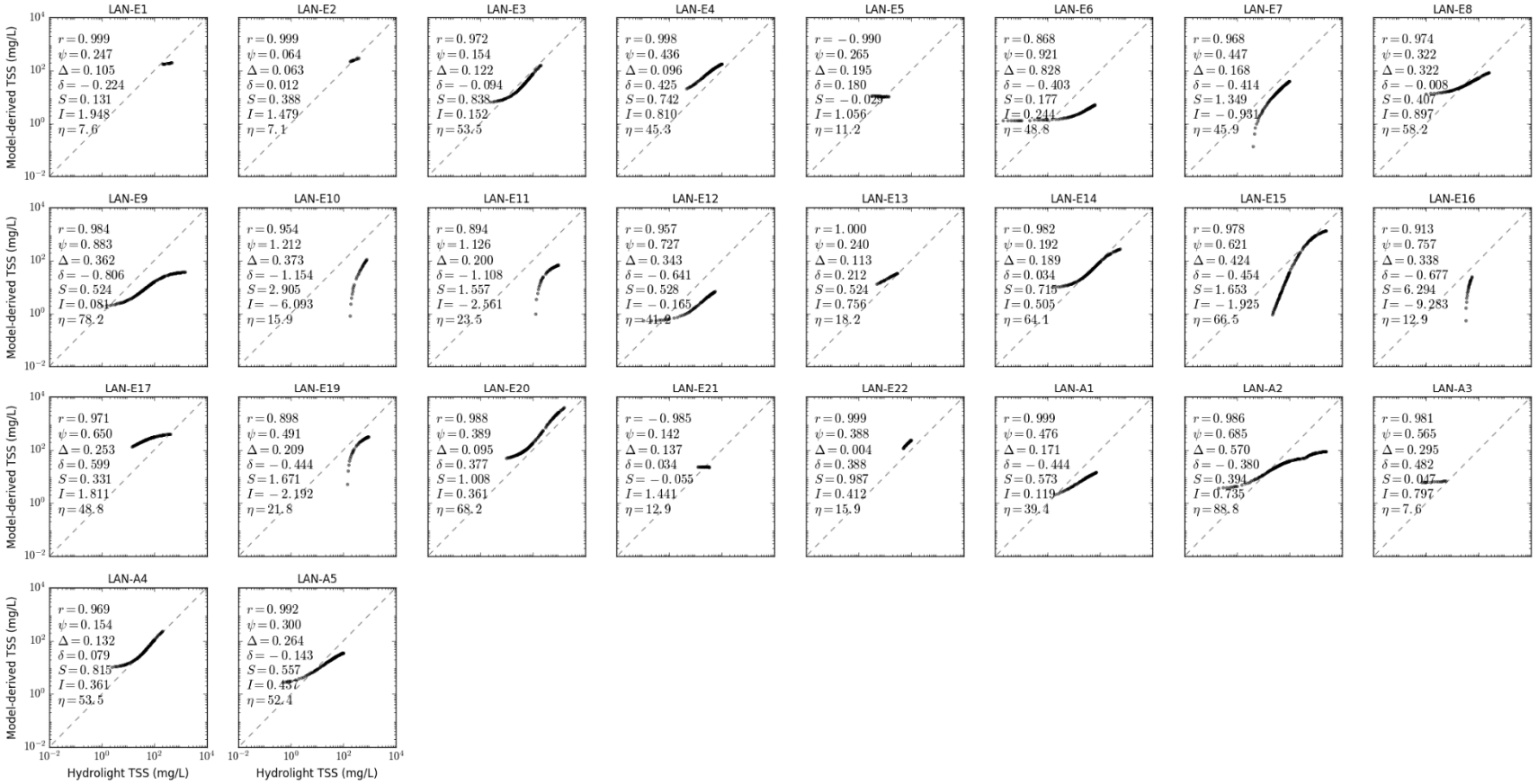

Figure S8.1. Scatter plot of LANDSAT TSS models in CLASS-III water for brown earth sediment, b_b/b ratio of 0.018, solar zenith angle of 30°.

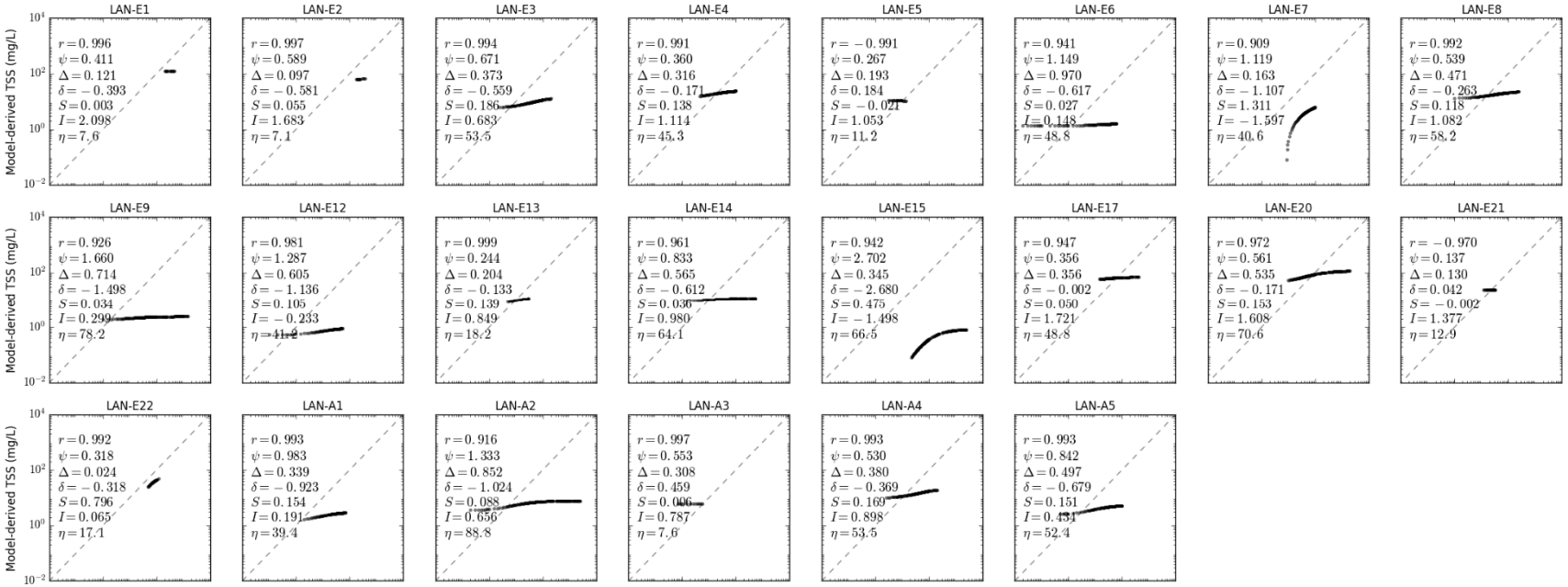

Figure S8.2. Scatter plot of LANDSAT TSS models in CLASS-III water for bukata sediment, b_b/b ratio of 0.018, solar zenith angle of 30°.

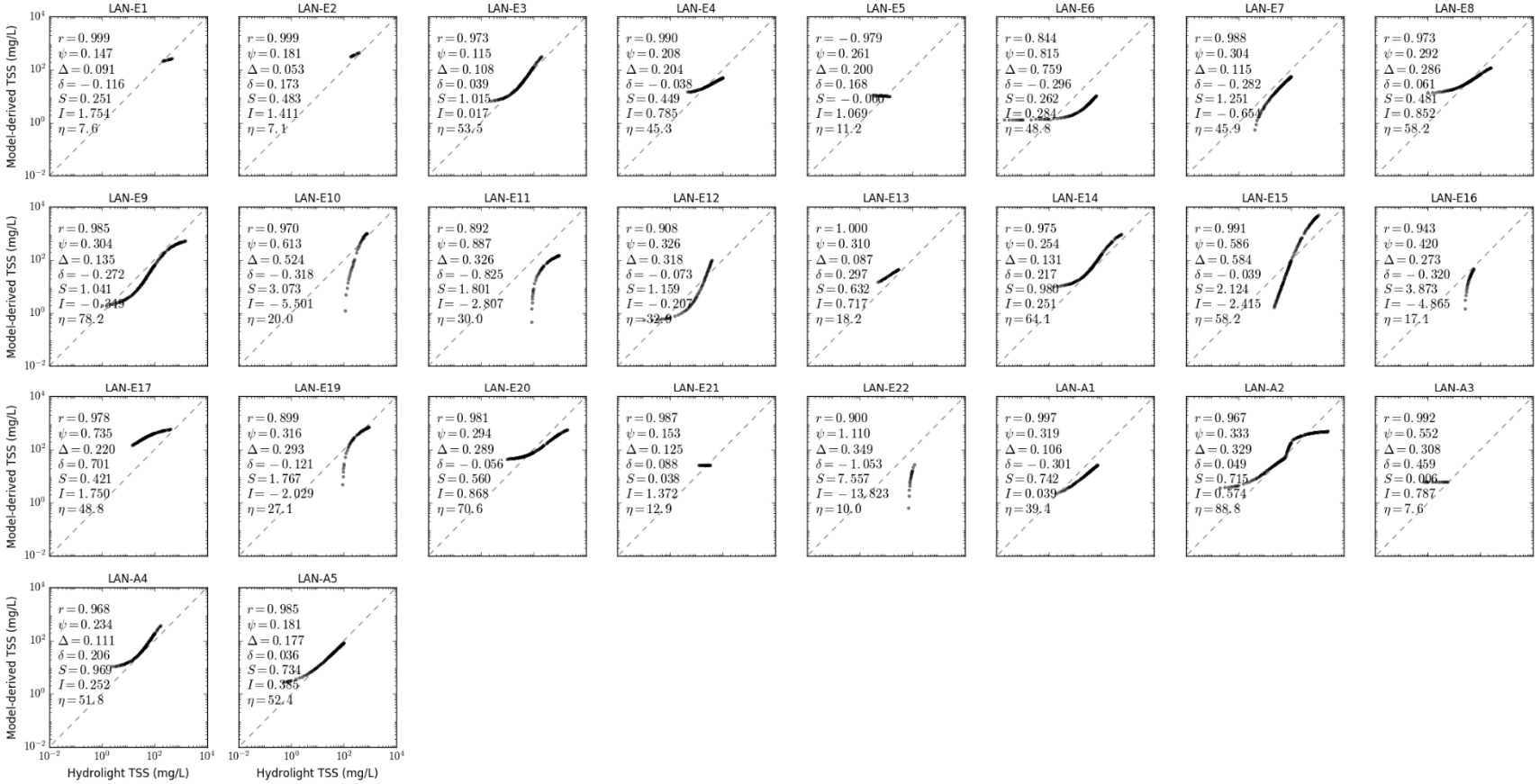

Figure S8.3. Scatter plot of LANDSAT TSS models in CLASS-III water for calcareous sand sediment, b_b/b ratio of 0.018, solar zenith angle of 30°.

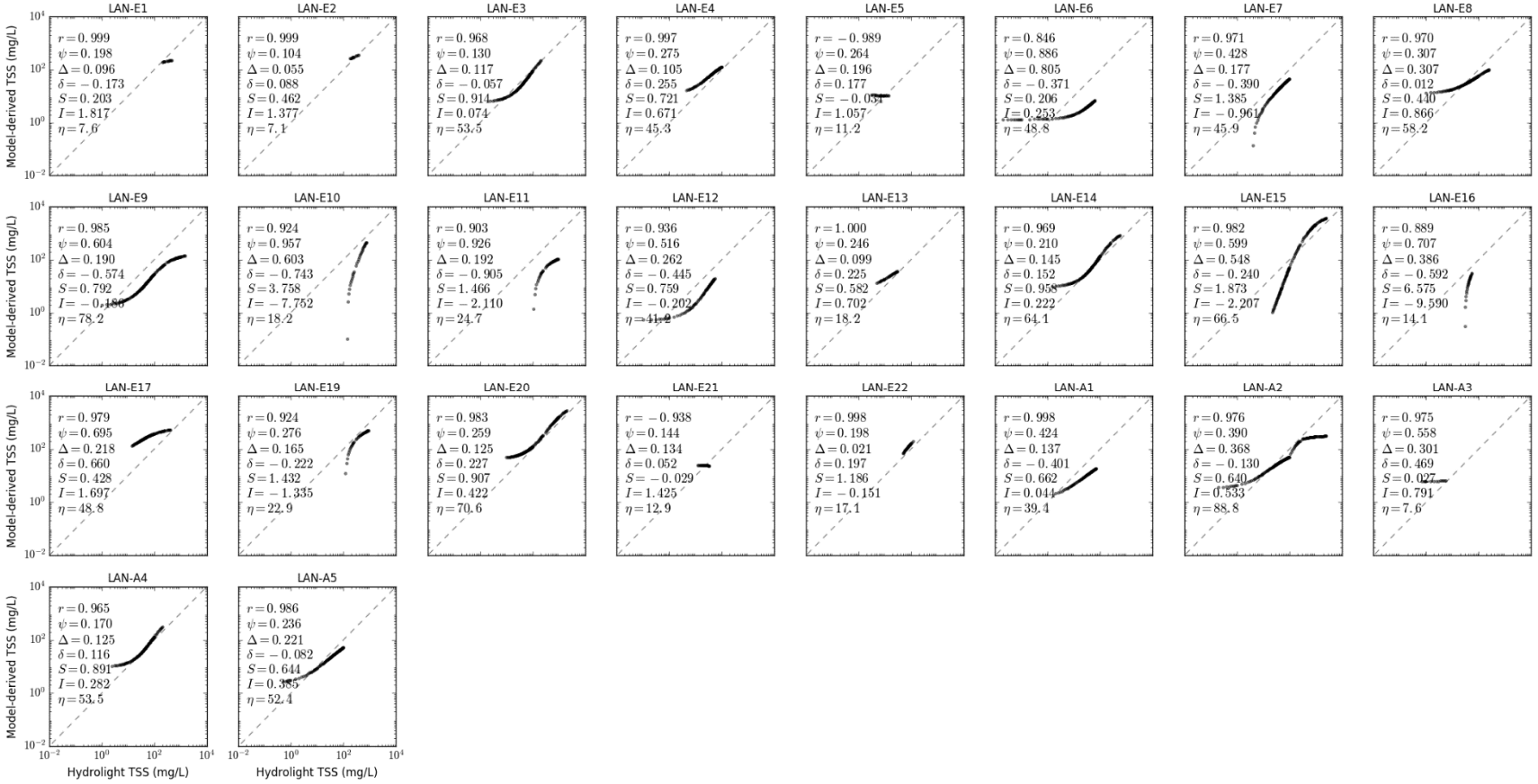

Figure S8.4. Scatter plot of LANDSAT TSS models in CLASS-III water for red clay sediment, b_b/b ratio of 0.018, solar zenith angle of 30°.

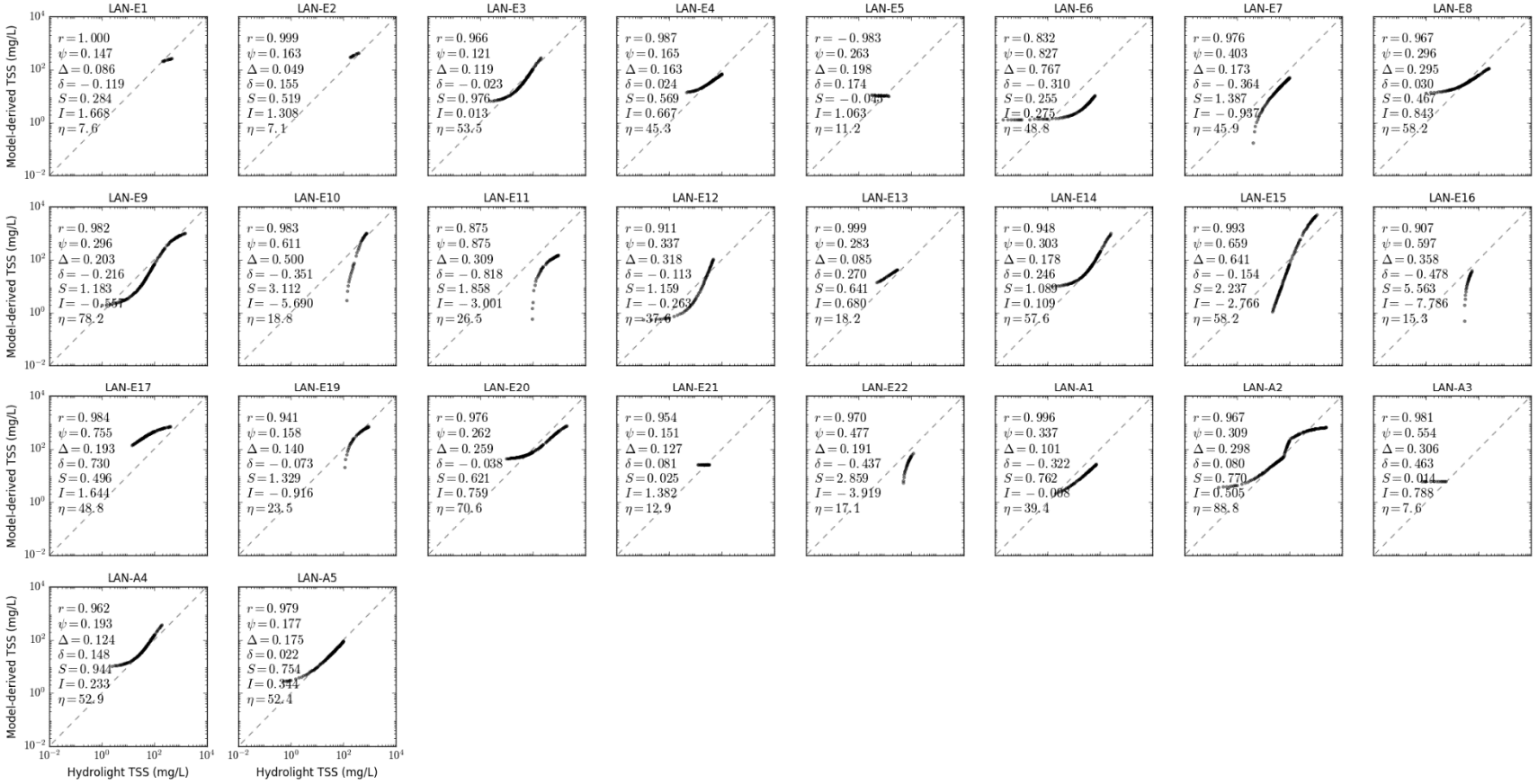

Figure S8.5. Scatter plot of LANDSAT TSS models in CLASS-III water for yellow clay sediment, b_b/b ratio of 0.018, solar zenith angle of 30°.

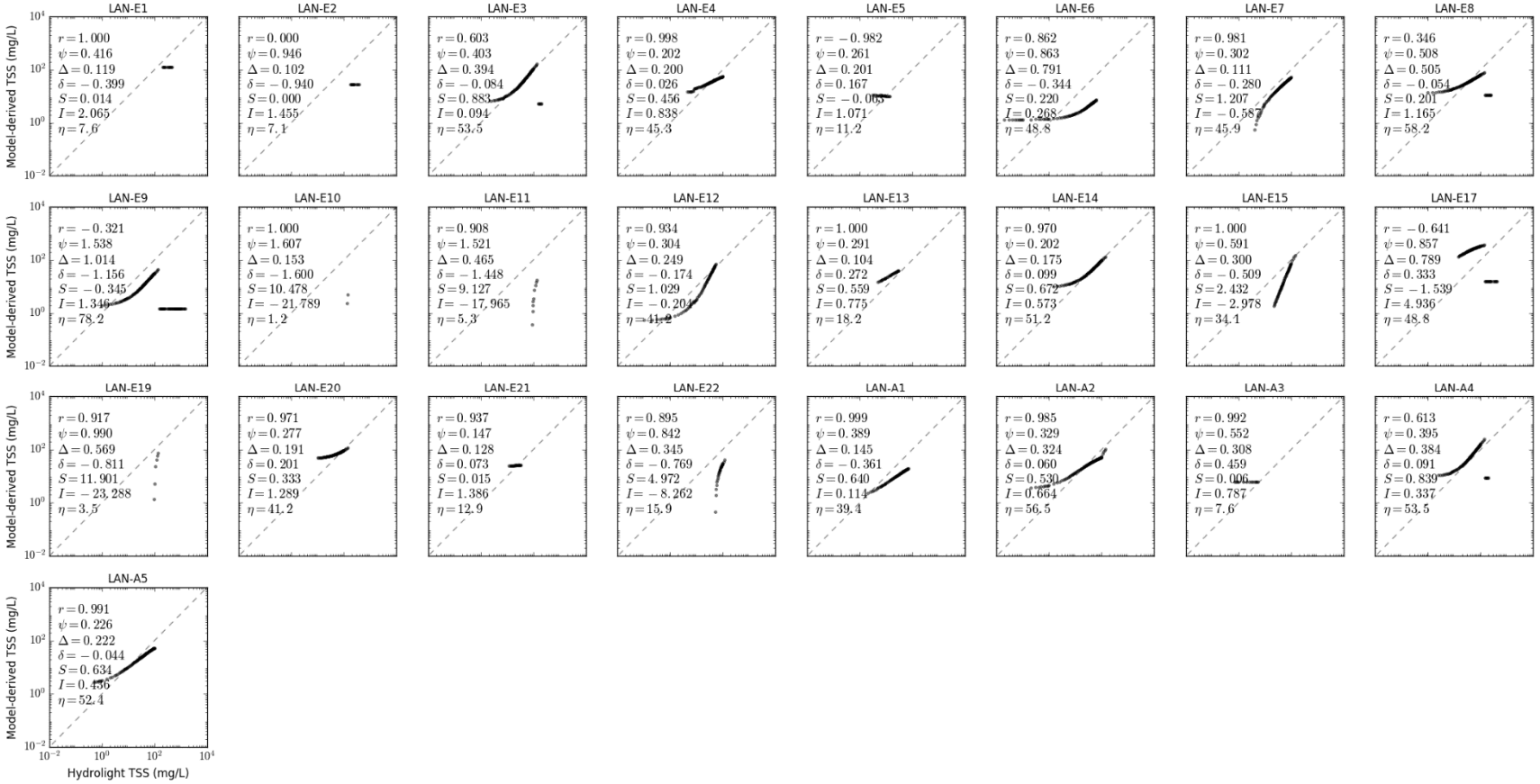

Figure S8.6. Scatter plot of LANDSAT TSS models in CLASS-III water for calcareous sand sediment, b_b/b ratio of 0.001, solar zenith angle of 30°.

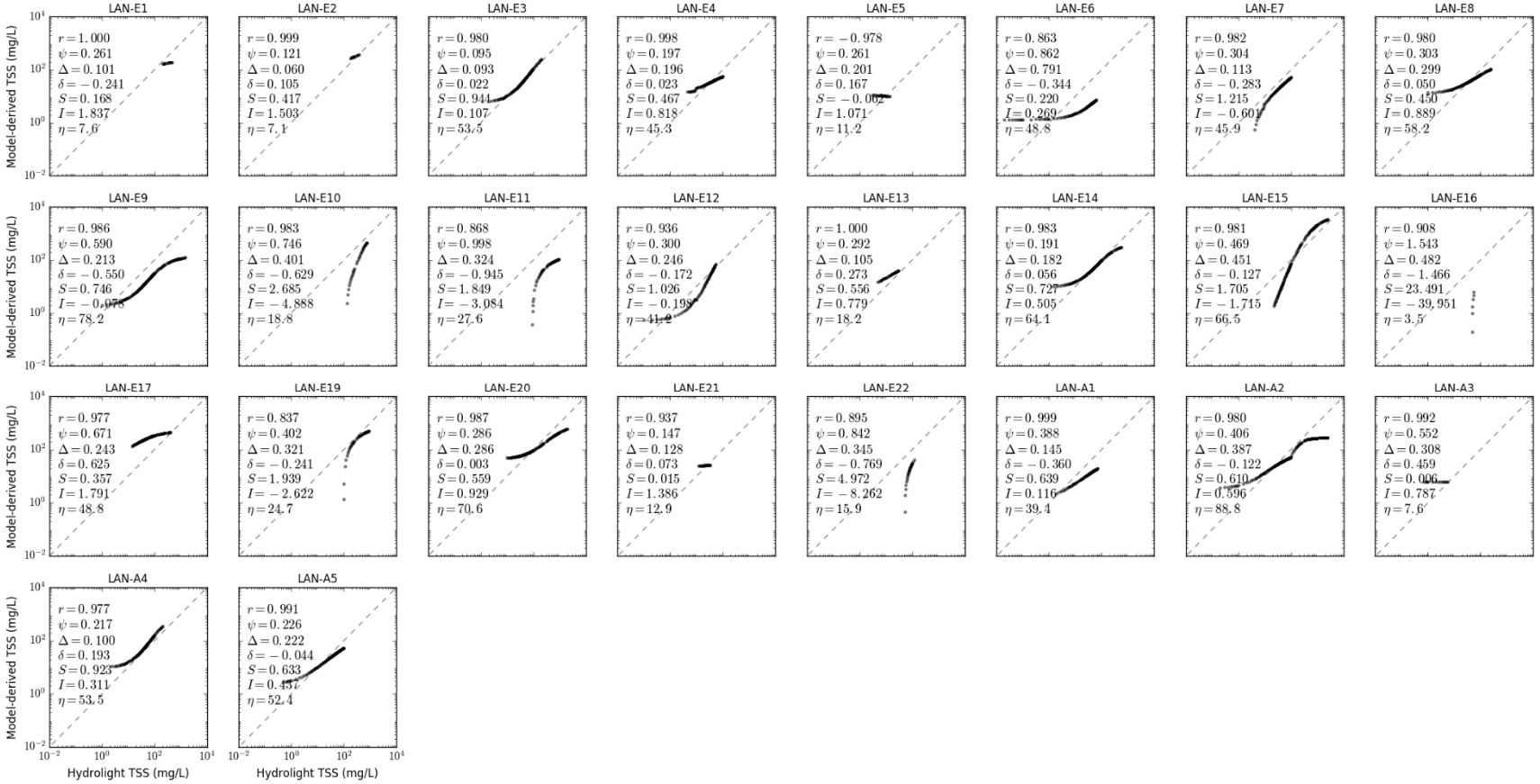

Figure S8.7. Scatter plot of LANDSAT TSS models in CLASS-III water for calcareous sand sediment, b_b/b ratio of 0.01, solar zenith angle of 30°.

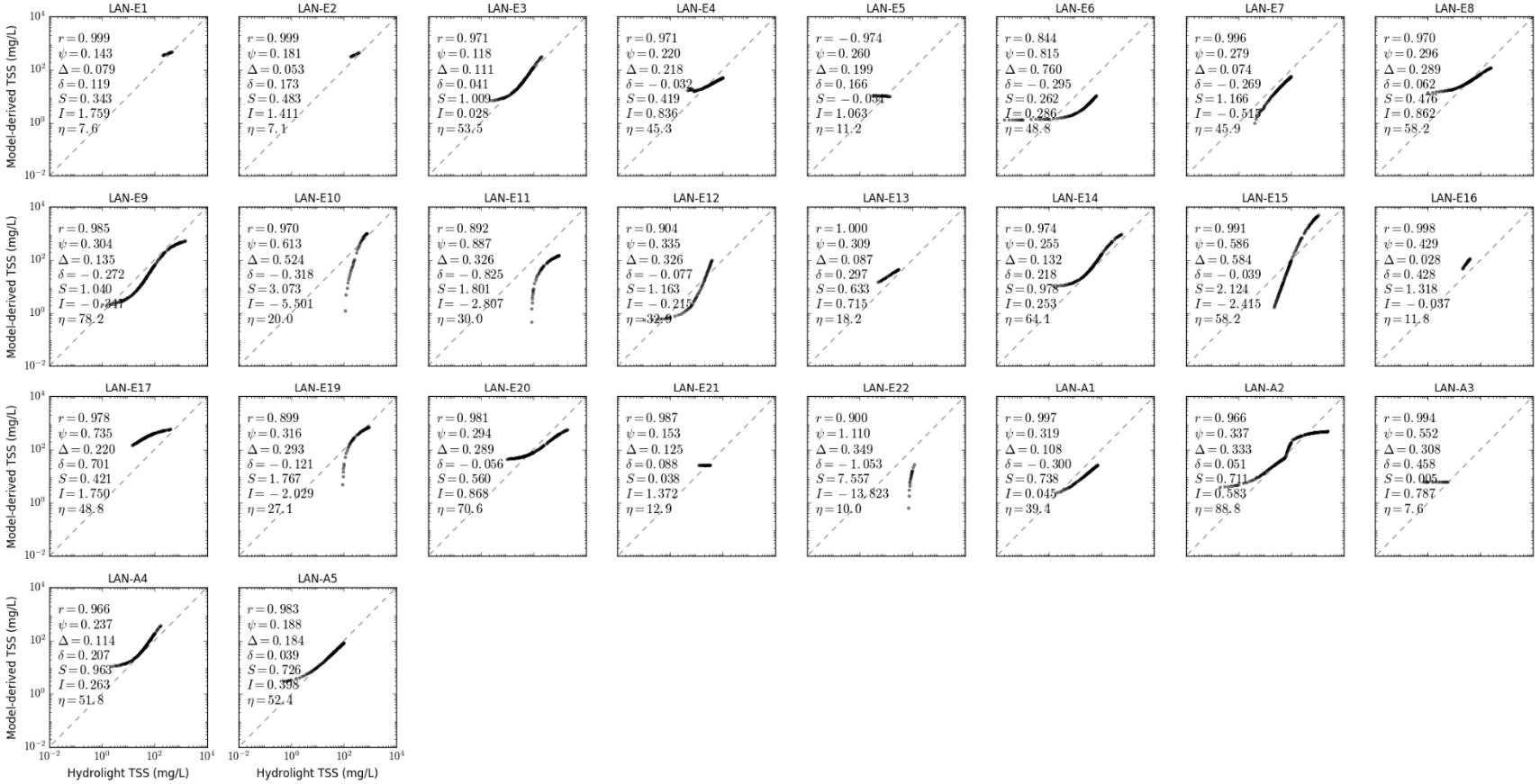

Figure S8.8. Scatter plot of LANDSAT TSS models in CLASS-III water for calcareous sand sediment, b_b/b ratio of 0.05, solar zenith angle of 30°.

Figure S8.9. Scatter plot of LANDSAT TSS models in CLASS-III water for calcareous sand sediment, b_b/b ratio of 0.1, solar zenith angle of 30°.

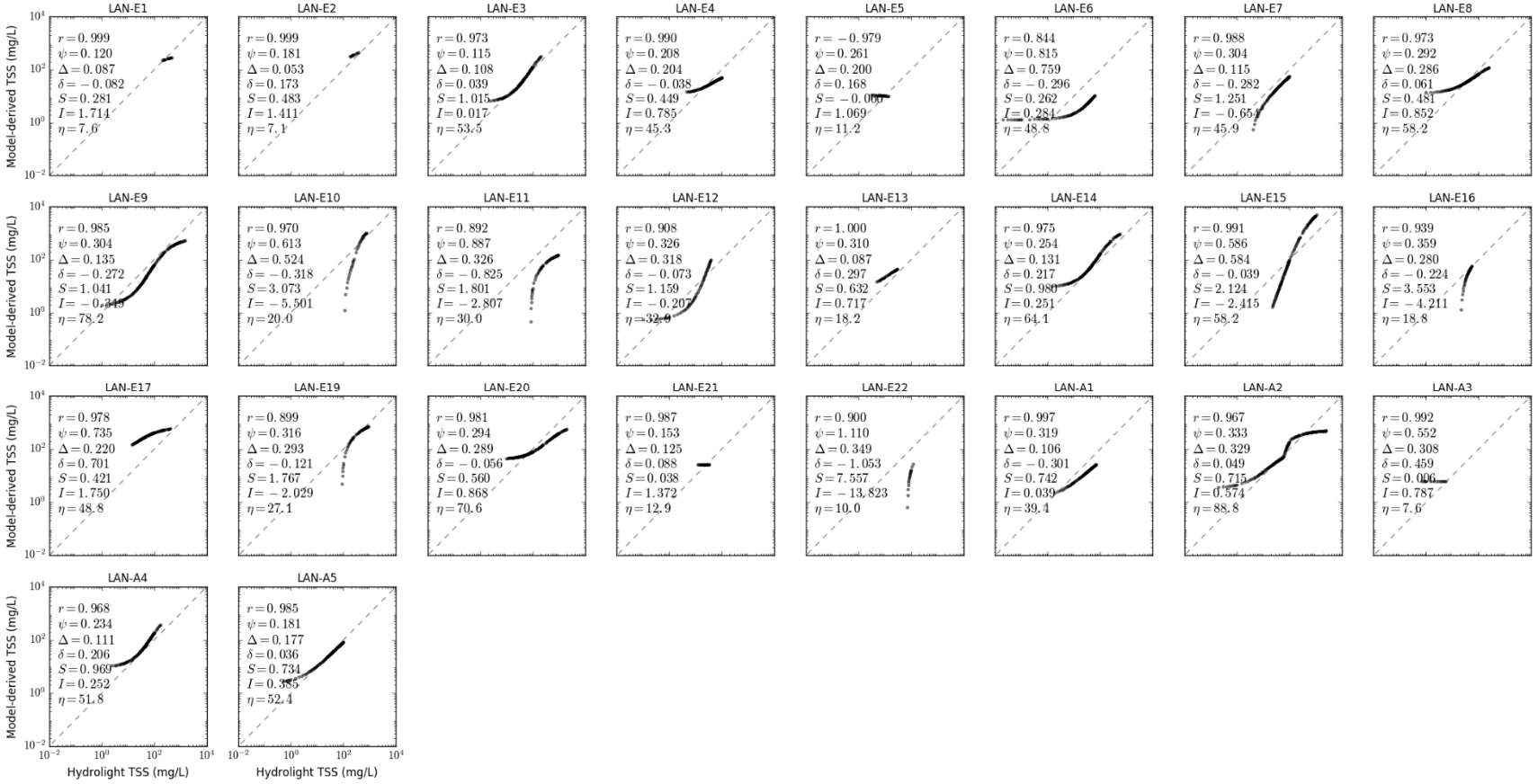

Figure S8.10. Scatter plot of LANDSAT TSS models in CLASS-III water for calcareous sand sediment, b_b/b ratio of 0.018, solar zenith angle of 15°.

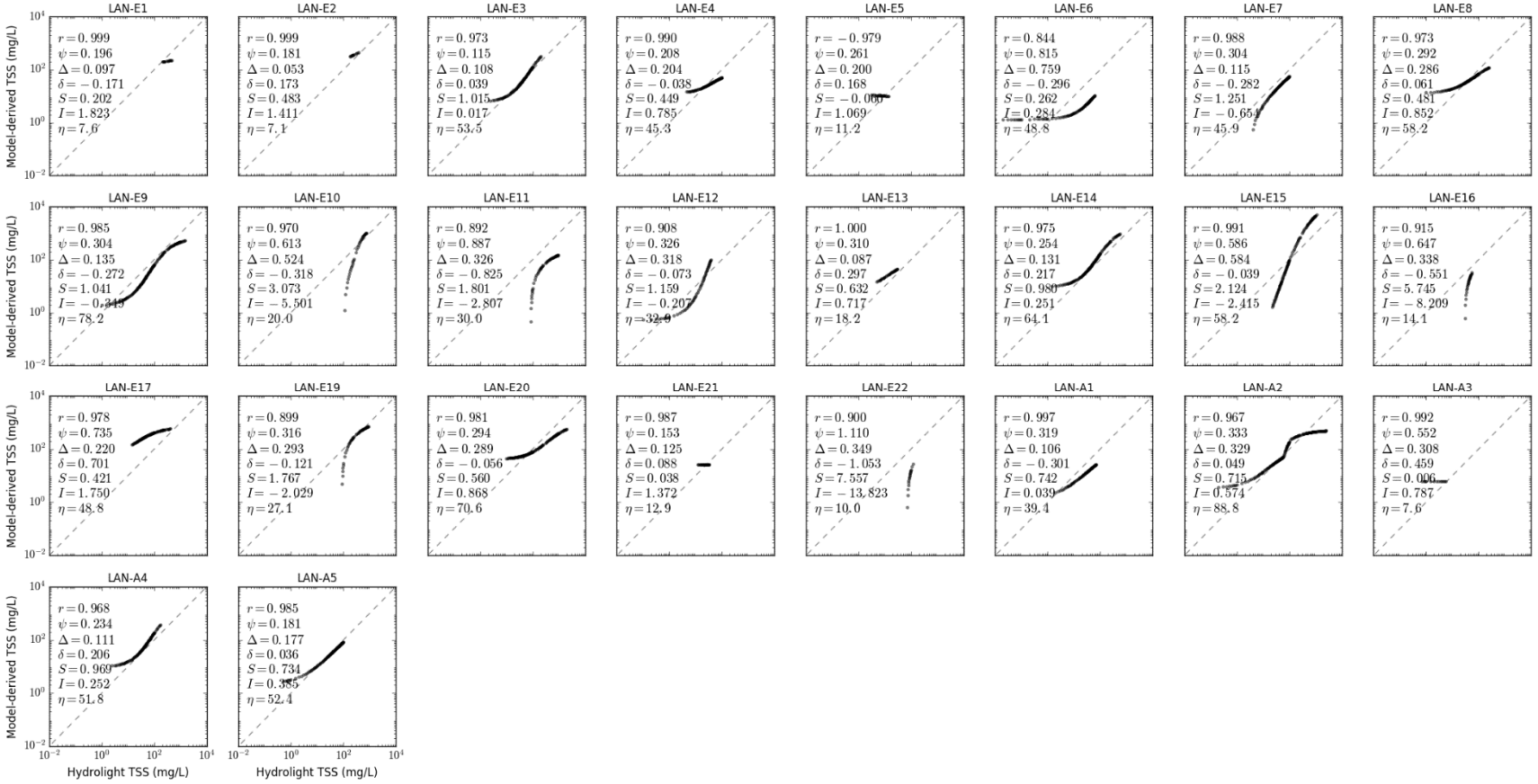

Figure S8.11. Scatter plot of LANDSAT TSS models in CLASS-III water for calcareous sand sediment, b_b/b ratio of 0.018, solar zenith angle of 45°.

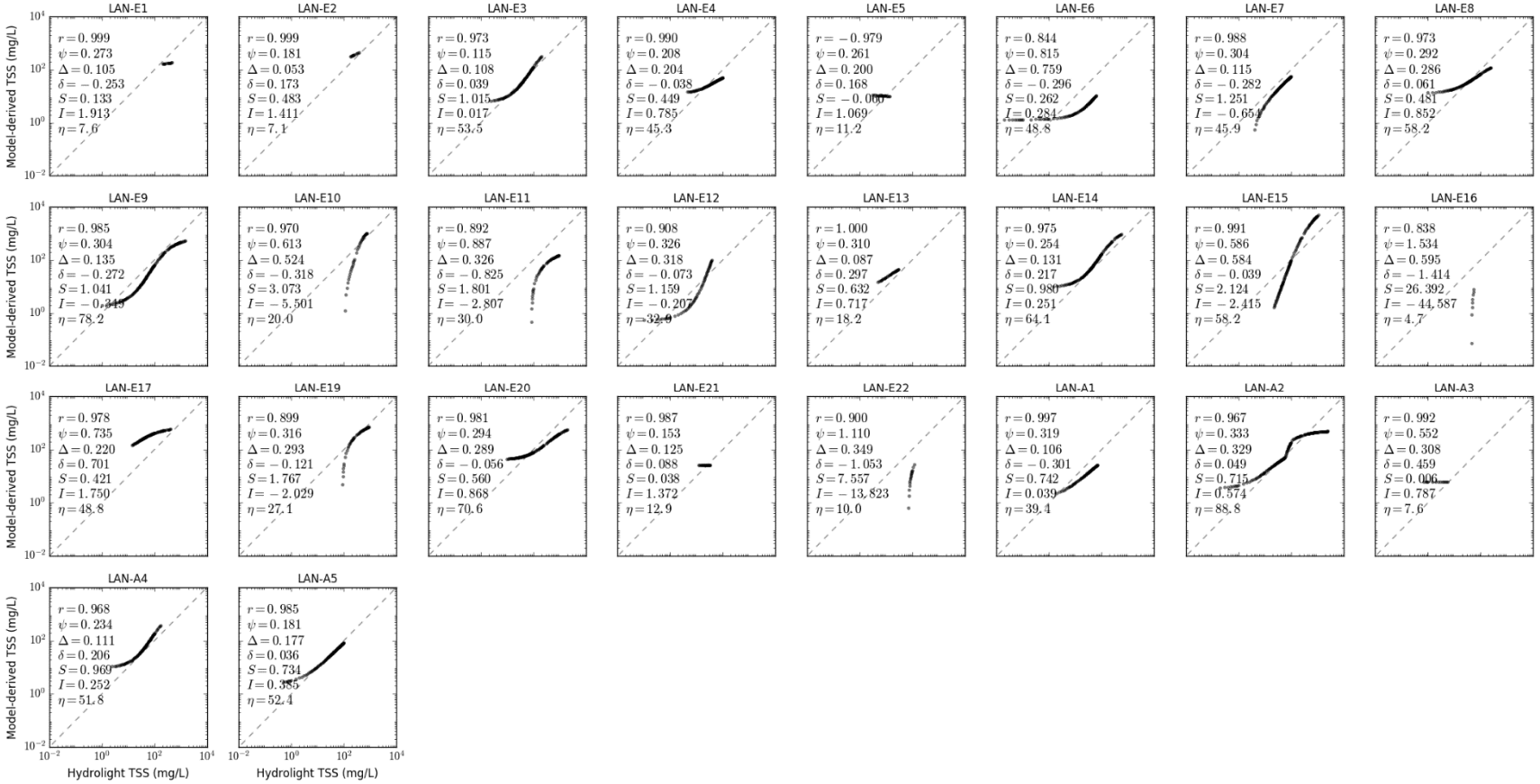

Figure S8.12. Scatter plot of LANDSAT TSS models in CLASS-III water for calcareous sand sediment, b_b/b ratio of 0.018, solar zenith angle of 60°.

Supplementary Materials S9. Scatter Plot of LANDSAT TSS Models for CLASS-IV Water

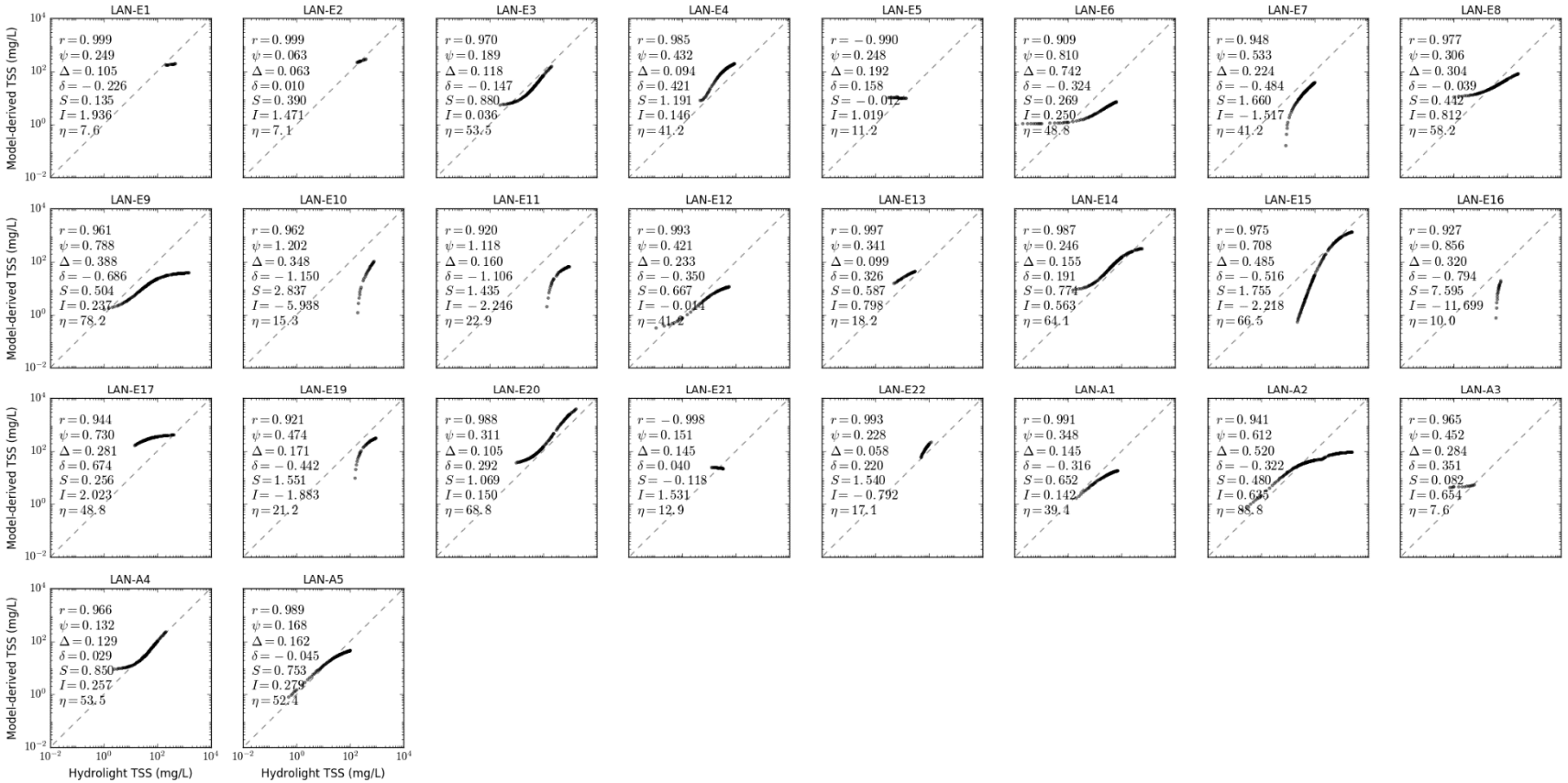

Figure S9.1. Scatter plot of LANDSAT TSS models in CLASS-IV water for brown earth sediment, b_b/b ratio of 0.018, solar zenith angle of 30°.

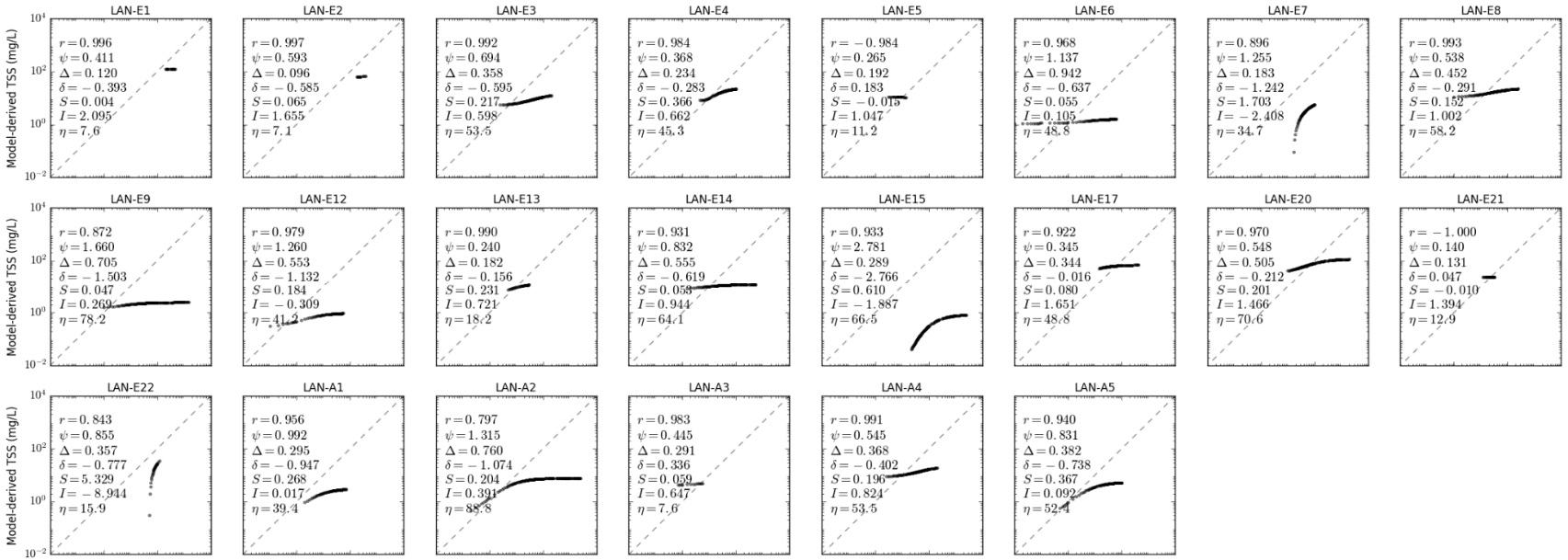

Figure S9.2. Scatter plot of LANDSAT TSS models in CLASS-IV water for bukata sediment, b_b/b ratio of 0.018, solar zenith angle of 30°.

Figure S9.3. Scatter plot of LANDSAT TSS models in CLASS-IV water for calcareous sand sediment, b_b/b ratio of 0.018, solar zenith angle of 30°.

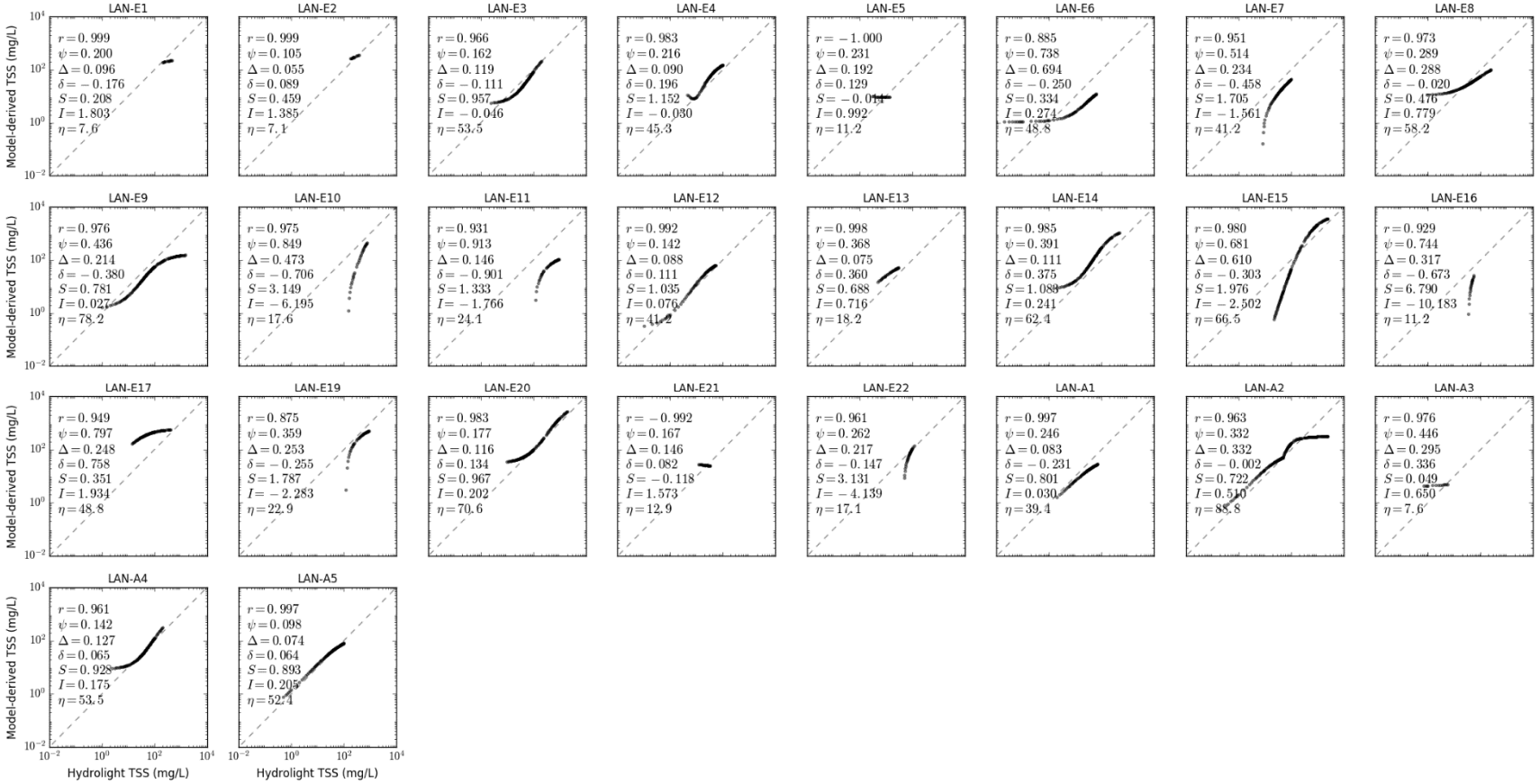

Figure S9.4. Scatter plot of LANDSAT TSS models in CLASS-IV water for red clay sediment, b_b/b ratio of 0.018, solar zenith angle of 30°.

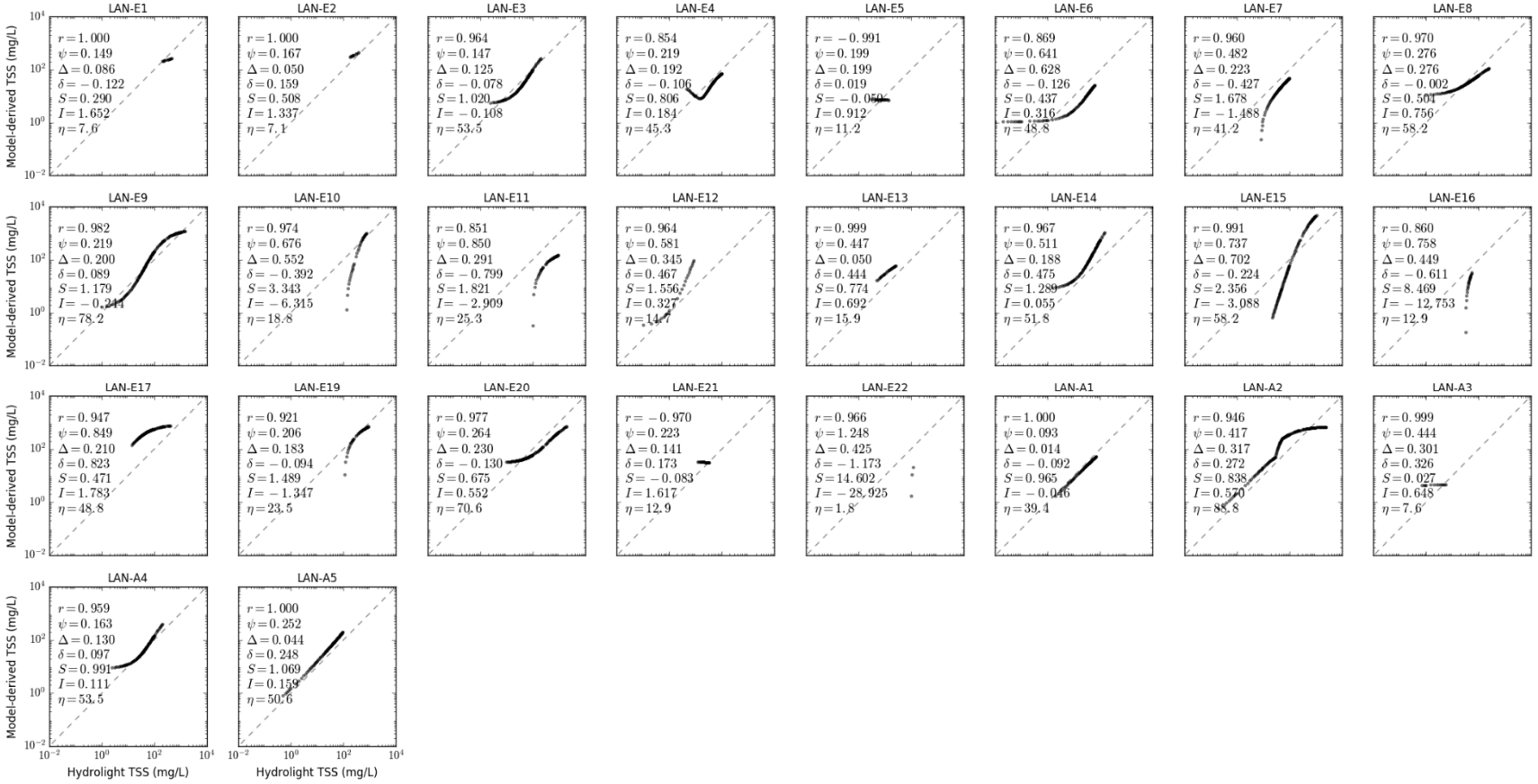

Figure S9.5. Scatter plot of LANDSAT TSS models in CLASS-IV water for yellow clay sediment, b_b/b ratio of 0.018, solar zenith angle of 30°.

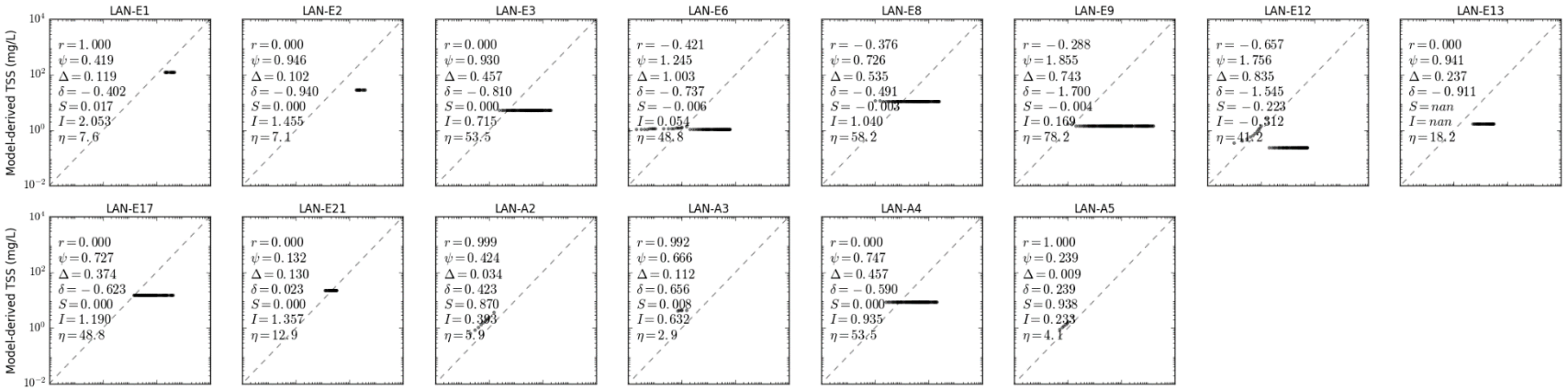

Figure S9.6. Scatter plot of LANDSAT TSS models in CLASS-IV water for calcareous sand sediment, b_b/b ratio of 0.001, solar zenith angle of 30°.

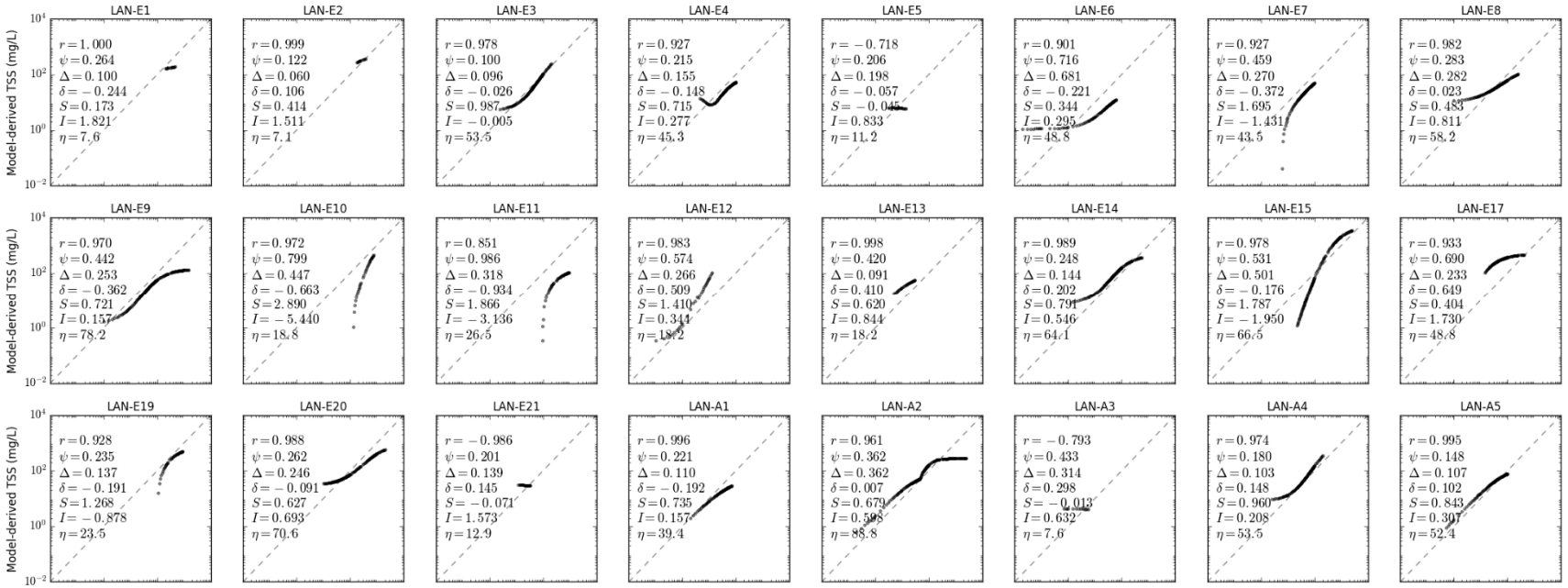

Figure S9.7. Scatter plot of LANDSAT TSS models in CLASS-IV water for calcareous sand sediment, b_b/b ratio of 0.01, solar zenith angle of 30°.

Figure S9.8. Scatter plot of LANDSAT TSS models in CLASS-IV water for calcareous sand sediment, b_b/b ratio of 0.05, solar zenith angle of 30°.

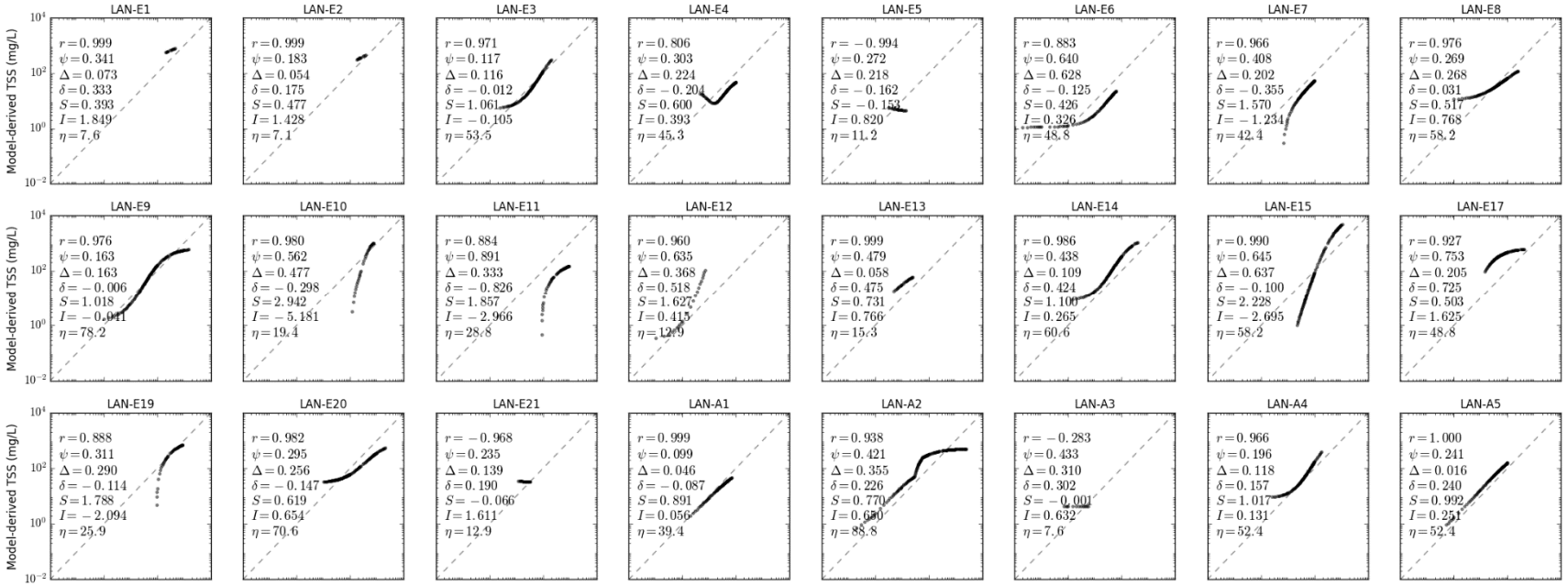

Figure S9.9. Scatter plot of LANDSAT TSS models in CLASS-IV water for calcareous sand sediment, b_b/b ratio of 0.1, solar zenith angle of 30°.

Figure S9.10. Scatter plot of LANDSAT TSS models in CLASS-IV water for calcareous sand sediment, b_b/b ratio of 0.018, solar zenith angle of 15°.

Figure S9.11. Scatter plot of LANDSAT TSS models in CLASS-IV water for calcareous sand sediment, b_b/b ratio of 0.018, solar zenith angle of 45°.

Figure S9.12. Scatter plot of LANDSAT TSS models in CLASS-IV water for calcareous sand sediment, b_b/b ratio of 0.018, solar zenith angle of 60°.

Supplementary Materials S10. Scatter Plot of LANDSAT TSS Models for CLASS-V Water

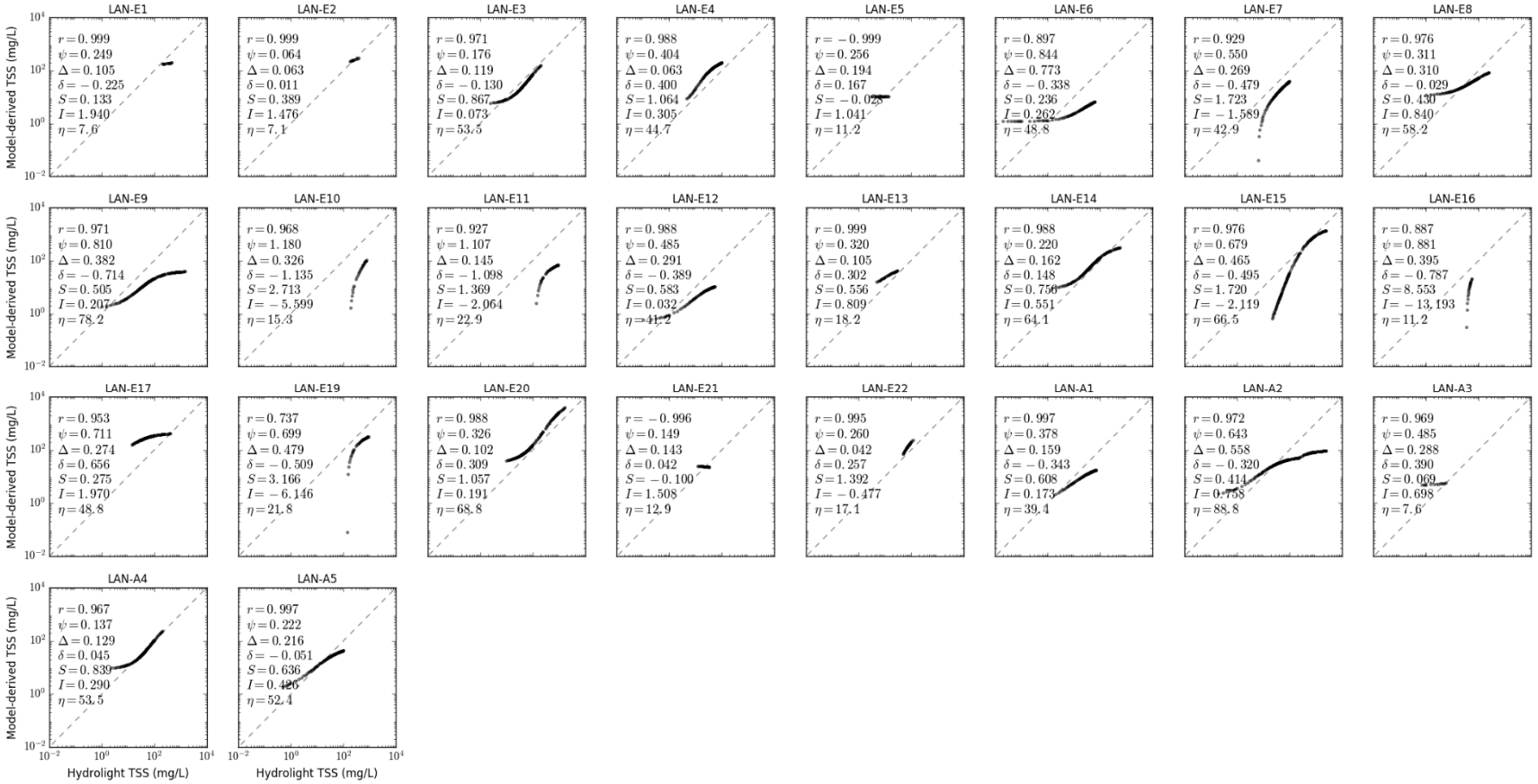

Figure S10.1. Scatter plot of LANDSAT TSS models in CLASS-V water for brown earth sediment, b_b/b ratio of 0.018, solar zenith angle of 30°.

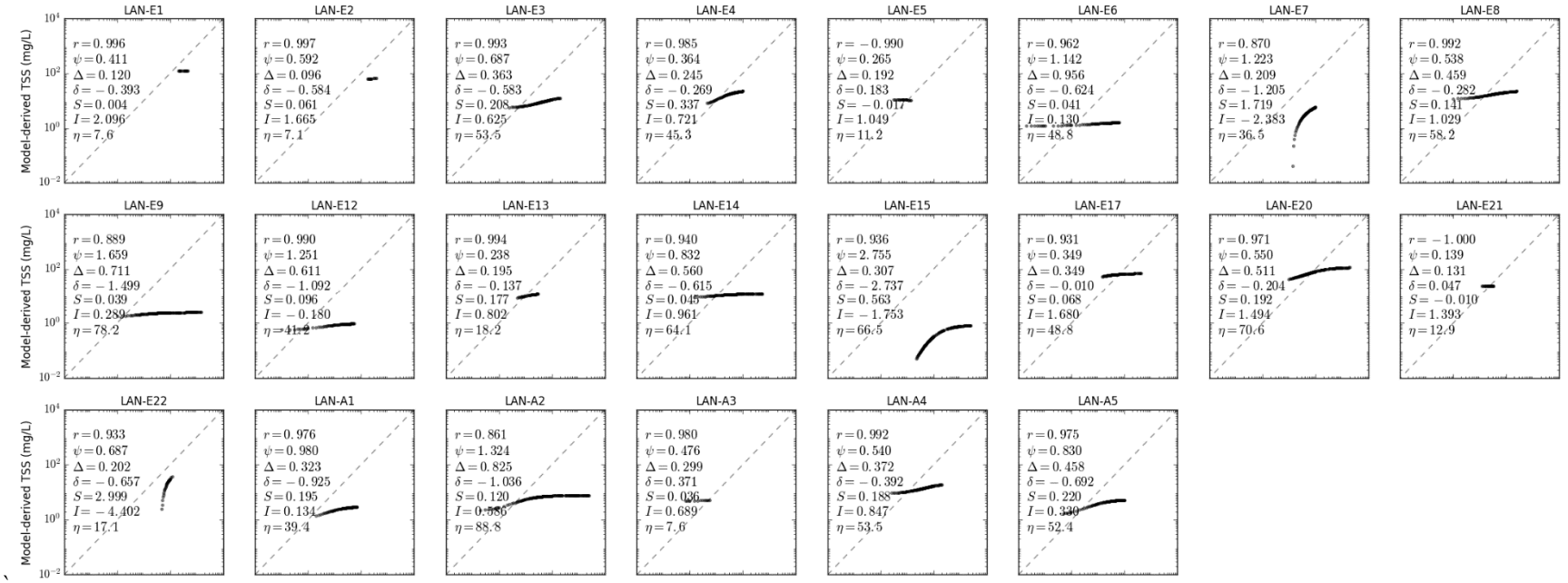

Figure S10.2. Scatter plot of LANDSAT TSS models in CLASS-V water for bukata sediment, b_b/b ratio of 0.018, solar zenith angle of 30°.

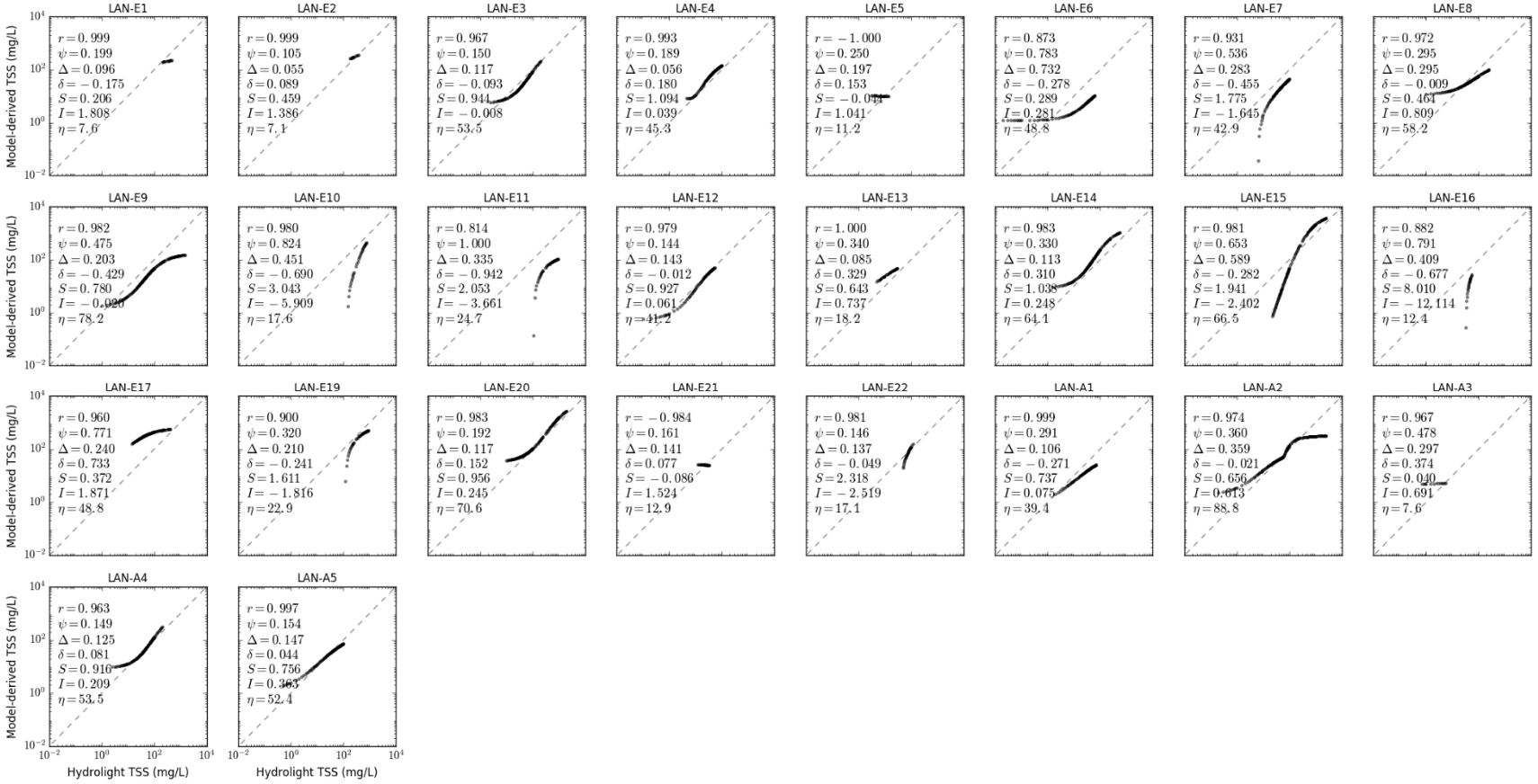

Figure S10.3. Scatter plot of LANDSAT TSS models in CLASS-V water for calcareous sand sediment, b_b/b ratio of 0.018, solar zenith angle of 30°.

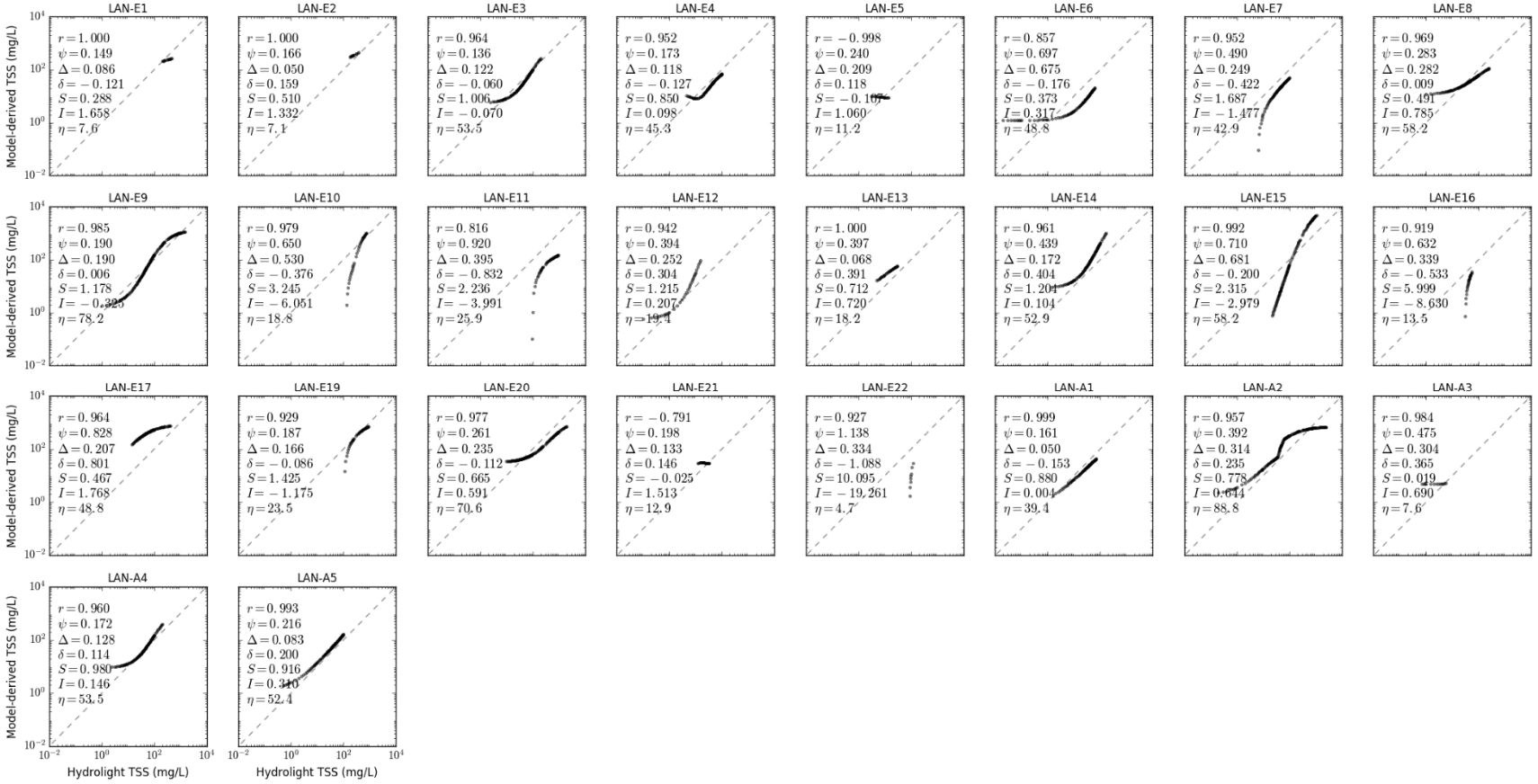

Figure S10.4. Scatter plot of LANDSAT TSS models in CLASS-V water for red clay sediment, b_b/b ratio of 0.018, solar zenith angle of 30°.

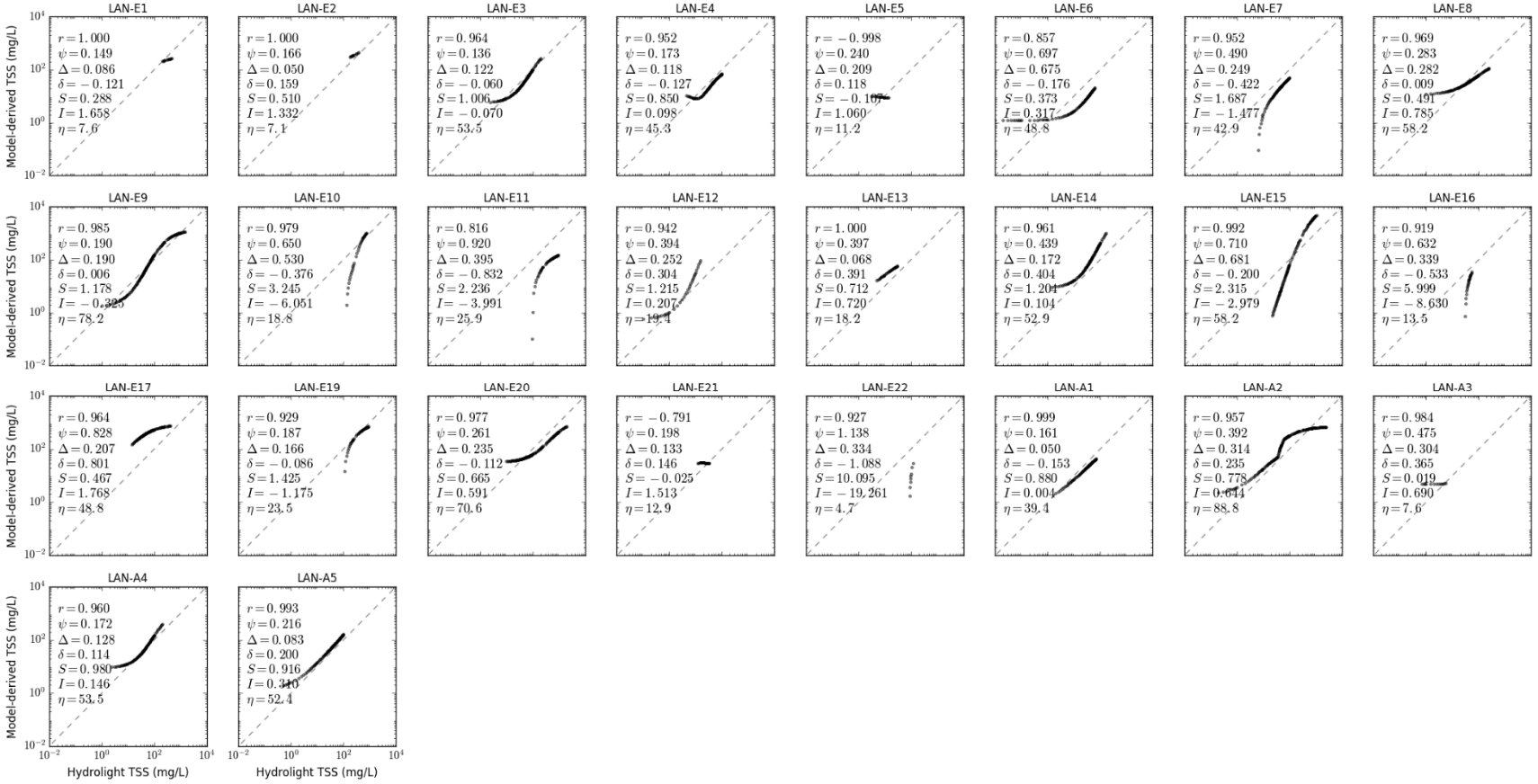

Figure S10.5. Scatter plot of LANDSAT TSS models in CLASS-V water for yellow clay sediment, b_b/b ratio of 0.018, solar zenith angle of 30°.

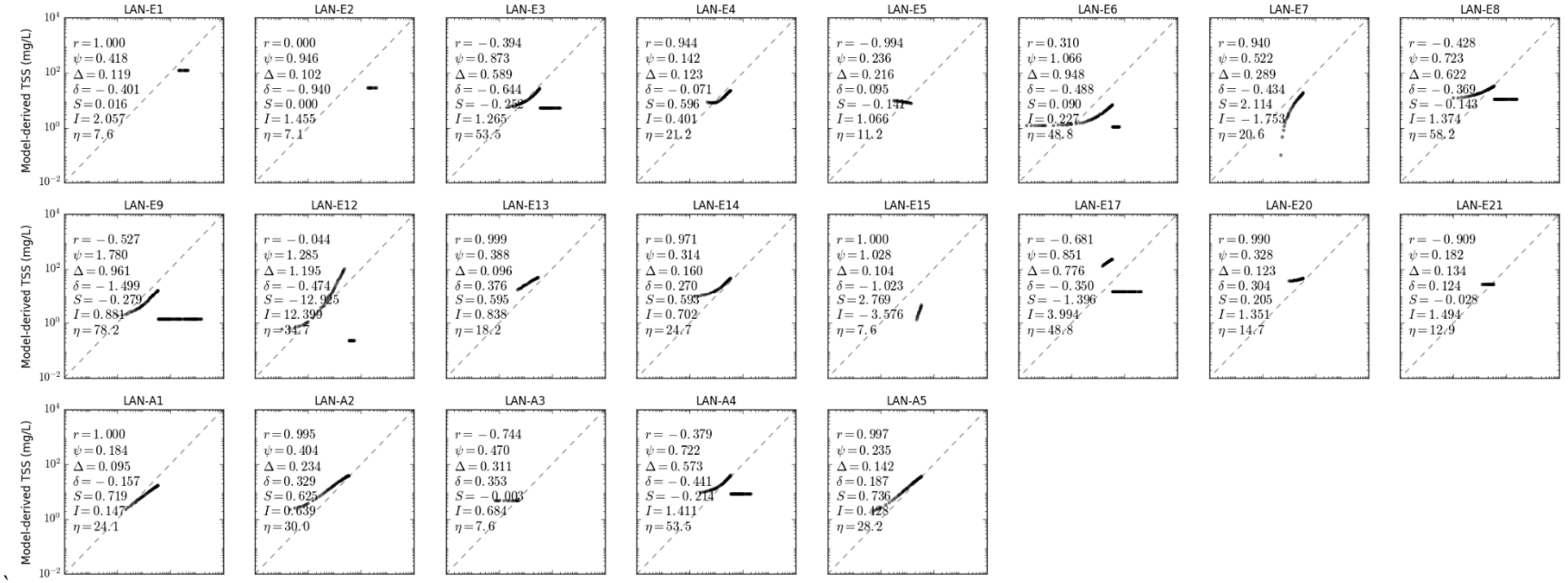

Figure S10.6. Scatter plot of LANDSAT TSS models in CLASS-V water for calcareous sand sediment, b_b/b ratio of 0.001, solar zenith angle of 30°.

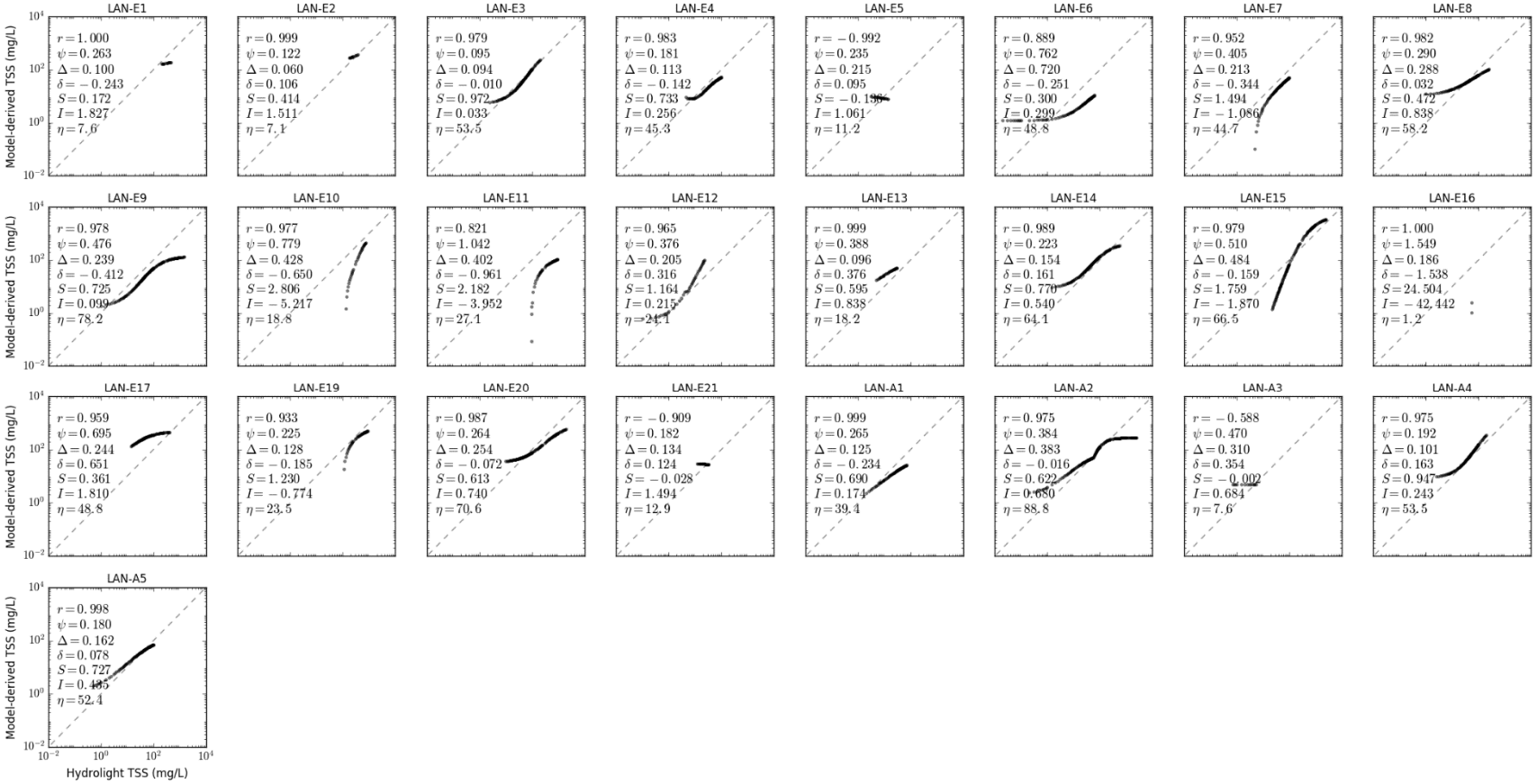

Figure S10.7. Scatter plot of LANDSAT TSS models in CLASS-V water for calcareous sand sediment, b_b/b ratio of 0.01, solar zenith angle of 30°.

Figure S10.8. Scatter plot of LANDSAT TSS models in CLASS-V water for calcareous sand sediment, b_b/b ratio of 0.05, solar zenith angle of 30°.

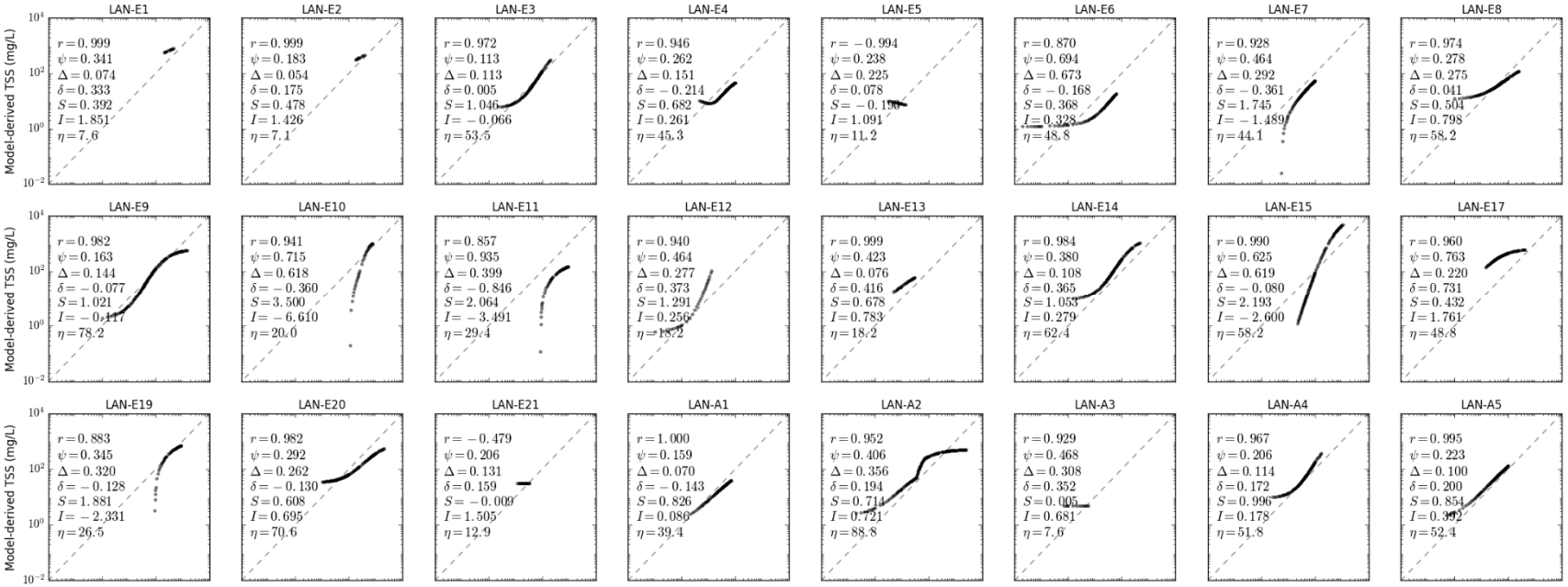

Figure S10.9. Scatter plot of LANDSAT TSS models in CLASS-V water for calcareous sand sediment, b_b/b ratio of 0.1, solar zenith angle of 30°.

Figure S10.10. Scatter plot of LANDSAT TSS models in CLASS-V water for calcareous sand sediment, b_b/b ratio of 0.018, solar zenith angle of 15°.

Figure S10.11. Scatter plot of LANDSAT TSS models in CLASS-V water for calcareous sand sediment, b_b/b ratio of 0.018, solar zenith angle of 45°.

Figure S10.12. Scatter plot of LANDSAT TSS models in CLASS-V water for calcareous sand sediment, b_b/b ratio of 0.018, solar zenith angle of 60°.

S11: This supplementary section shows the scoring of each of the MODIS (MOD) and LANDSAT (LAN) TSS models for the individual water types, sediment types, backscattering ratios and solar zenith angles.

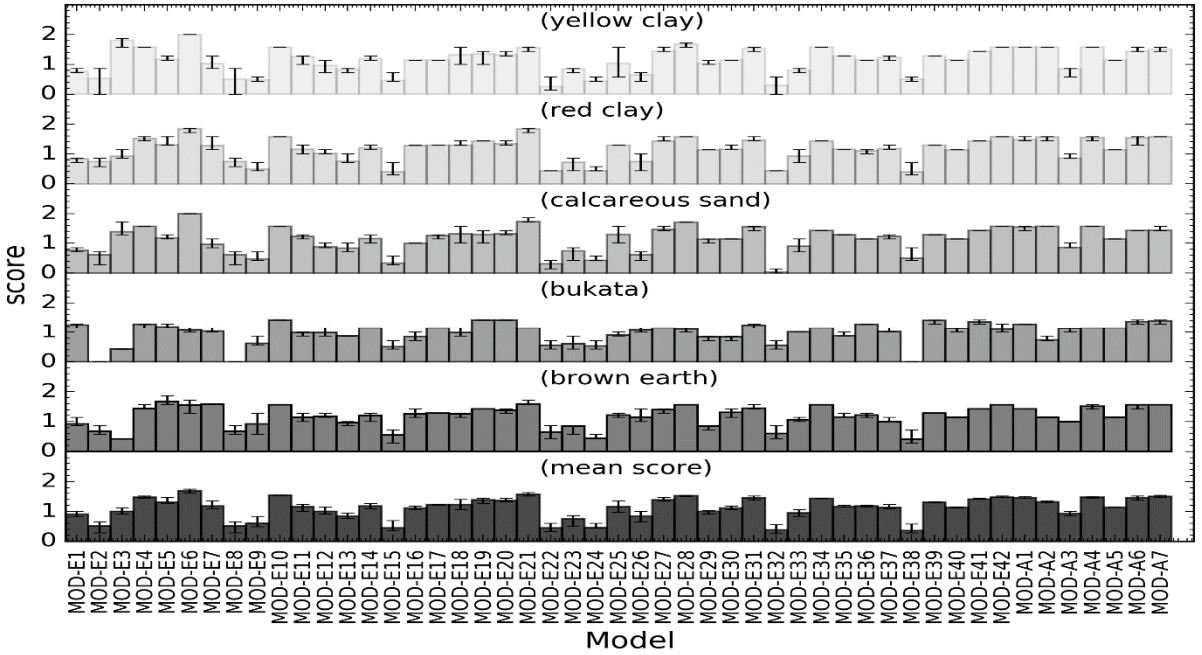

Figure S11.1. Total scores for different sediments and the average scores across all five sediments in CLASS-I water.

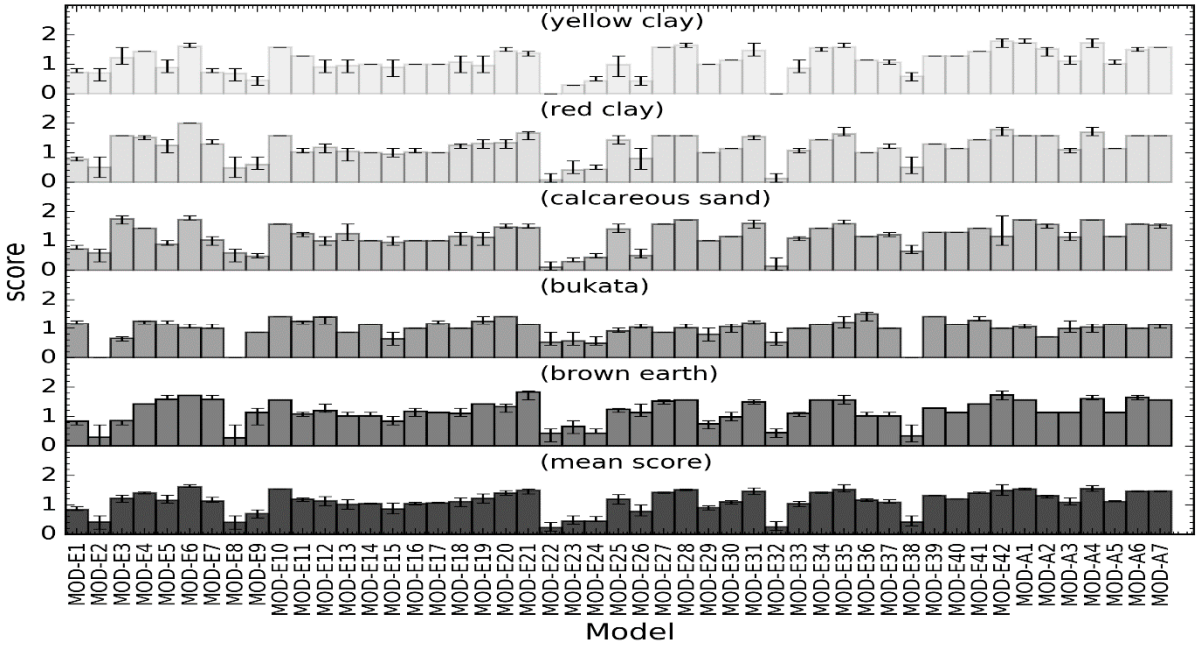

Figure S11.2. Total scores for different sediments and the average scores across all five sediments in CLASS-II water.

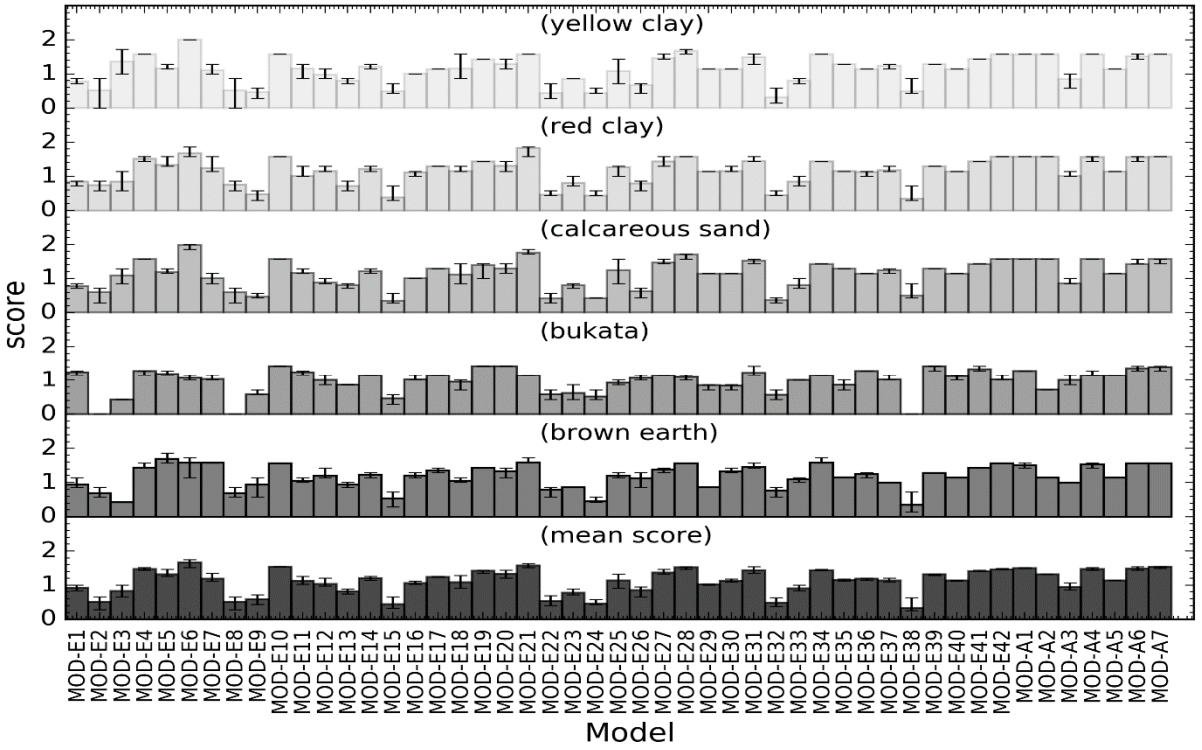

Figure S11.3. Total scores for different sediments and the average scores across all five sediments in CLASS-III water.

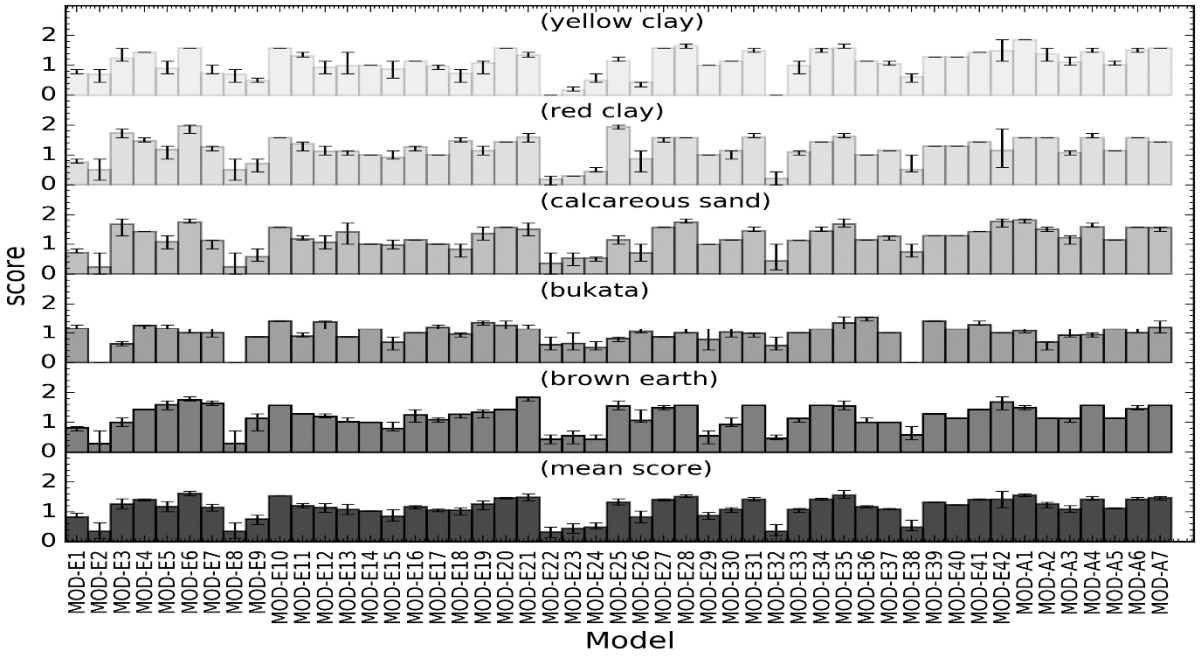

Figure S11.4. Total scores for different sediments and the average scores across all five sediments in CLASS-IV water.

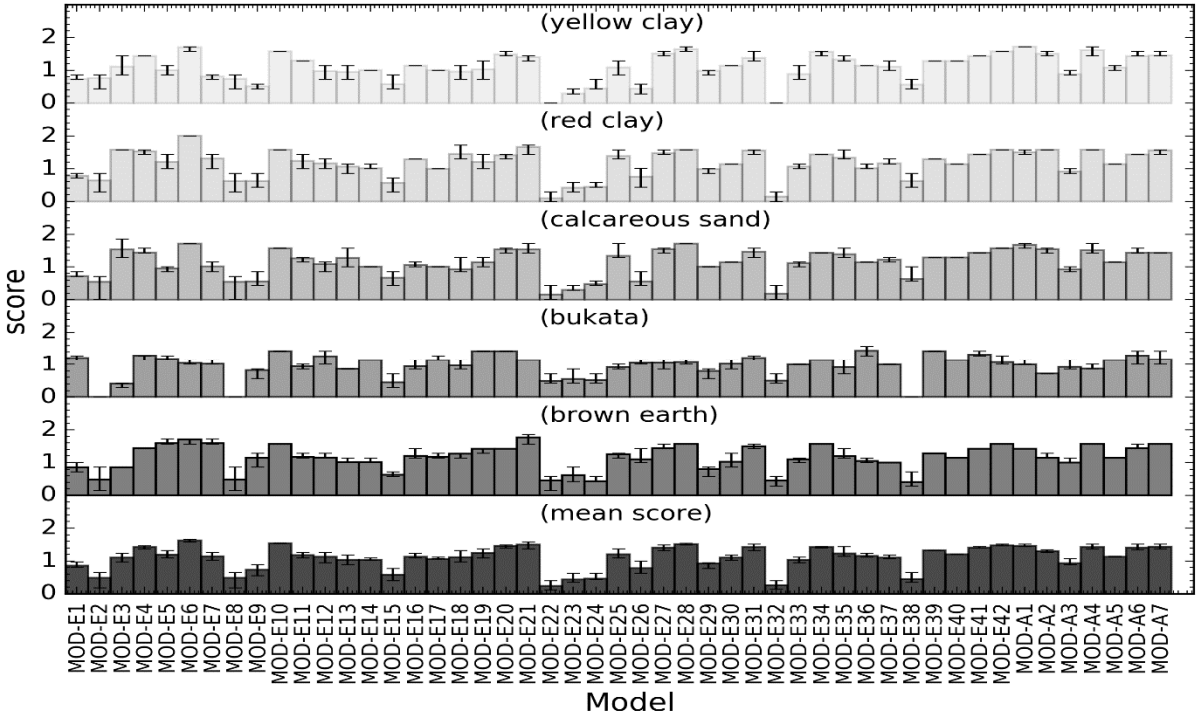

Figure S11.5. Total scores for different sediments and the average scores across all five sediments in CLASS-V water.

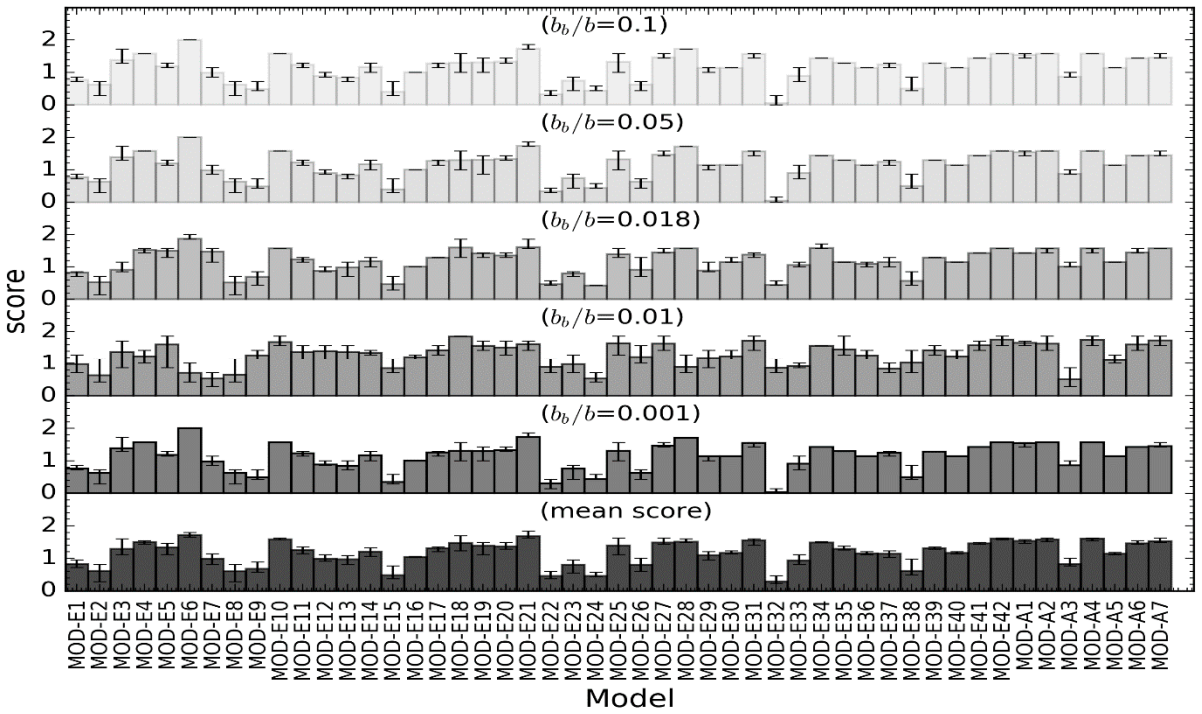

Figure S11.6. Total scores for different backscattering ratios and the average scores across all backscattering ratios in CLASS-I water for Calcareous sand.

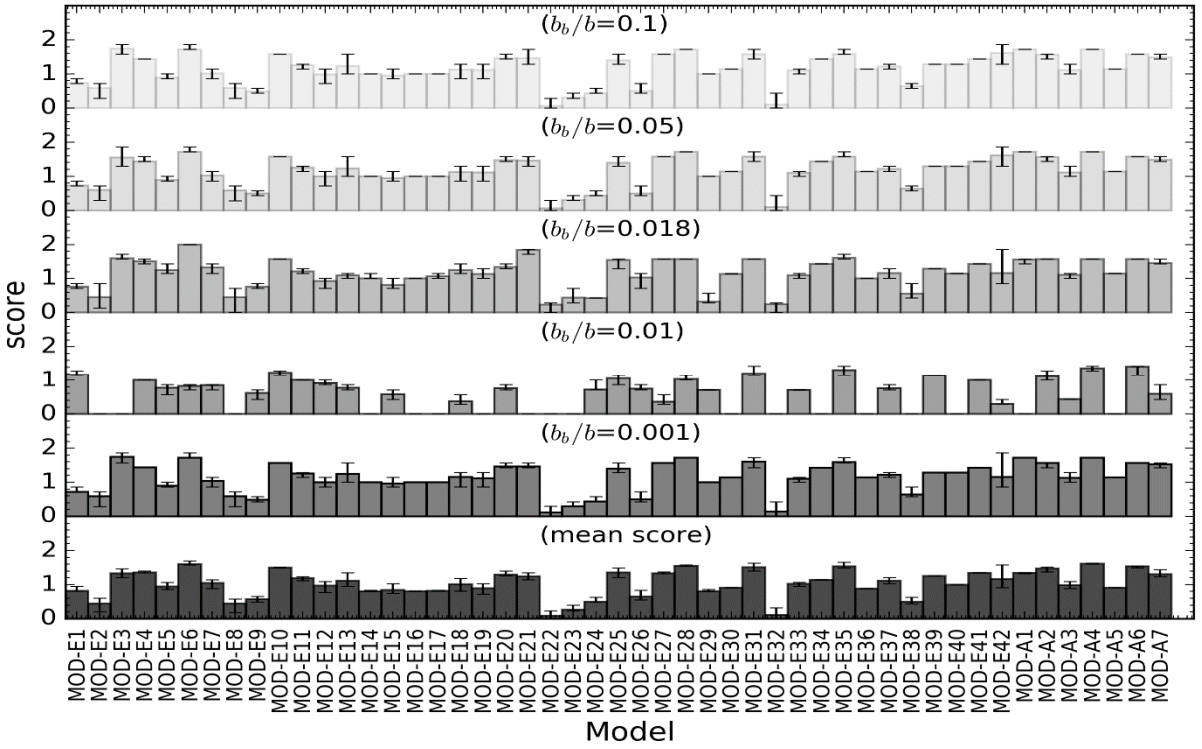

Figure S11.7. Total scores for different backscattering ratios and the average scores across all backscattering ratios in CLASS-II water for Calcareous sand.

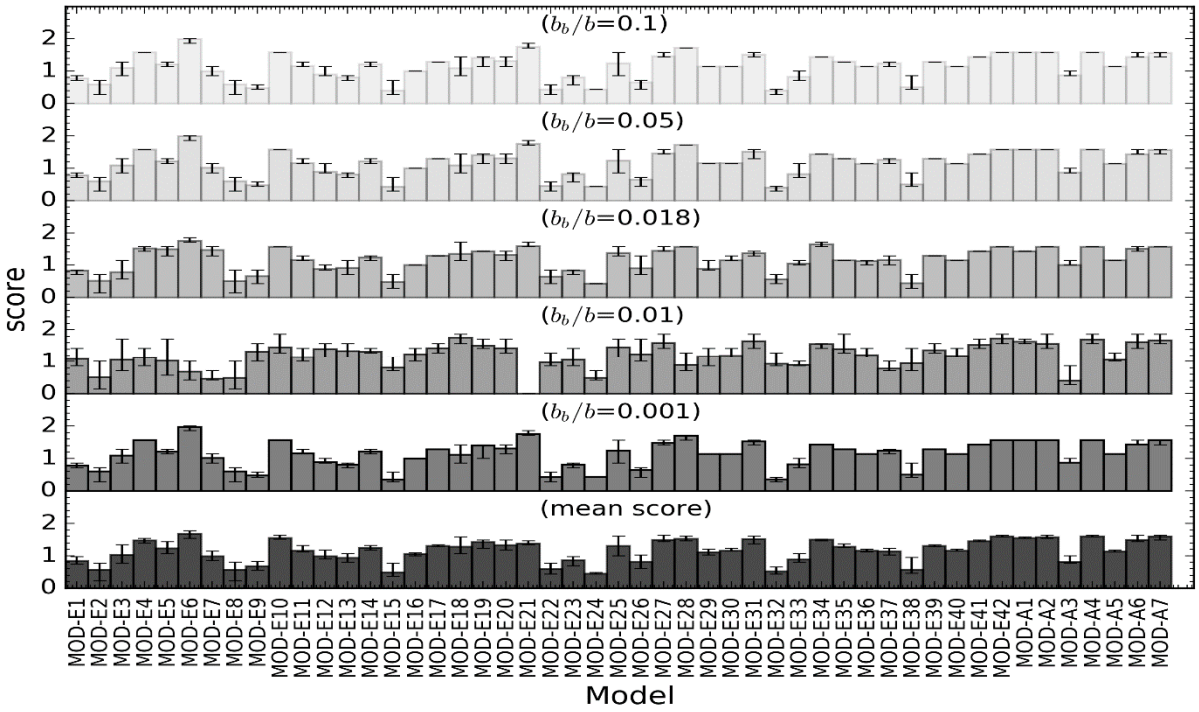

Figure S11.8. Total scores for different backscattering ratios and the average scores across all backscattering ratios in CLASS-III water for Calcareous sand.

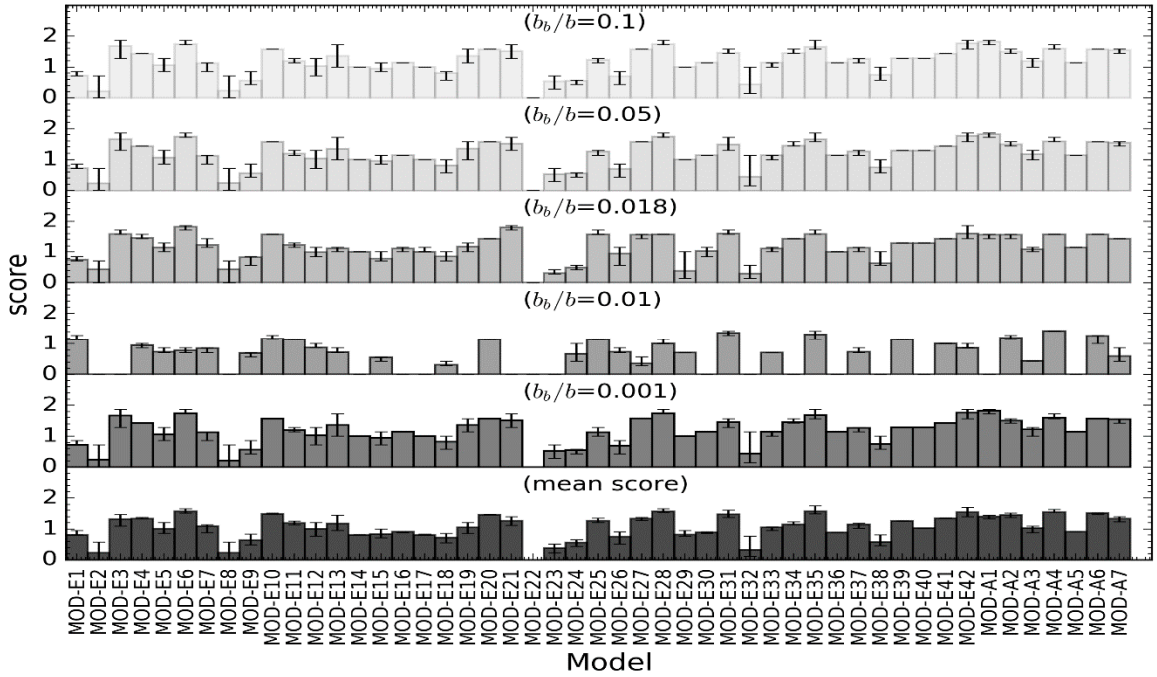

Figure S11.9. Total scores for different backscattering ratios and the average scores across all backscattering ratios in CLASS-IV water for Calcareous sand.

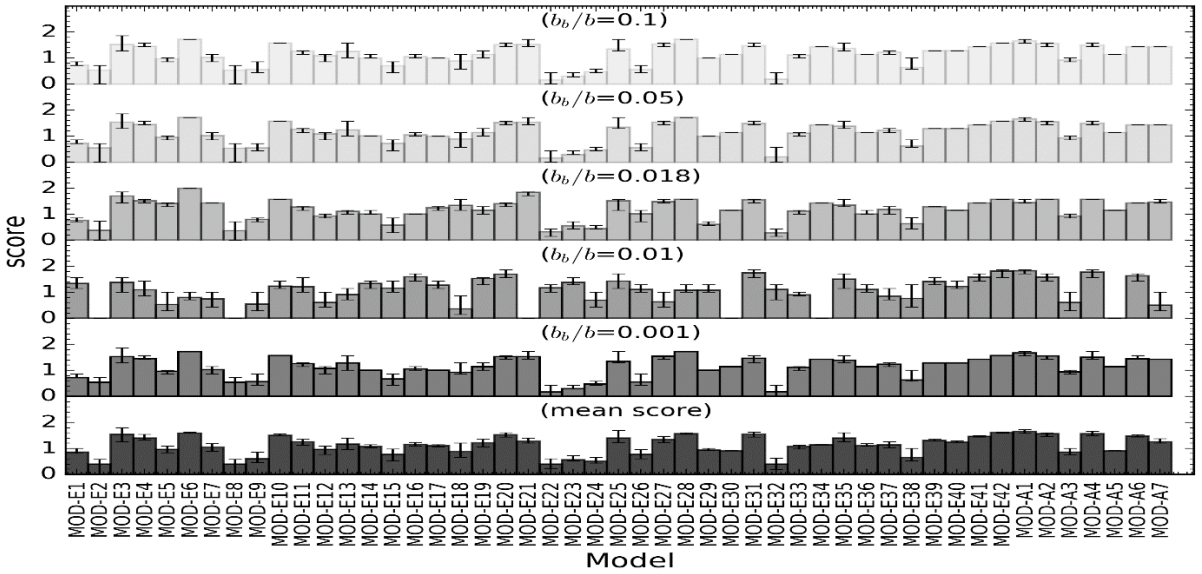

Figure S11.10. Total scores for different backscattering ratios and the average scores across all backscattering ratios in CLASS-V water for Calcareous sand.

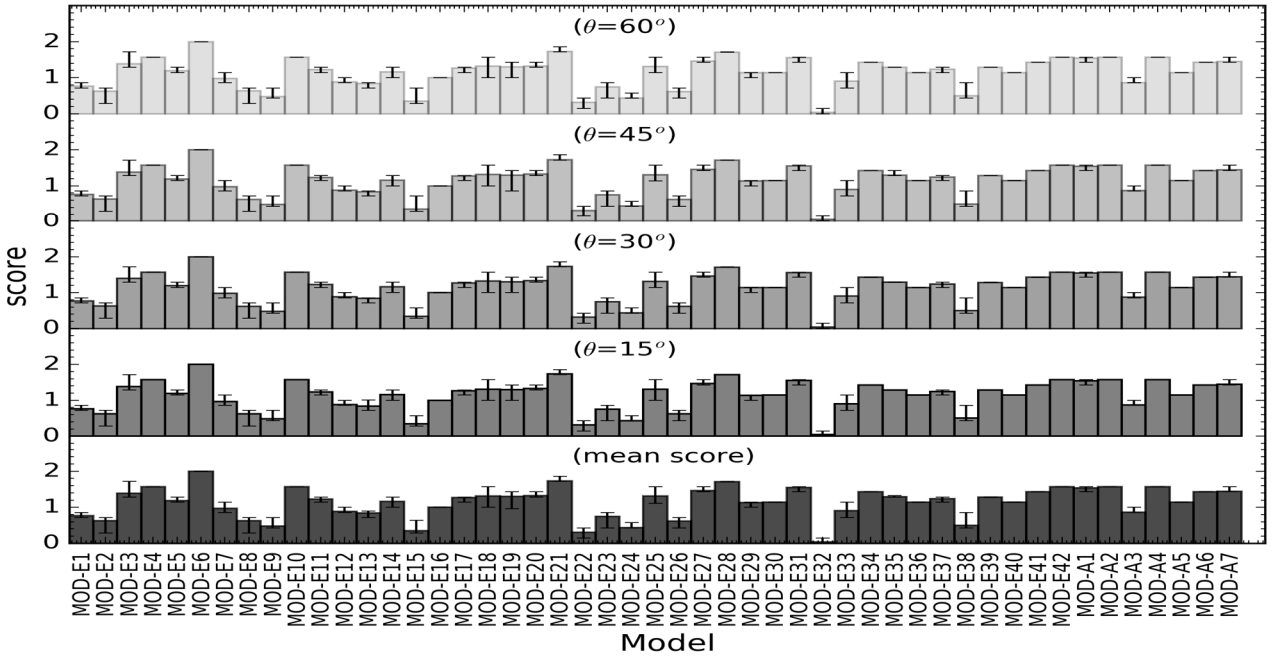

Figure S11.11. Total scores for different solar zenith angles and the average scores across all solar zenith angles in CLASS-I water for Calcareous sand.

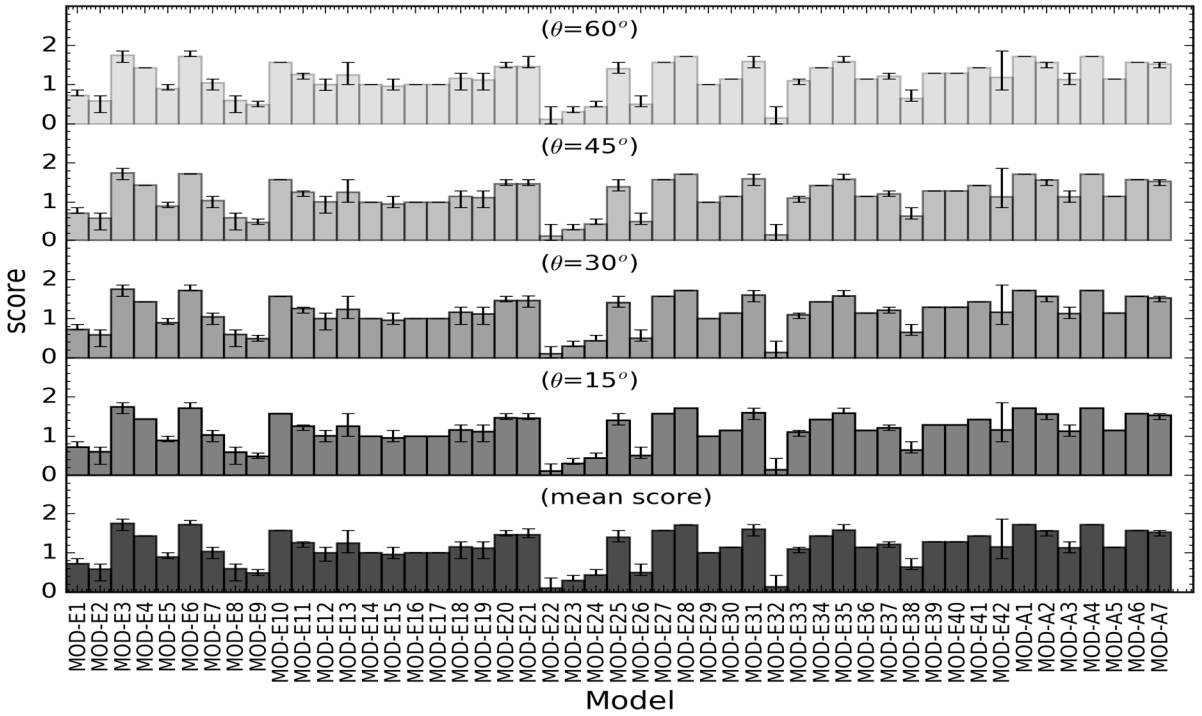

Figure S11.12. Total scores for different solar zenith angles and the average scores across all solar zenith angles in CLASS-II water for Calcareous sand.

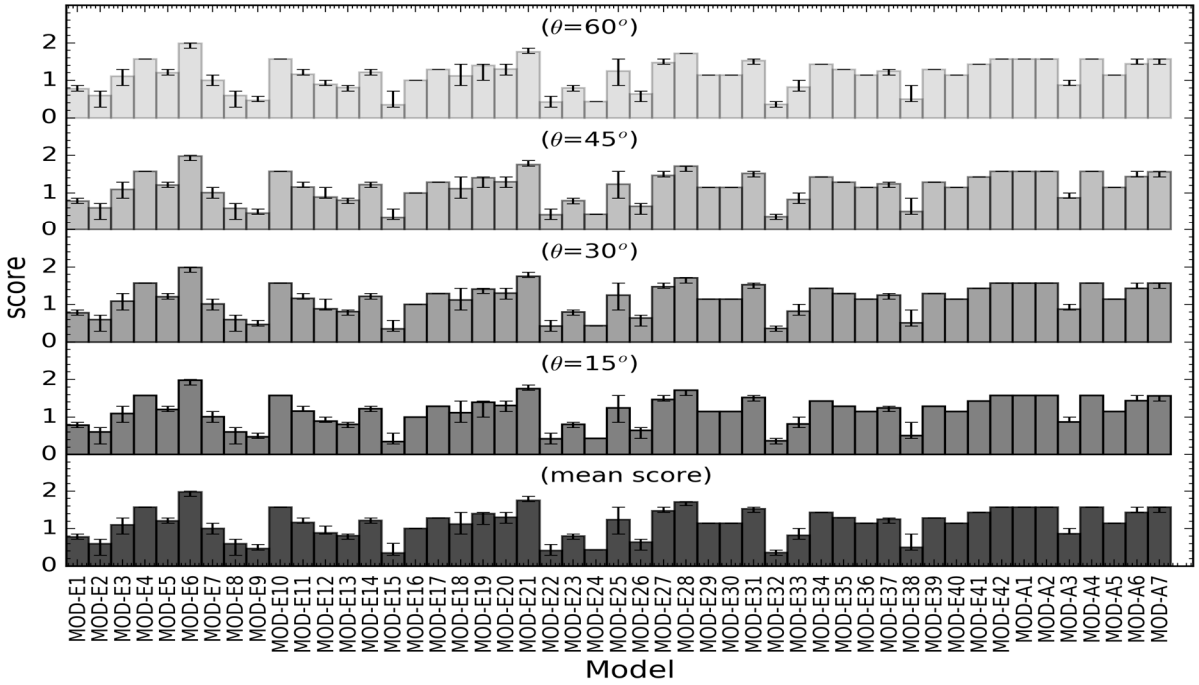

Figure S11.13. Total scores for different solar zenith angles and the average scores across all solar zenith angles in CLASS-III water for Calcareous sand.

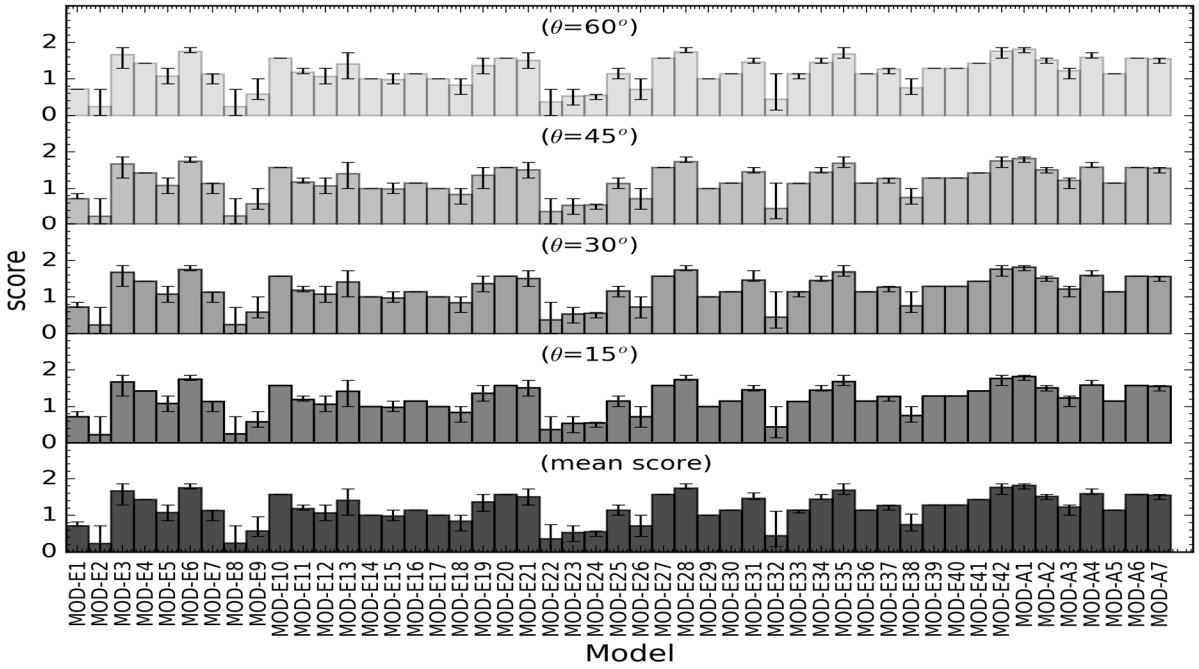

Figure S11.14. Total scores for different solar zenith angles and the average scores across all solar zenith angles in CLASS-IV water for Calcareous sand.

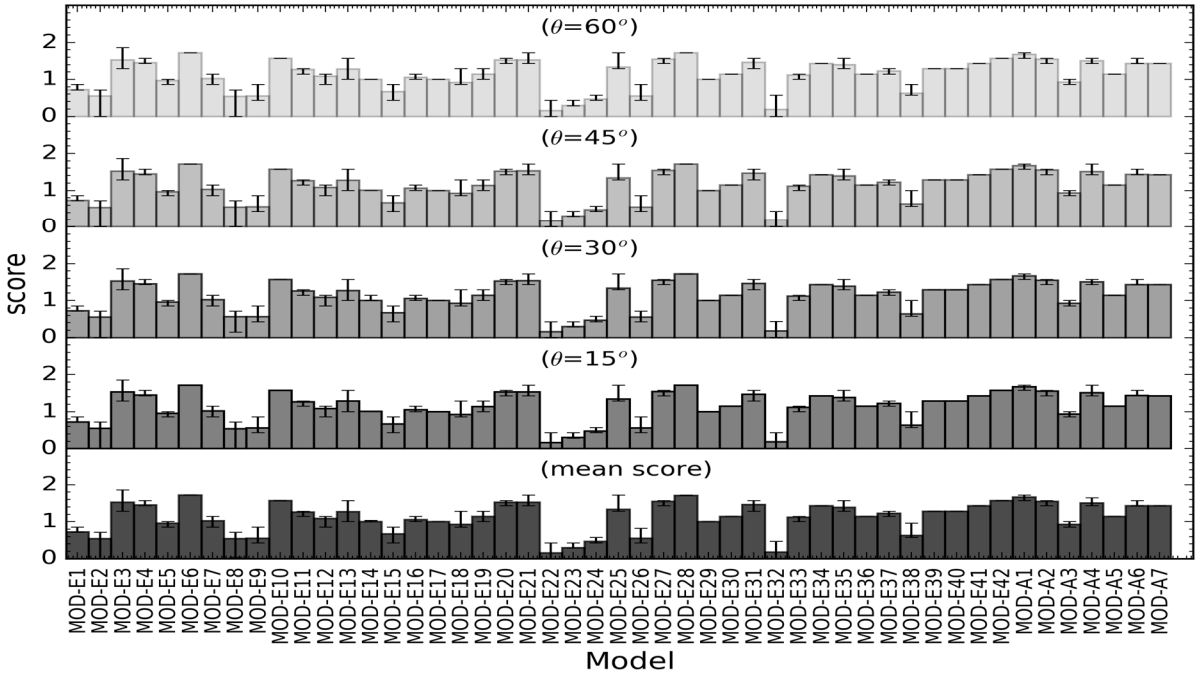

Figure S11.15 Total scores for different solar zenith angles and the average scores across all solar zenith angles in CLASS-V water for Calcareous sand.

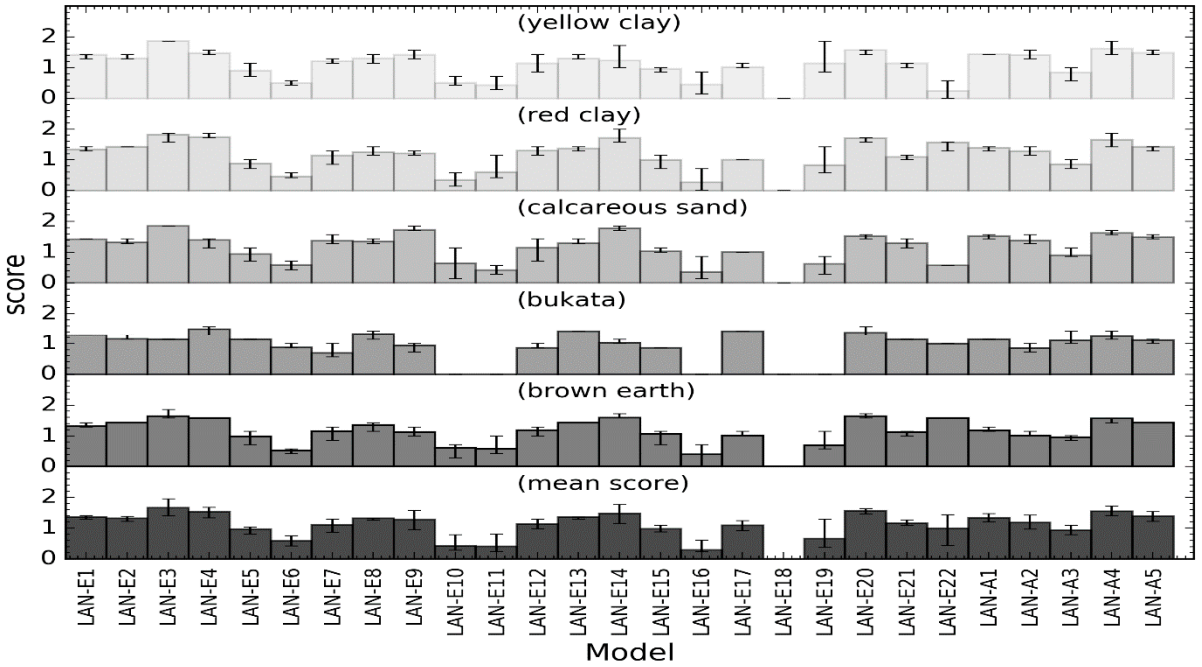

Figure S11.16. Total scores for different sediments and the average scores across all five sediments in CLASS-I water.

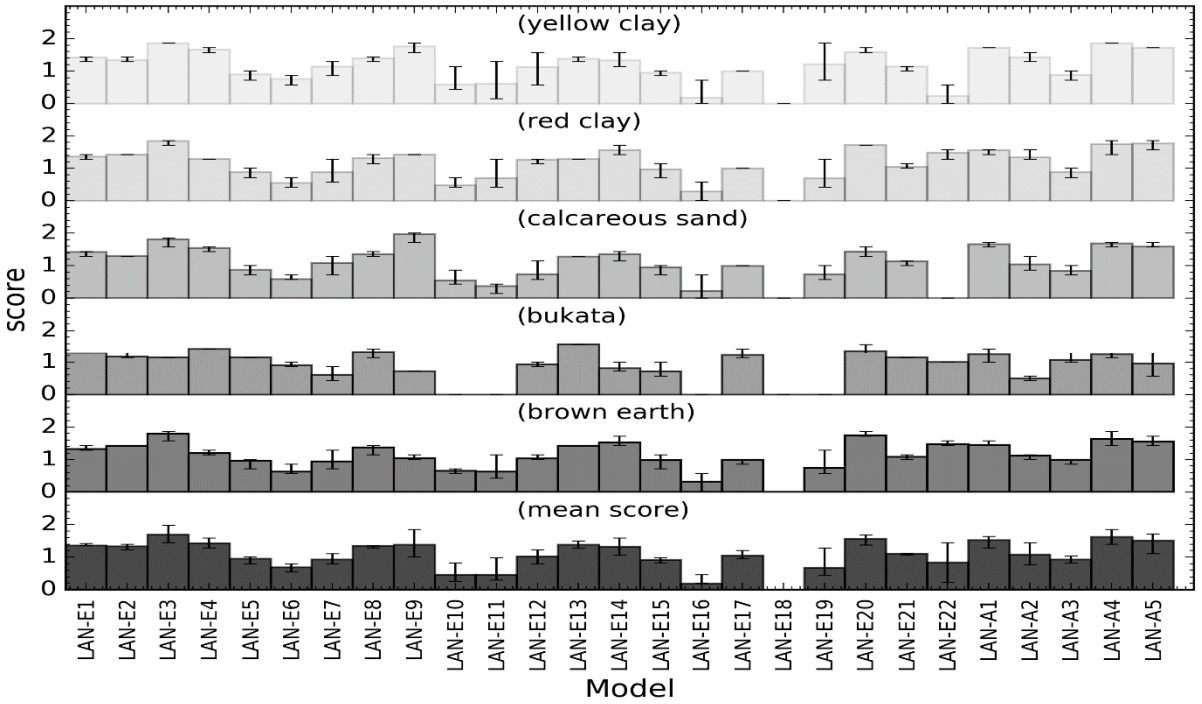

Figure S11.17. Total scores for different sediments and the average scores across all five sediments in CLASS-II water.

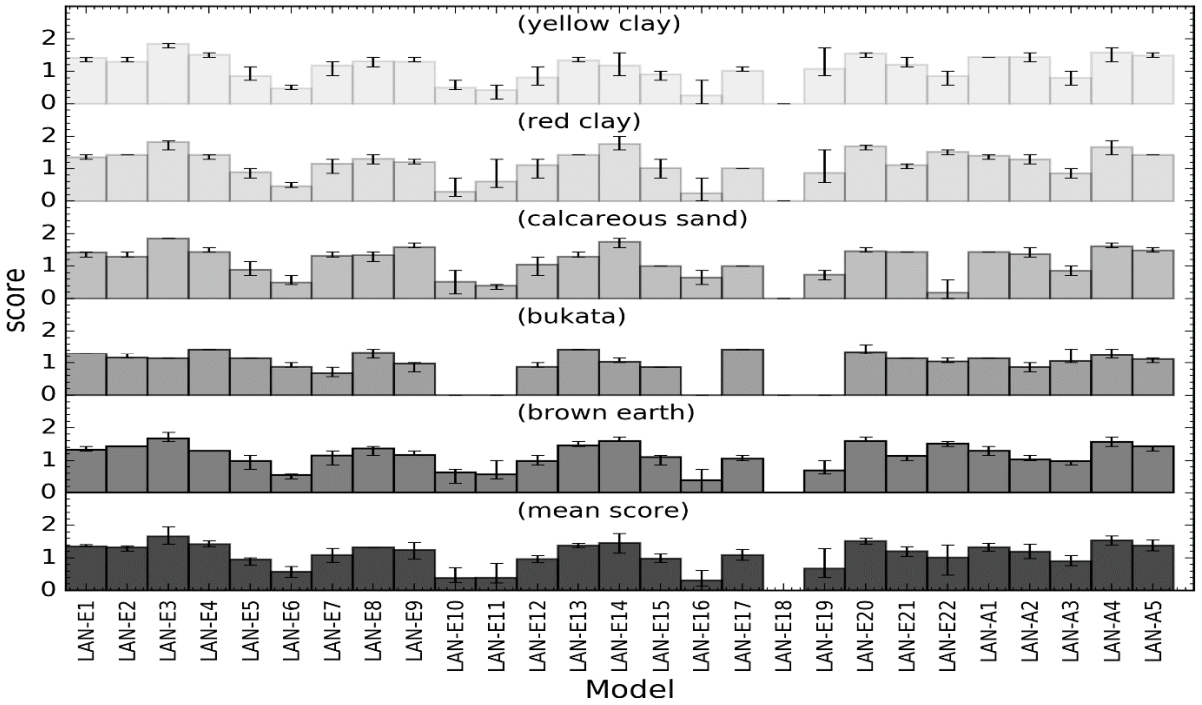

Figure S11.18. Total scores for different sediments and the average scores across all five sediments in CLASS-III water.

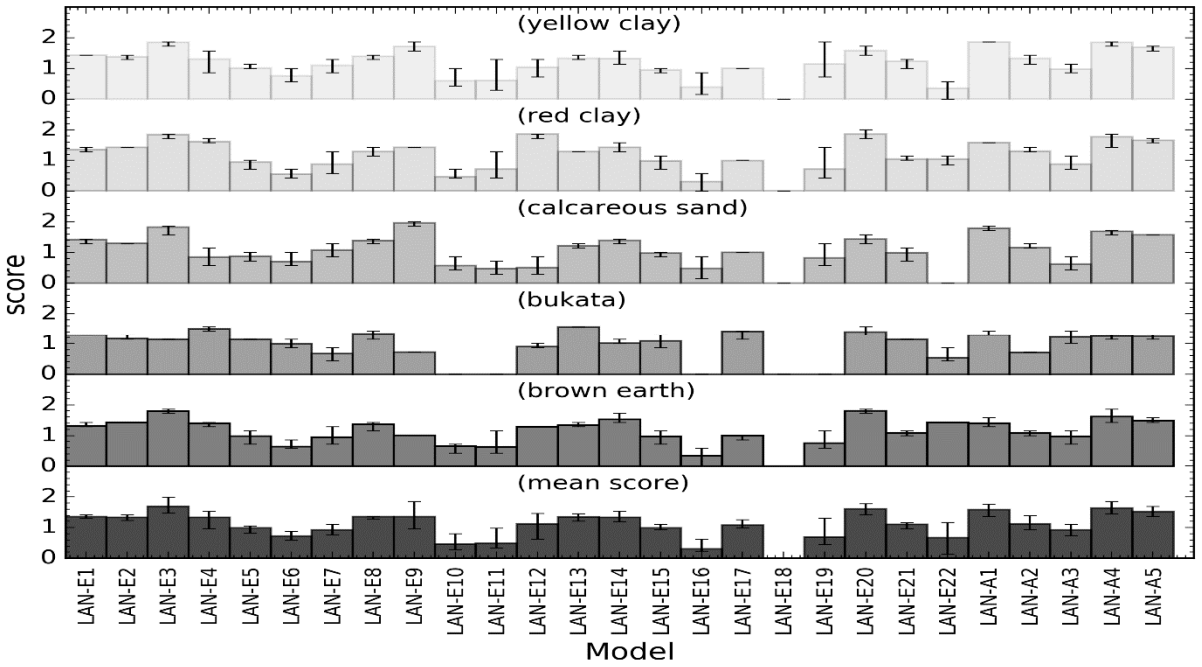

Figure S11.19. Total scores for different sediments and the average scores across all five sediments in CLASS-IV water.

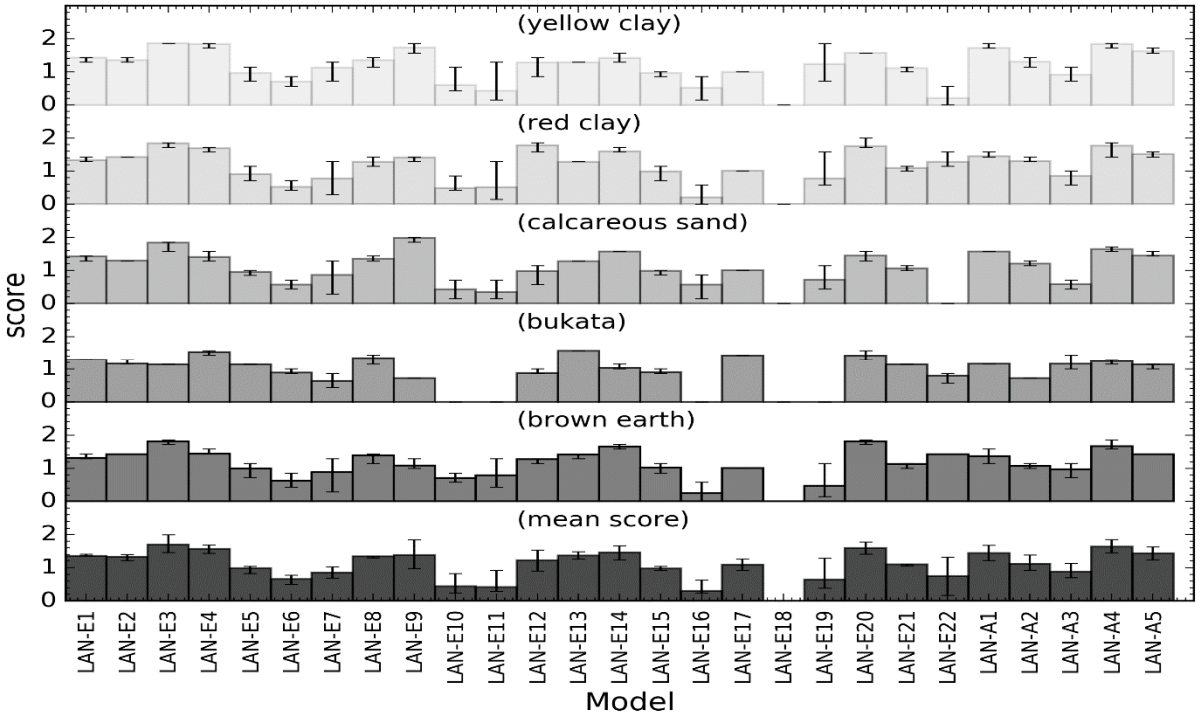

Figure S11.20. Total scores for different sediments and the average scores across all five sediments in CLASS-V water.

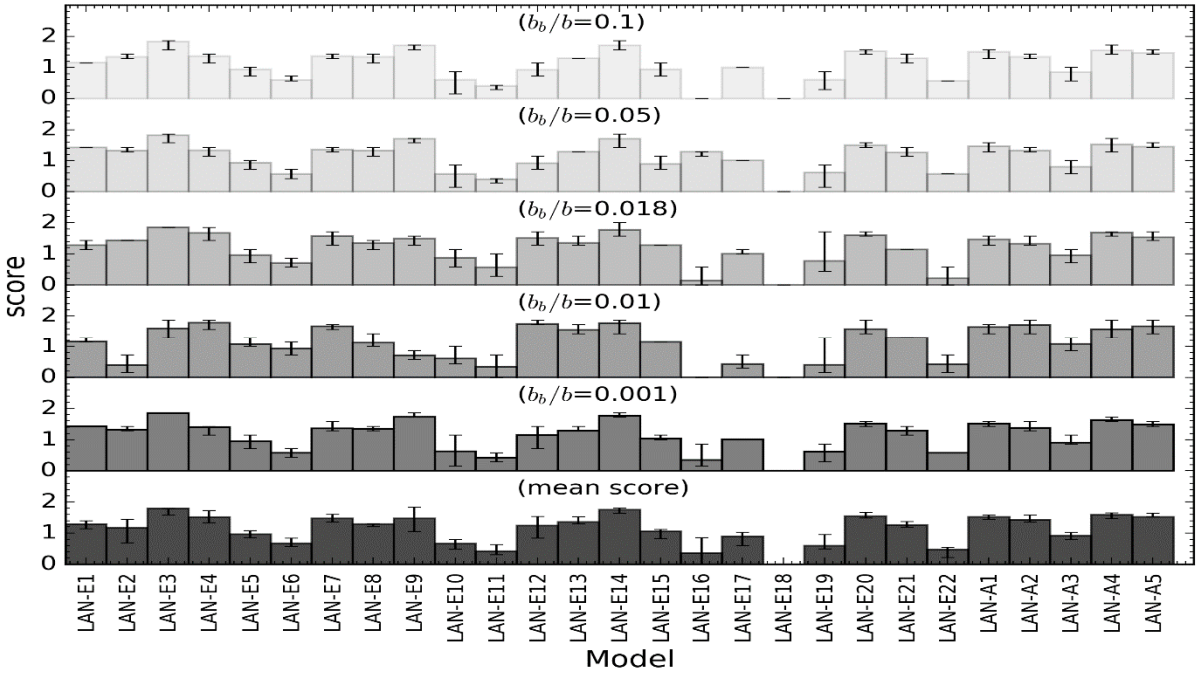

Figure S11.21. Total scores for different backscattering ratios and the average scores across all backscattering ratios in CLASS-I water for Calcareous sand.

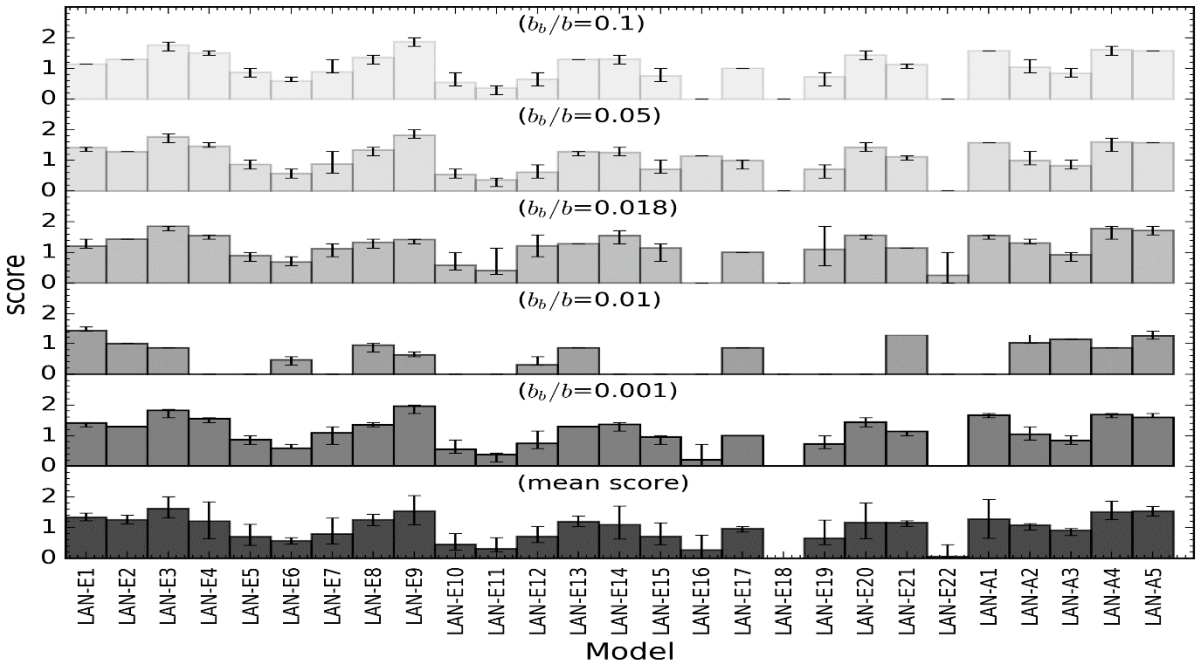

Figure S11.22. Total scores for different backscattering ratios and the average scores across all backscattering ratios in CLASS-II water for Calcareous sand.

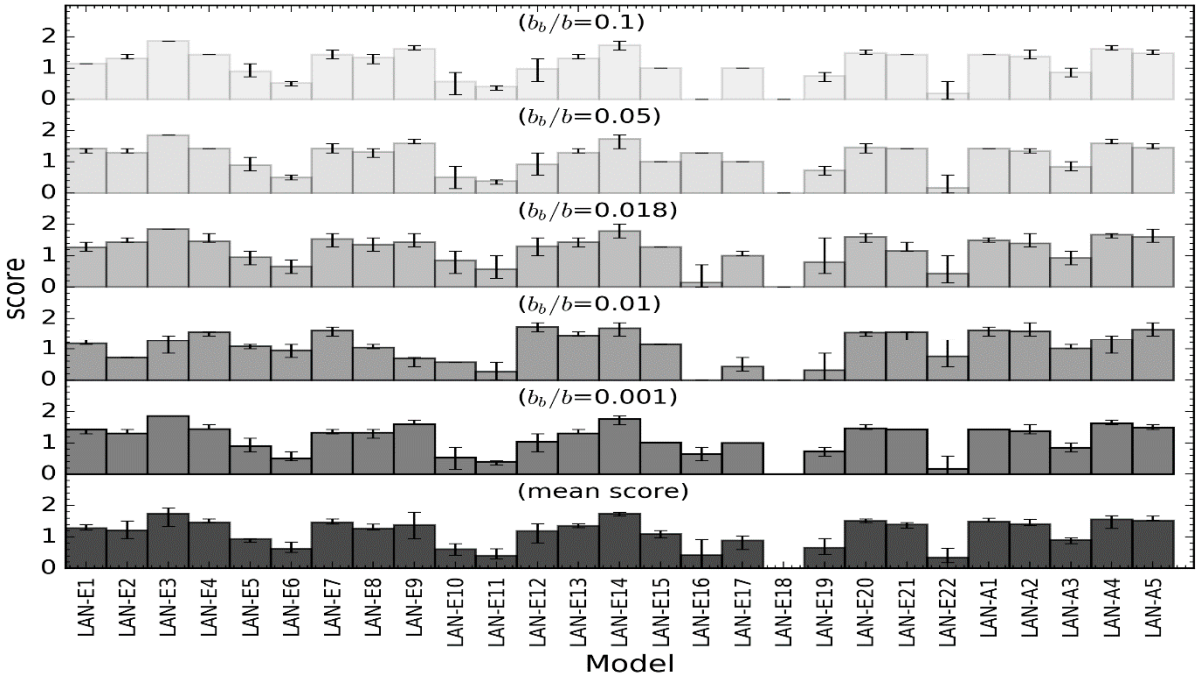

Figure S11.23. Total scores for different backscattering ratios and the average scores across all backscattering ratios in CLASS-III water for Calcareous sand.

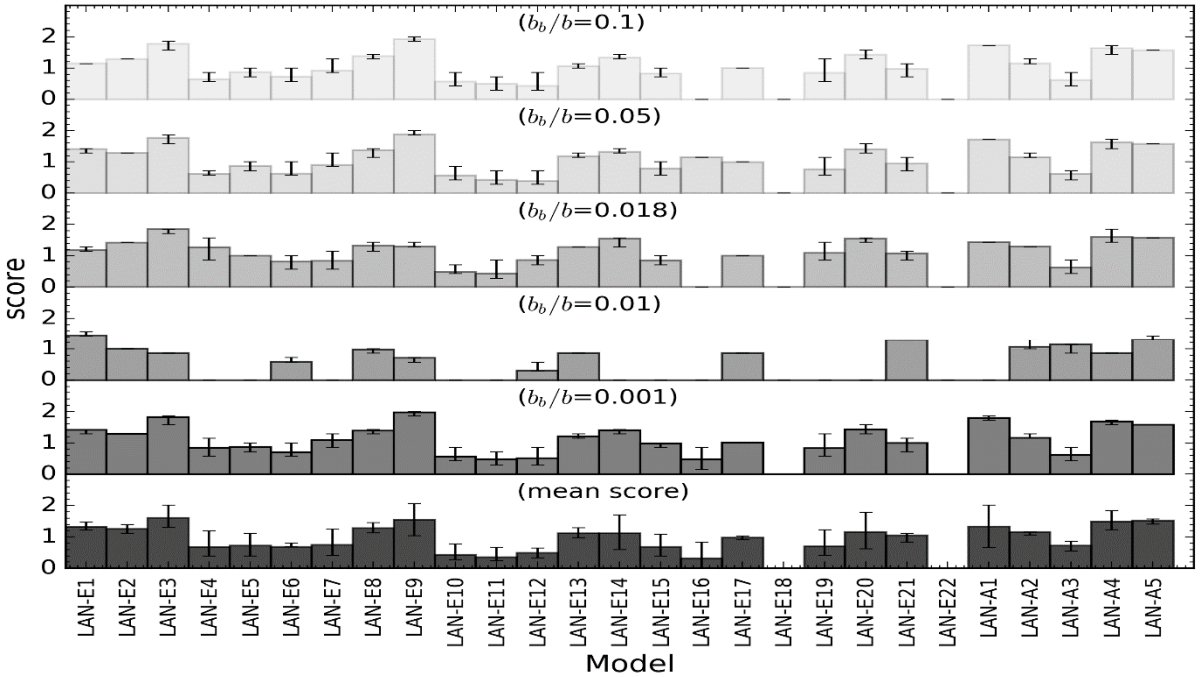

Figure S11.24. Total scores for different backscattering ratios and the average scores across all backscattering ratios in CLASS-IV water for Calcareous sand.

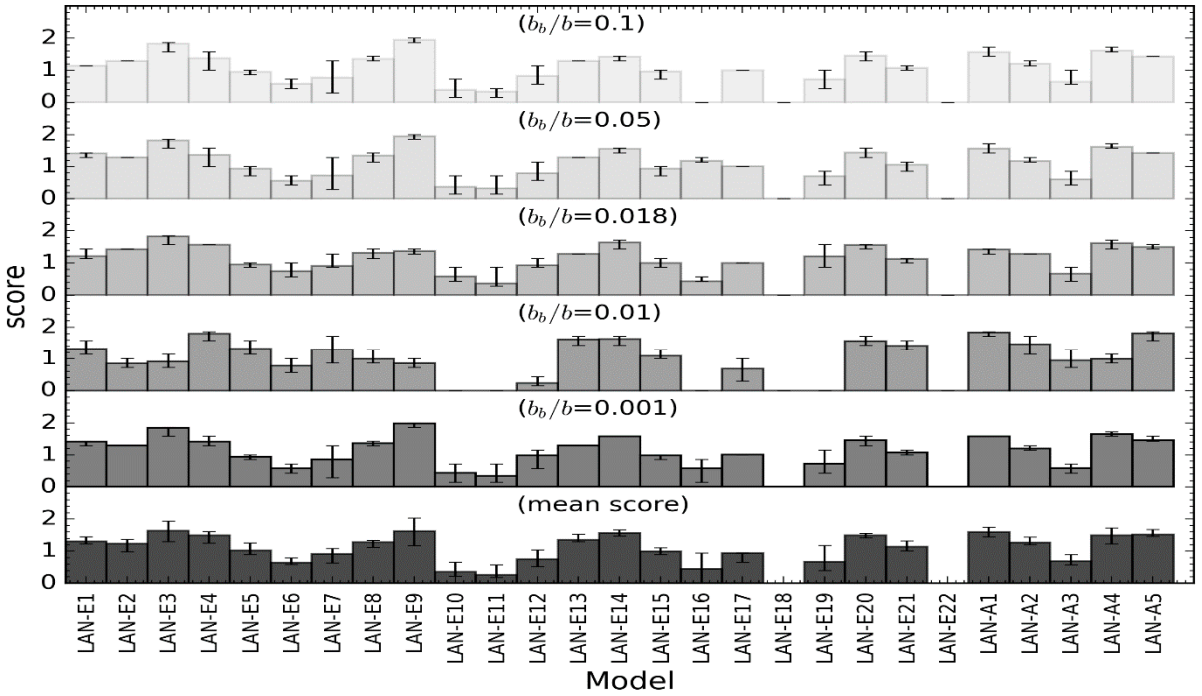

Figure S11.25. Total scores for different backscattering ratios and the average scores across all backscattering ratios in CLASS-V water for Calcareous sand.

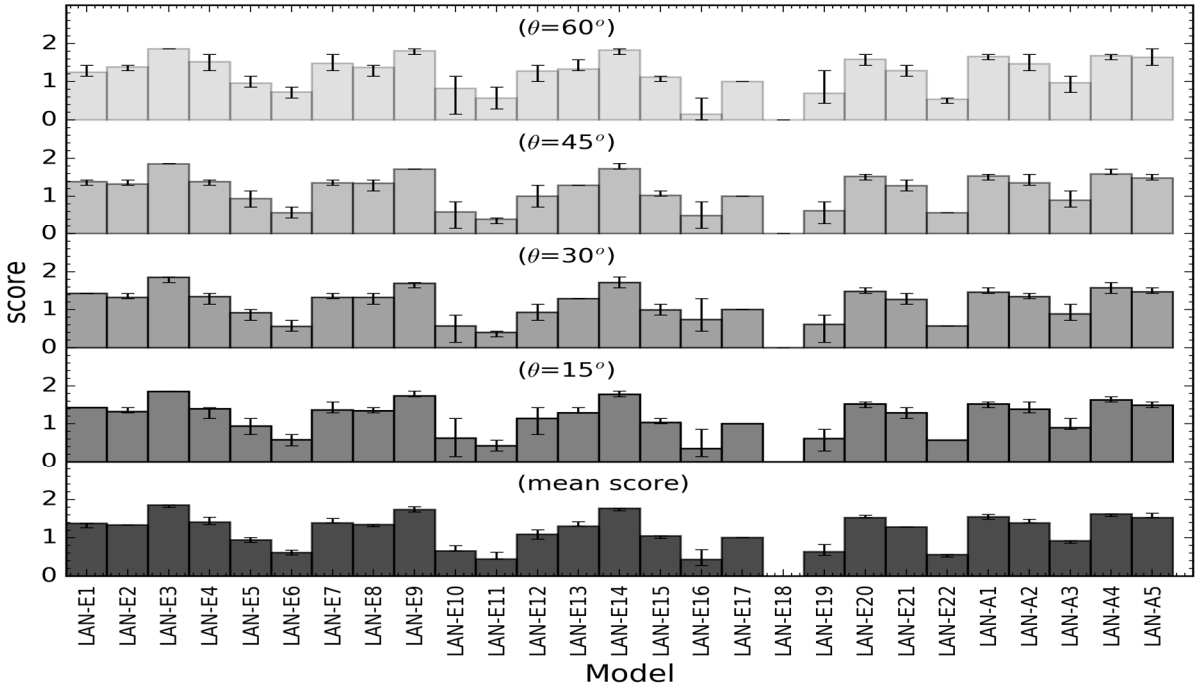

Figure S11.26. Total scores for different solar zenith angles and the average scores across all solar zenith angles in CLASS-I water for Calcareous sand.

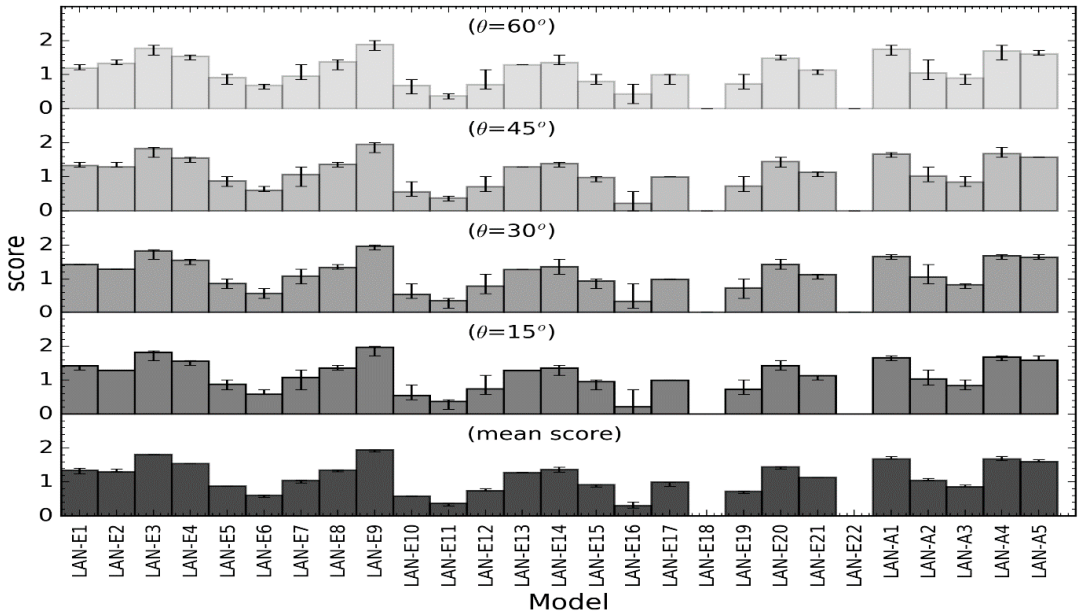

Figure S11.27. Total scores for different solar zenith angles and the average scores across all solar zenith angles in CLASS-II water for Calcareous sand.

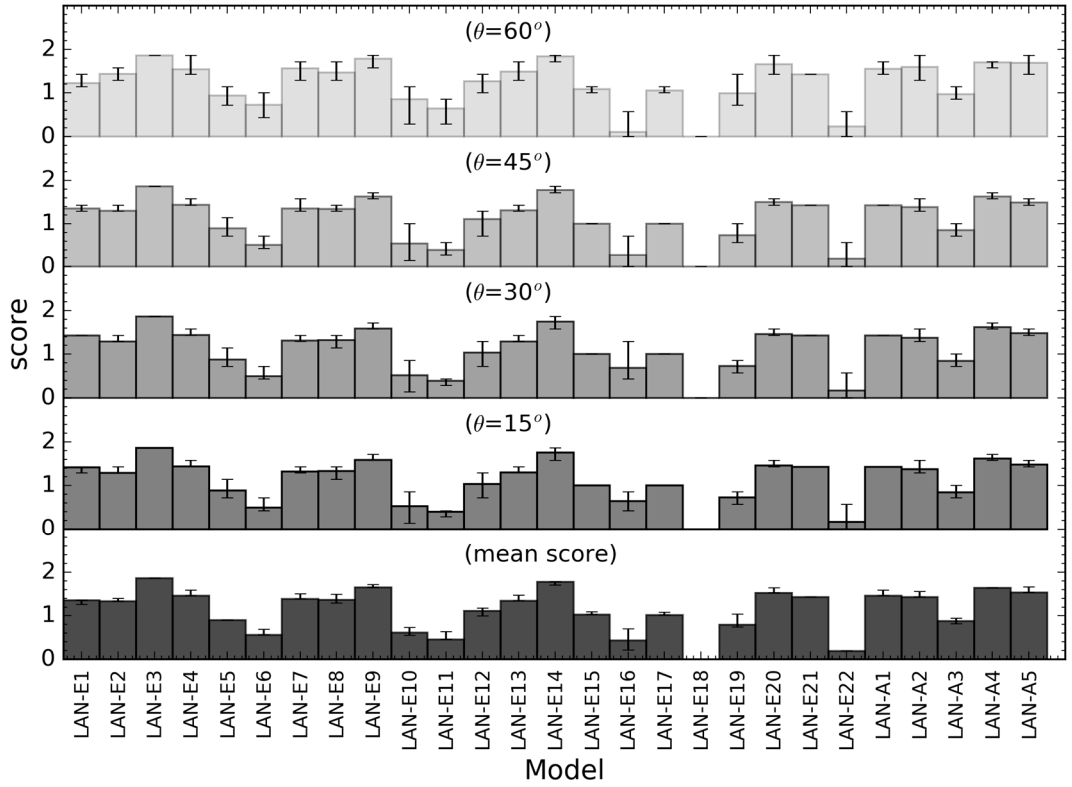

Figure S11.28. Total scores for different solar zenith angles and the average scores across all solar zenith angles in CLASS-III water for Calcareous sand.

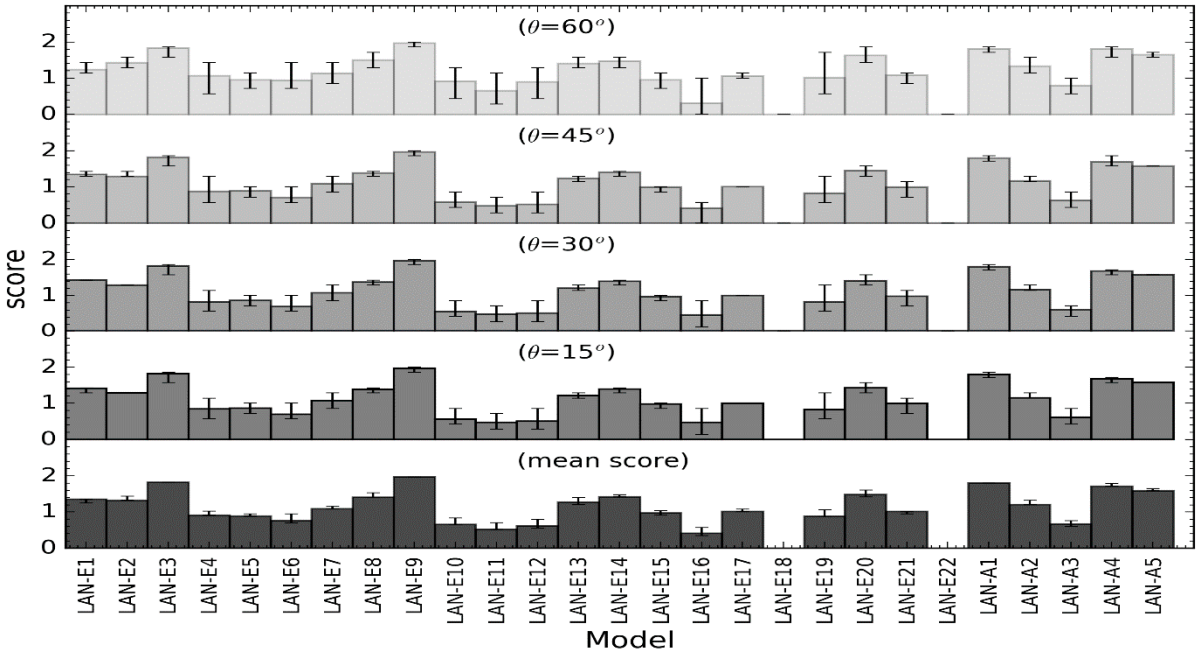

Figure S11.29. Total scores for different solar zenith angles and the average scores across all solar zenith angles in CLASS-IV water for Calcareous sand.

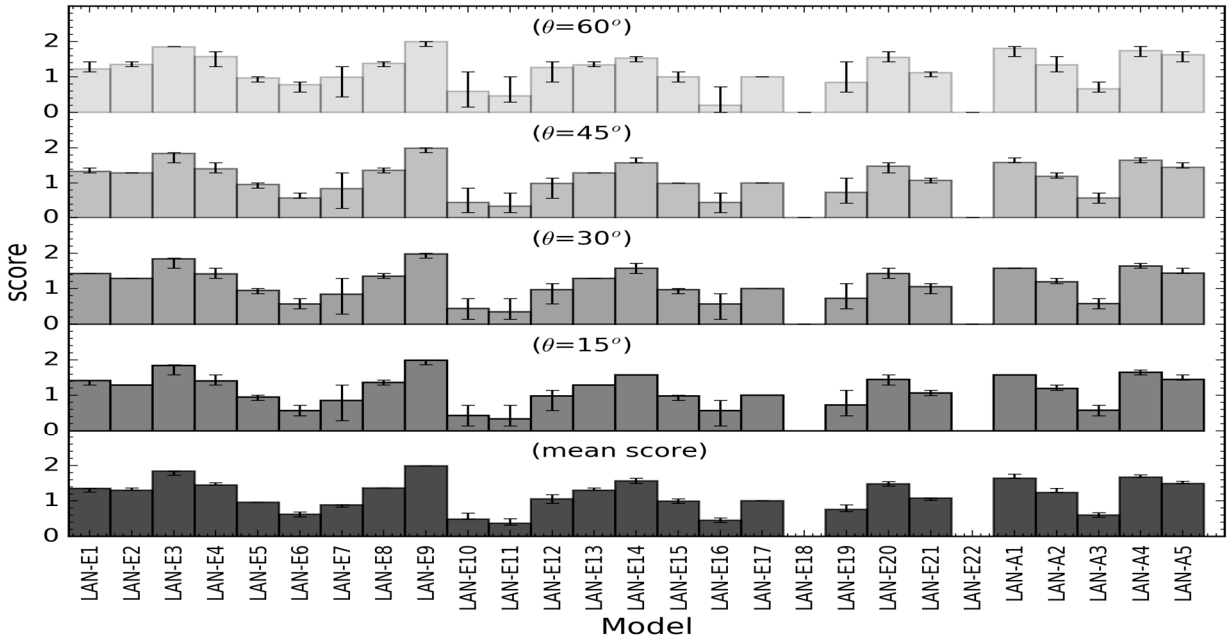

Figure S11.30. Total scores for different solar zenith angles and the average scores across all solar zenith angles in CLASS-V water for Calcareous sand.